PRESSURE EFFECTS OF TRANSOM LIFT DEVICES ON PRISMATIC PLANING HULLS

by

Declan Gaylo and Daniel Roske

A thesis submitted in partial fulfillment of the requirements for the Bachelor of Science Degree in Naval Architecture and Marine Engineering.

Declan Gaylo
Declan Gaylo

Daniel Roske
Daniel Roske

Certification of Approval

Matthew Werner, Dean

JUNE 19, 2019
Date

Richard Royce, Principal Adviser

6/18/2019
Date

Webb Institute
Glen Cove, New York

ACKNOWLEDGMENTS

First, we would like to thank our principal advisor, Professor Richard Royce, for his continued support and guidance throughout this project. We would like to thank Pat Doherty for his significant technical assistance in Robinson Model Basin and his work on the electrical components necessary for our testing. We would like to thank Professor Neil Gallagher and Jamie Swan for their help in manufacturing components for our testing. Finally, we would like to thank Stevens Institute's Davidson Laboratory for providing us use of its tank, specifically Professor Raju Datla for organizing our use of the tank and Uihoon Chung for running the tank for our tests.

ABSTRACT

This thesis investigates the effects of trim tabs and interceptors on the performance of a prismatic planing hull. Pressure measurements taken in way of the devices were used to characterize the lift generated by these devices as well as the devices' effect on running trim and resistance. Results were compared to existing prediction methodologies, which were found to inadequately model the effects of the added pressure created by these devices, especially interceptors. Recommendations were made for improvements. Additionally, the effectiveness of the devices was studied. It was found that interceptors have a higher lift to drag ratio at $F_{\nabla} = 2.49$. Both devices increase residual resistance at $F_{\nabla} > 2.7$.

TABLE OF CONTENTS

TABLE OF CONTENTS iii
LIST OF FIGURES v
LIST OF TABLES vi
NOMENCLATURE viii
INTRODUCTION 1
OBJECTIVE 2
BACKGROUND 2
THEORY OF PLANING 2
TRANSOM LIFT DEVICES 4
PREVIOUS WORK 6
THEORY 14
STILL-WATER TESTING 14
PRESSURE COEFFICIENT 16
APPENDAGE EFFECTIVENESS 17
UNCERTAINTY 18
DESIGN AND CONSTRUCTION 18
HULL MODEL 18
PRESSURE TAPS 20
TRIM TABS 21
INTERCEPTOR PLATE 24
PROCEDURE 26
TEST MATRIX 26
TANK TESTING EQUIPMENT 28
CALIBRATION 30
RESULTS 32
ERROR ANALYSIS 33
TRIM REDUCTION 34
RESISTANCE 38
PRESSURE 42
ANALYSIS 49
TRIM TAB PREDICTION METHODS 49
INTERCEPTOR PREDICTION METHODS 52
CONCLUSION 56
TRANSOM LIFT DEVICE EFFECTIVENESS 56
TRIM TAB PERFORMANCE PREDICTIONS 57
INTERCEPTOR PERFORMANCE PREDICTIONS 57
RECOMMENDATIONS FOR FUTURE WORK 58
LIST OF REFERENCES 58

APPENDIX A. INTERCEPTOR DEPLOYMENT UNCERTAINTY A-1
APPENDIX B. MOUNTING LAYOUT B-1
APPENDIX C. APPENDAGE BUOYANCY CORRECTION C-1
APPENDIX D. RUN DATA AND COEFFICIENT CALCULATIONS D-1
APPENDIX E. RESISTANCE, TRIM, AND SINKAGE RESULTS E-1
APPENDIX F. PRESSURE RESULTS F-1
APPENDIX G. UNCERTAINTY ANALYSIS G-1
APPENDIX H. PREDICTION CALCULATIONS H-1
APPENDIX I. EQUIVALENCE MATCHING CALCULATIONS I-1

LIST OF FIGURES

Figure 1. Planing Flat-Plate Pressure Distribution 2

Figure 2. Planing Vessel Regions of Resistance 3

Figure 3. Example Trim Tab Force Diagram 5

Figure 4. Example Interceptor Force Diagram 5

Figure 5. Planing Free-Body Diagram 7

Figure 6. Definition of Variables for Trim Tab Prediction 8

Figure 7. Interceptor and Trim Tab Equivalence Diagram (L_C=L_T) 10

Figure 8. CFD Trim Tab C_P Curve 12

Figure 9. CFD Interceptor C_P Curve 12

Figure 10. Model Test Interceptor C_P Curve 13

Figure 11. Underside Photo – Trim Tab C at RMB ($F\nabla = 2.77$) 14

Figure 12. Underside Photo – Trim Tab C at DL ($F\nabla = 2.77$) 15

Figure 13. Modified Leshnover C-1 Model 19

Figure 14. Pressure Manifold Layout 21

Figure 15. Trim Tabs as Mounted 23

Figure 16. Starboard Trim Tab Pressure Tap Layout 23

Figure 17. Effect of Pressure Relief on Trim Tab Pressure Distribution 24

Figure 18. Interceptor Plate 25

Figure 19. Equivalent Appendage Weights 26

Figure 20. Pressure Calibration Stand 31

Figure 21. Running Trim - Bare Hull 35

Figure 22. Reduction in Running Trim - Trim Tabs 36

Figure 23. Reduction in Running Trim - Interceptors 37

Figure 24. Resistance - Bare Hull 38

Figure 25. Reduction in Resistance - Trim Tabs 40

Figure 26. Reduction in Resistance - Interceptors 41

Figure 27. Typical Trim Tab Pressure Distribution ($F\nabla = 2.77$) 43

Figure 28. Trim Tab Peak Induced Pressure 44

Figure 29. Selected 5.00° Trim Tab C Induced Pressure Distributions 45

Figure 30. Example Interceptor Pressure Distribution ($F\nabla = 2.77$) 46

Figure 31. Interceptor Peak Induced Pressure 47

Figure 32. Selected 0.045" Interceptor C Induced Pressure Distributions 48

Figure 33. Selected 0.036" Interceptor B Induced Pressure Distributions 48

Figure 34. Bare Hull Trim Compared to Savitsky's Prediction Method 49

Figure 35. Bare Hull Resistance Compared to Savitsky's Prediction Method 50

Figure 36. Reduction in Running Trim - Measured versus Predicted 51

Figure 37. Equivalence Prediction Models versus Experimental Values 53

Figure 38. Comparison of Interceptor C and Trim Tab C 55

LIST OF TABLES

Table 1. Principal Geometric Characteristics of Model 19

Table 2. Characteristics of Model as Tested 20

Table 3. Pressure Tap Locations – Manifold 21

Table 4. Trim Tab Geometry 22

Table 5. Pressure Tap Locations – Trim Tabs 23

Table 6. Interceptor Geometry and Uncertainty 25

Table 7. Bare Hull Ballasting – RMB 27

Table 8. Bare Hull Ballasting – DL 27

Table 9. Average Uncertainty 33

Table 10. Average Uncertainty – Pressure 34

Table 11. Direct Comparison of Resistance Reduction ($F\nabla = 2.49$) 42

NOMENCLATURE

A_P – Projected Area of Planing Surface

A_{WP} – Area of Waterplane

B_{OA} – Beam Overall

B_P – Projected Chine Beam

C_{AP} – Longitudinal Center of Projected Planing Area

C_F – Frictional Coefficient of Resistance

C_p– Pressure Coefficient

C_R– Residual Coefficient of Resistance

C_T– Total Coefficient of Resistance

C_{WP}– Waterplane Coefficient

D_f – Drag Force of Total Planing Surface

D_T – Drag Force of Trim Tabs

DL – Davidson Laboratory

F_∇ –Volumetric Froude Number

g – Acceleration due to Gravity

L_C – Wetted Chine Length

L_K – Wetted Keel Length

L_m – Mean Wetted Length

L_T – Trim Tab Chord

L_P – Length of Planing Surface

L_{OA} – Length Overall

L_{WL} – Length of Waterline

LCG – Longitudinal Center of Gravity

P_D – Hydrodynamic Pressure

P_T – Total Pressure (Gauge)

R_N – Reynold's Number

R_T – Total Resistance

RMB – Robinson Model Basin

S – Wetted Surface Area, Dynamic

S_0 – Wetted Surface Area, Static

T – Design Draft

V – Vessel Speed

z – Vertical Distance from Static Free Surface

α_t – Trim Tab Deployment

β – Angle of Deadrise of Planing Surface

Δ – Displacement

ΔC_p – Appendage-Induced Pressure Coefficient

λ – Mean Wetted Length to Beam Ratio

ρ – Fluid Density

σ – Total Horizontal Span to Beam Ratio

τ – Trim

∇ – Displaced Volume

INTRODUCTION

High-speed craft operate in the planing regime where, as opposed to displacement vessels, dynamic forces become significant relative to buoyant forces. In the planing regime, the center of gravity rises, decreasing frictional resistance. Additionally, the length of the generated wave system is greater than the length of the vessel, which reduces wave resistance. To reach this regime, planing craft must first get past the heightened resistance caused by the length of the wave systems being approximately equal to the hull's waterline length. This transitional speed range is referred to as the hump region because of the local increase in resistance.

The increase in resistance associated with the hump region is in part due to a bow-up running trim of the vessel, which leads to a large form drag, often amplified by a transom stern. Decreasing the bow-up running trim decreases the resistance through the hump region, making the transition from displacement to planing easier. On small recreational boats, simply shifting a passenger's weight forward can be sufficient to decrease the running trim, allowing a boat, otherwise unable to transition from displacement to planing, to transition easily. The same effect is possible on larger craft with the aid of devices, referred to as transom lift devices, designed to create a forward trimming moment by moving the center of the hydrodynamic lifting force aft. Examples include hydrofoils, trim tabs, and interceptors. Many of these devices are adjustable, so they can also be used to actively decrease motions in a seaway; however, this thesis examines trim tabs and interceptors in calm water and their ability to decrease running trim and resistance.

OBJECTIVE

The objective of this thesis is to produce data and performance prediction recommendations that will allow naval architects to understand the effects of interceptors and trim tabs on planing craft more accurately. A better understanding will ultimately allow naval architects to better size optimal interceptors and trim tabs. The data will be produced through model testing of a prismatic planing hull, while measuring pressures near the transom in way of the lifting devices. The analysis will focus on how the pressures are affected by the presence of these devices. The results will be compared to existing prediction methods, and conclusions will be made on their accuracy. Additionally, this thesis will compare the effectiveness of trim tabs and interceptors over a range of speeds to help determine which is better suited for planing craft.

BACKGROUND

THEORY OF PLANING

Unlike a typical displacement vessel, the weight of which is supported entirely by buoyancy, a planing vessel's weight is supported by a combination of buoyancy and dynamic lift. Figure 1 shows a simplified drawing of a planing flat plate.

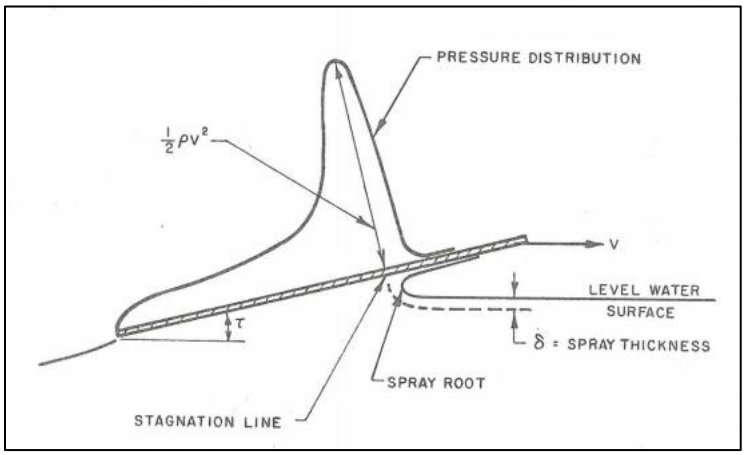

Figure 1. Planing Flat-Plate Pressure Distribution
Source: Savitsky (1964)

The flat plate moves at a velocity, V, through the water at some trim angle, τ, accelerating the flow downward. The resulting dynamic pressure distribution creates a reaction force on the plate. The component of the reaction force perpendicular to the direction of travel is dynamic lift, and the tangential component is dynamic drag. The peak of the dynamic pressure distribution occurs at the stagnation point on the plate. The distribution then decreases aft of the stagnation point until it reaches a value of zero at the trailing edge of the plate.

As a vessel accelerates to planing speeds, it passes through three characteristic regions of resistance. The general boundaries of the regions are described by a non-dimensionalized speed characteristic called the volumetric Froude number, F_∇. V is the model velocity and ∇ is the static displaced volume.

$$F_\nabla = \frac{V}{\sqrt{g\sqrt[3]{\nabla}}} \tag{1}$$

In the slowest region, the displacement region, the vessel is supported entirely by buoyancy. The second region is the transition, or semi-displacement, region. In this region, dynamic forces begin to become significant. This region contains the "hump" of a planing hull's resistance curve, as shown in Figure 2.

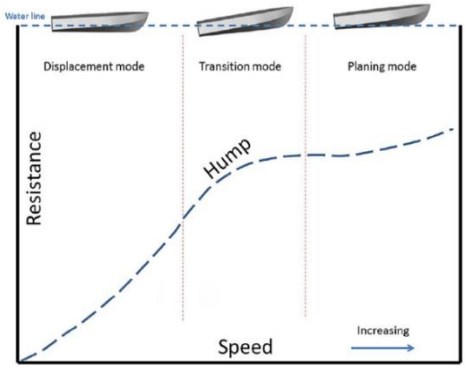

Figure 2. Planing Vessel Regions of Resistance
Source: Mansoori & Fernandes (2017)

This hump is partially caused by a large running trim of the vessel, which increases the form drag. The fastest region is the planing region, where the majority of the craft's weight is supported by dynamic lift. The running trim is reduced and the center of gravity rises. As there is a much smaller wetted surface, there is less frictional and wave-making drag.

TRANSOM LIFT DEVICES

Often the increased resistance within the hump region can be partially alleviated using transom lift devices, which are appendages that are outfitted on the transom of a planing vessel to create a forward trimming moment to counteract the bow-up running trim. The two transom lift devices explored in this thesis are trim tabs and interceptors.

When sizing transom lift devices, it is vital to accurately predict the amount of running trim reduction that will be created. An excessive amount of running trim reduction could result in a loss of directional stability of the vessel and would be inefficient. Too little running trim reduction means the device would be adding drag with little beneficial effect. Blount (2014) suggests that all transom lift devices should be designed such that they provide 1° to 1.5° of running trim reduction at the vessel's greatest running trim angle.

Theory of Trim Tabs

Trim tabs are inclined plates that extend behind the transom and direct flow downward, as shown in Figure 3. The tab accelerates the fluid flow downward, creating a reaction force on the trim tab, causing a forward trimming moment.

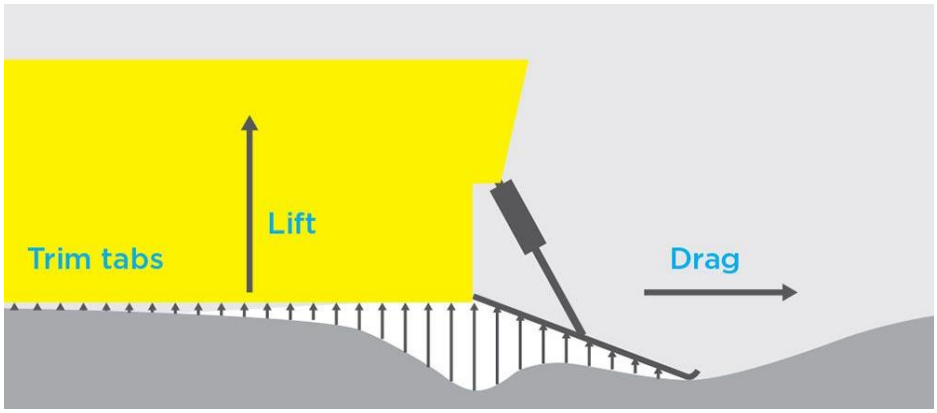

Figure 3. Example Trim Tab Force Diagram
Source: Zipwake.com

A trim tab adds additional surface area to the vessel, increasing the frictional resistance. To a similar effect, the extension of the trim tab hanging below the baseline of the vessel increases the form drag of the vessel, although in practice this slight increase in form drag because of the extension of the tab is made up for by the large decrease in form drag caused by the running trim reduction created by the tab's lift.

Theory of Interceptors

Interceptors are flat blades that extend directly below the transom and create a stagnation point in the flow, which increases the pressure at the transom, as shown in Figure 4.

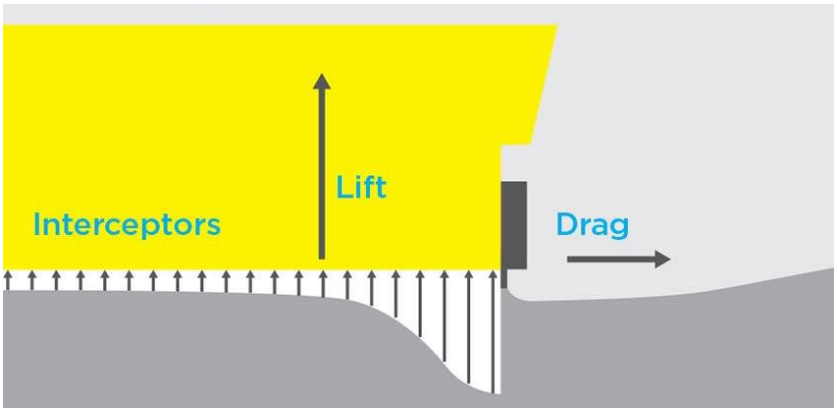

Figure 4. Example Interceptor Force Diagram
Source: Zipwake.com

A stagnation point is a point in the flow where the particles are decelerated to zero relative velocity to the vessel. The theoretical pressure at this point can be found using Bernoulli's equation,

$$\frac{1}{2}\rho v^2 + \rho g z + P = constant \tag{2}$$

where ρ is the fluid density, v is the fluid velocity, g is the acceleration due to gravity, z is the fluid height, and P is the fluid static pressure. At a stagnation point, all dynamic pressure, as expressed by the first term of Equation 2, is converted to static pressure, the third term, as the velocity of the fluid slows from the far-field velocity to zero. The converted dynamic pressure is added to the static pressure, P_0. If there is no change in height along the streamline, absolute stagnation pressure is given by the following equation.

$$P_{Stagnation} = P_0 + \frac{1}{2}\rho v^2 \tag{3}$$

The pressure developed is greatly dependent on the far-field velocity; however, the boundary layer thickness and the corresponding velocity gradient play a role in the magnitude of the stagnation pressure at the interceptor. The velocity within the boundary layer will be lower than that of the fluid outside it; therefore, the stagnation pressure is lower. Generally, the interceptor blade does not penetrate the boundary layer (Molini & Brizzolara, 2005) (Mansoori & Fernandes, 2017).

PREVIOUS WORK

Predicting Basic Planing-Hull Performance

The starting point for performance prediction of a planing hull is a series of semi-empirical equations, developed by researchers at Stevens Institute's Davidson Laboratory,

which describe the dynamics of planing. Savitsky (1964) synthesized these equations and applied them to the free-body system shown in Figure 5. Using this method, he developed a prediction method for planing-hull performance which is suited to design. Most subsequent work on planing-hull performance prediction has used the Savitsky method as a starting point and has applied correction factors or modifications.

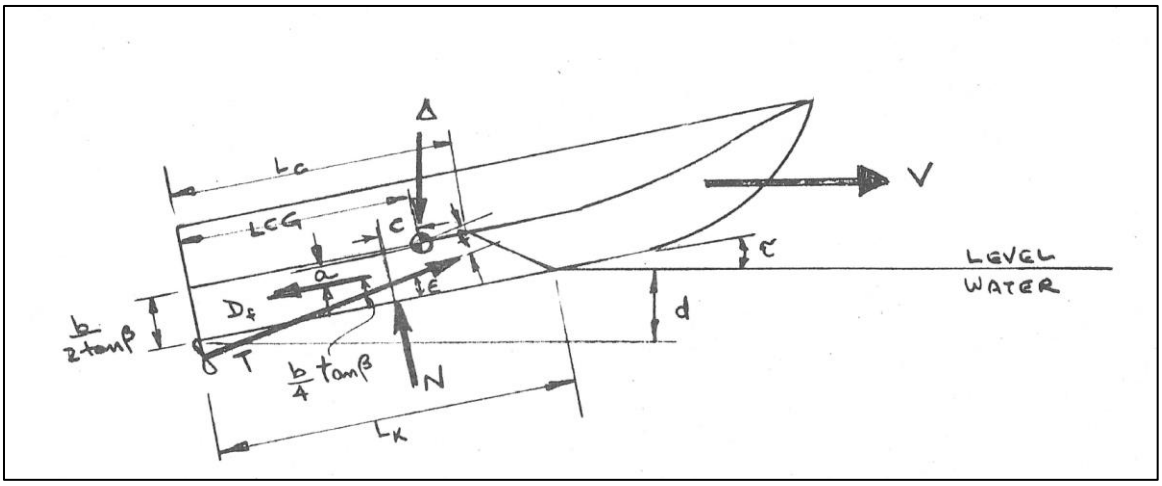

Figure 5. Planing Free-Body Diagram
Source: Savitsky (1964)

According to Blount and Fox (1976), the Savitsky method has been found to accurately predict model test resistance for planing speeds. However, this method has consistently been observed to under predict resistance at hump speeds. To correct the underprediction of resistance at hump speeds, Blount and Fox proposed the following correction factor, M, based off regressions of typical heavy-loaded planing craft ($\frac{A_p}{\nabla^{2/3}} = 6.0\ to\ 6.5$). This correction factor approaches unity at higher speeds.

$$M = 0.98 + 2\left(\frac{LCG}{B_P}\right)^{1.45} e^{-2(F_\nabla - 0.85)} - 3\left(\frac{LCG}{B_P}\right) e^{-3(F_\nabla - 0.85)} \quad (4)$$

LCG is the longitudinal distance of the center of gravity, measured from the transom, B_P is the beam of the planing surface. For the vessel tested in this thesis, the B_P is equal to the B_{OA}. The predicted resistance is thus calculated:

$$R_T = M \cdot R_{Savitsky} \tag{5}$$

Predicting Trim Tab Performance

The dimensions used for predicting trim tab performance are shown in Figure 6.

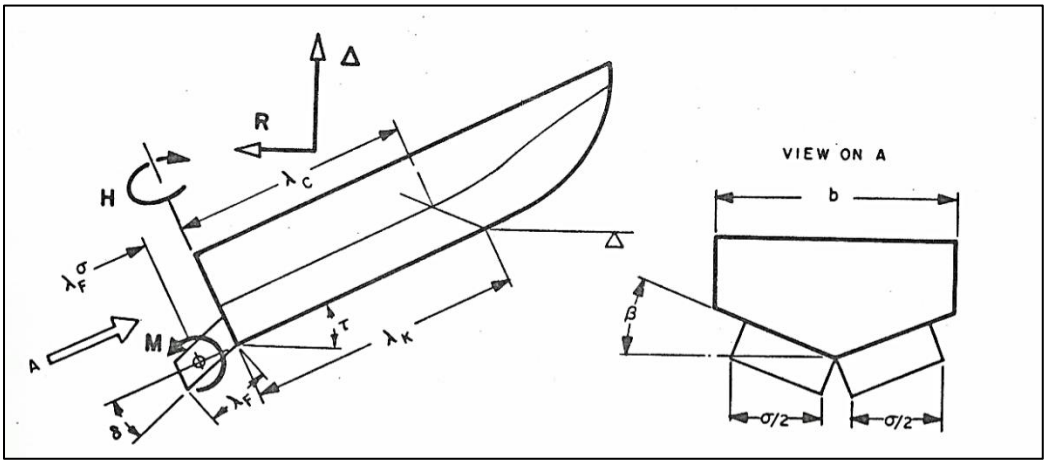

Figure 6. Definition of Variables for Trim Tab Prediction
Source: Brown (1971)

From model tests, Brown (1971) developed the following equations to predict change in lift, Δ_T, and resistance, D_T, caused by the trim tabs. L_T is the chord of the tabs, α_t is the trim tab deployment angle (labeled as δ in Figure 6), and σ is the span to beam ratio.

$$\Delta_T = 0.046\, L_T\, \alpha_t \sigma B_P \left[\frac{\rho}{2} V^2\right] \tag{6}$$

$$D_T = 0.0052\, \Delta_T\, (\tau + \alpha_t) \tag{7}$$

For these equations, the span of the trim tab is measured in the horizontal plane, so σ is calculated as follows, where s is the span of a single tab as measured in the plane parallel to the trim tab's face. Also, note that σ refers to the total span of both trim tabs.

$$\sigma = \frac{2\, s\, \cos\beta}{B_P} \tag{8}$$

Rather than considering the change in lift as a force that must be directly accounted for in the free body equations of a planing hull (Figure 5), the lift is accounted for through an effective change in weight of the vessel and an effective forward shift in the LCG. Savitsky and Brown (1976) together developed a method to do this, creating the following equation, which predicts the hydrodynamic moment, M_T, created by the trim tabs.

$$M_T = \Delta_T[0.6\, B_{PX} + L_T(1-\sigma)] \tag{9}$$

Effective displacement, Δ_e, and effective LCG, LCG_e, are calculated as follows, where Δ_T is the lift of the trim tabs.

$$\Delta_e = \Delta - \Delta_T \tag{10}$$

$$LCG_e = [\Delta(LCG) - M_T]/\Delta_e \tag{11}$$

These values are then used instead of the real values for displacement and LCG throughout the Savitsky method. Using these effective values accounts for trim tab lift but does not account for trim tab drag. The drag force of the trim tabs, D_T, is accounted for as follows:

$$D_f = D_{f\,Savitsky} + D_T \tag{12}$$

This modified drag force, combined with the effective weight and LCG change, allows full integration of the predicted trim tab forces into the Savitsky method.

Predicting Interceptor Performance

Dawson and Blount (2002) proposed a method to find an interceptor deployment that would give the same running trim reduction as a given trim tab. This method is based on a correlation equation that determines an effective interceptor angle for a given trim tab deployment angle,

$$\alpha_i = 0.175\alpha_t + 0.0154{\alpha_t}^2 \tag{13}$$

where α_t, is the trim tab angle of attack, and α_i is the theoretical equivalent interceptor deployment angle as shown in Figure 7. This equation is valid only when the span of the interceptor is chosen to match the given trim tab.

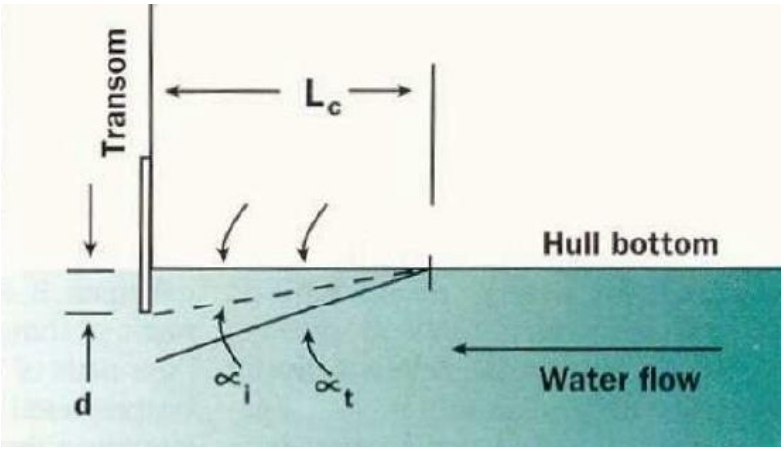

Figure 7. Interceptor and Trim Tab Equivalence Diagram (L_C=L_T)
Source: Dawson & Blount (2002)

This equivalence model can be used to find interceptor deployment with the following equation, where L_C is the projected longitudinal span of the trim tab, as shown in Figure 7.

$$d = L_c tan(\alpha_i) \tag{14}$$

This method is useful when considering replacing a trim tab with an interceptor; however, it cannot be used to predict directly the effect of an interceptor on a vessel. Because this equivalence method relies on angles, and Equation 13 is nonlinear, it cannot be integrated into Equation 6 without knowledge of a representative chord length. Dawson and Blount did not provide information on the chord-to-span ratios they examined to arrive at Equation 13.

Villa and Brizzolara (2009) used Blount and Dawson's equivalence equation when sizing the appendages for their CFD study. However, after the study, Villa and Brizzolara created their own equivalence equation, as follows, based on the correlation of their results.

$$\alpha_i = 0.102\alpha_t + 0.0134{\alpha_t}^2 \tag{15}$$

Villa and Brizzolara tested trim tabs with a span to chord ratio of 1.88. Thus, a representative equivalent trim tab span for a given interceptor could be calculated as follows.

$$L_T = \frac{\sigma}{2 \times 1.88} \tag{16}$$

Using this assumption and solving Equation 15 for α_t, the effects of an interceptor could be integrated into the Savitsky method using the Brown method of trim tab performance prediction. This approach is still not perfect, as it does not account for the difference in drag between interceptors and trim tabs. Neither Villa and Brizzolara nor Dawson and Blount provide predictions of the drag effects of an interceptor.

Predicting Pressures

Villa and Brizzolara (2009) explored the hydrodynamic performance of both interceptors and trim tabs through a systematic CFD analysis. In the study, a prismatic hard-chine vessel was modeled with a series of trim tabs at deployment angles ranging from 0° to 30°. From the analysis, they were able to extract the C_P curves at the centerline of the interceptor and trim tab. As expected, the study found a large increase in the pressure at the transom. For the 4° trim tab deployment, which is closest to the deployments explored in this research, the peak pressure coefficient was 0.19, as shown in Figure 8.

For the equivalent interceptor deployment (1.5 mm), the pressure coefficient at the transom was 0.4, as shown in Figure 9. The study also included testing to see the influence of speed on the C_P curves. It was found that, as speed varied, C_P remained approximately constant at each point along the bottom of the hull. This relationship is significant to predicting interceptor performance because it implies that the lift generated by an interceptor has a quadratic relationship with vessel velocity (Villa & Brizzolara, 2009).

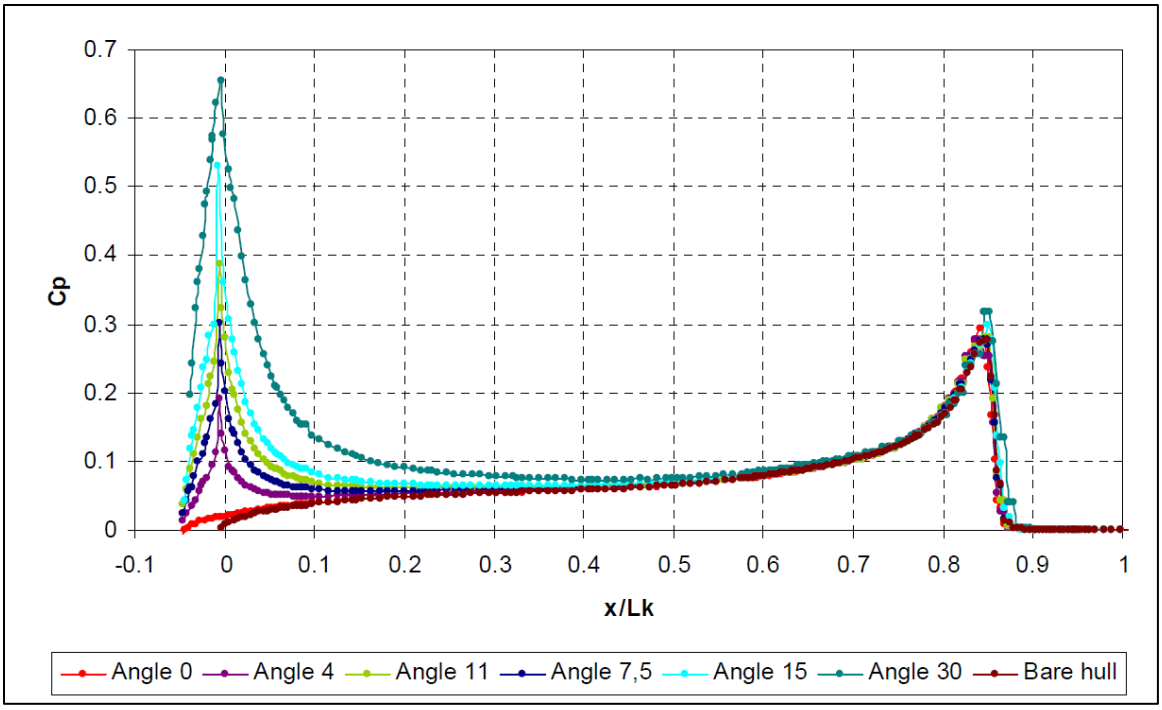

Figure 8. CFD Trim Tab C_P Curve
Source: Villa & Brizzolara (2009)

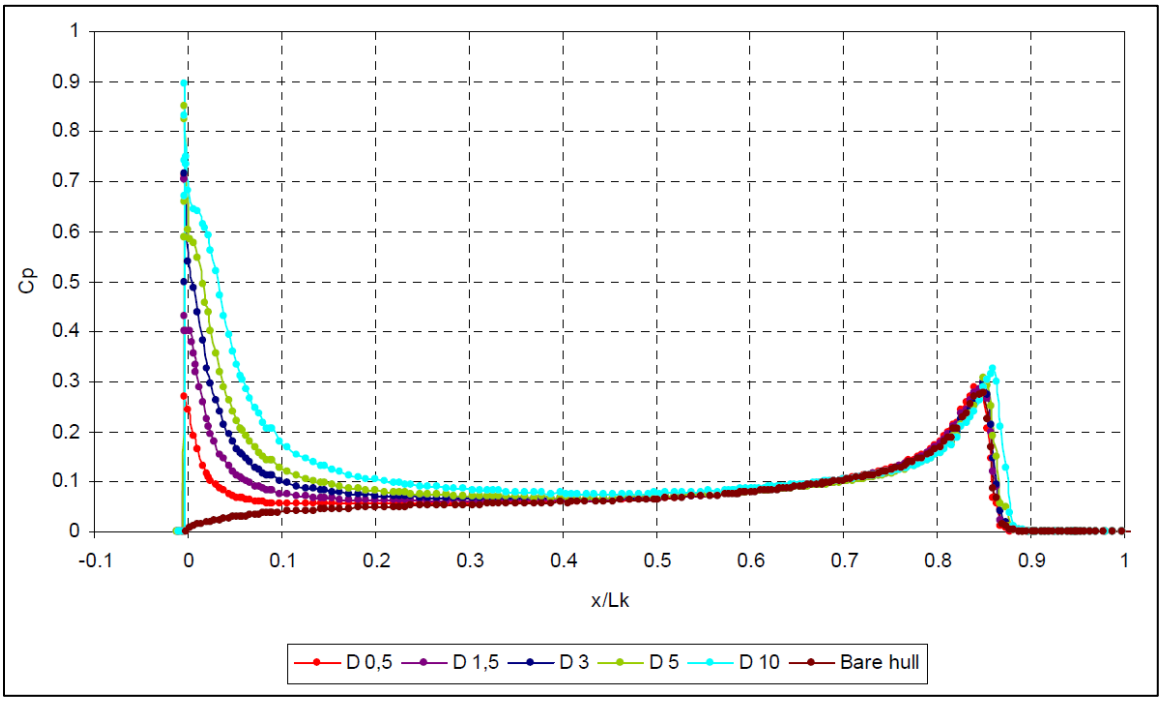

Figure 9. CFD Interceptor C_P Curve
Source: Villa & Brizzolara (2009)

Steen (2007) conducted model testing on a prismatic planing hull fitted with interceptors as well as several pressure cells. Throughout the model testing, trim and heave were fixed. The model (L_{OA}=2.5 m, B_P=0.5 m) was run at 4° of trim with a draft of 14.4 cm at the stern. Figure 10 shows a plot obtained by Steen of ***difference*** in pressure between bare hull and interceptors versus the longitudinal location of the pressure sensors, measured from the transom, for various deployments and speeds. Steen observed similar pressure distribution shapes as those calculated by Villa & Brizzolara using CFD.

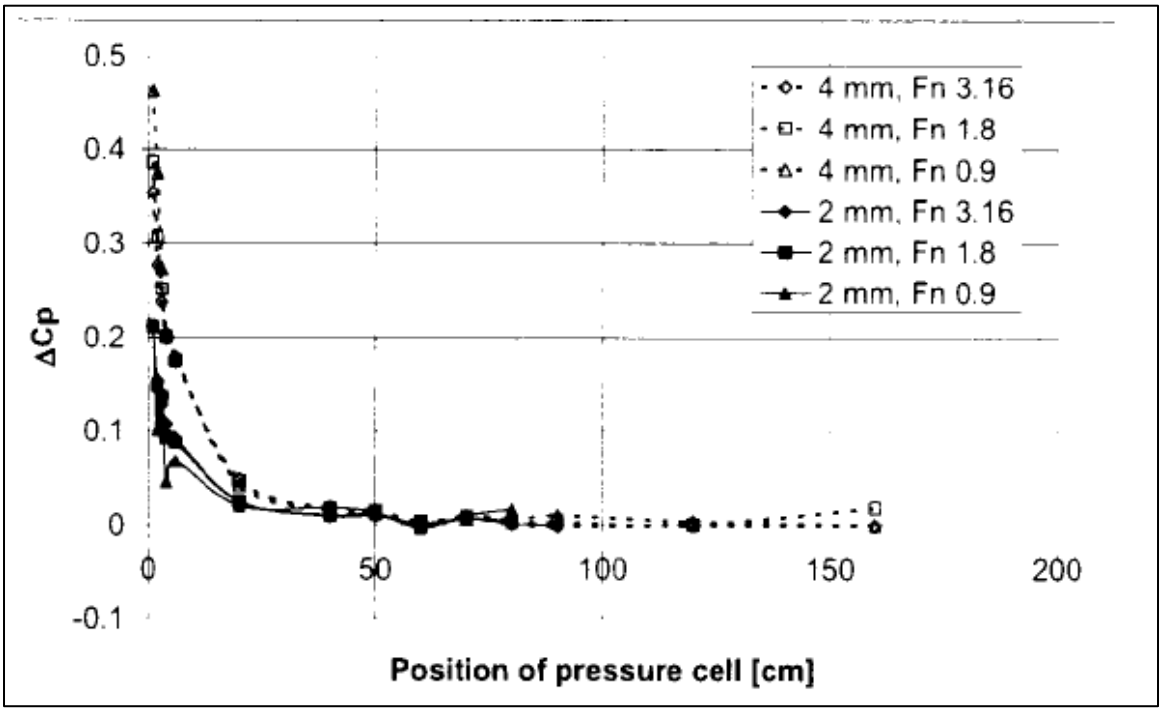

Figure 10. Model Test Interceptor C_P Curve
Source: Steen (2007)

Steen also attempted to capture a two-dimensional image of the pressure distribution near the interceptor using a pressure sensitive film; however, this approach was not reliable, as the film would often become entrained with water.

THEORY

STILL-WATER TESTING

The non-dimensional resistance of a model can be separated into two main components using Froude's Hypothesis, with a modification for the dynamic wetted surface area of high-speed craft (International Towing Tank Conference, 2008).

$$C_T = C_R + C_F * S/S_0 \quad (17)$$

C_T is the total resistance coefficient, C_R is the residuary resistance coefficient, and C_F is the frictional resistance coefficient. S_0 is the static wetted surface area of the model, and S is the dynamic wetted surface of the model. To measure the dynamic wetted surface area, an underside photo was taken for every run. Example underside photos from the Robinson Model Basin (RMB) at Webb Institute and the Davidson Laboratory (DL) at Stevens Institute of Technology are shown in Figure 11 and Figure 12. Quadratic interpolation was used to adjust for distortions in the photo due to the setup.

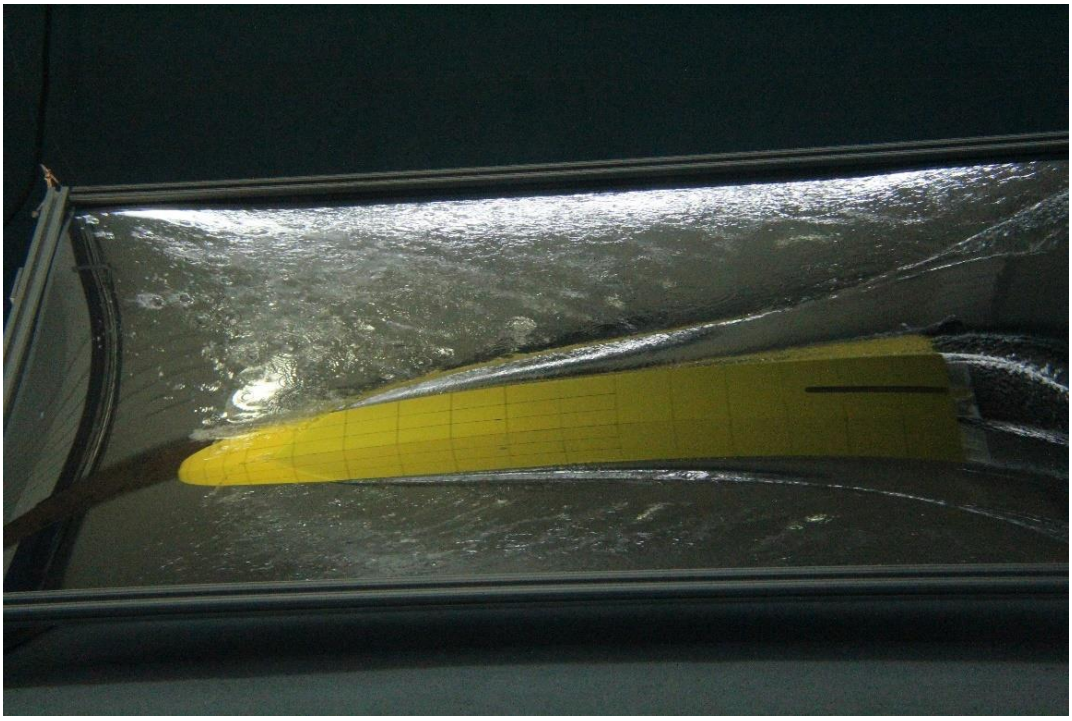

Figure 11. Underside Photo – Trim Tab C at RMB ($F_\nabla = 2.77$)

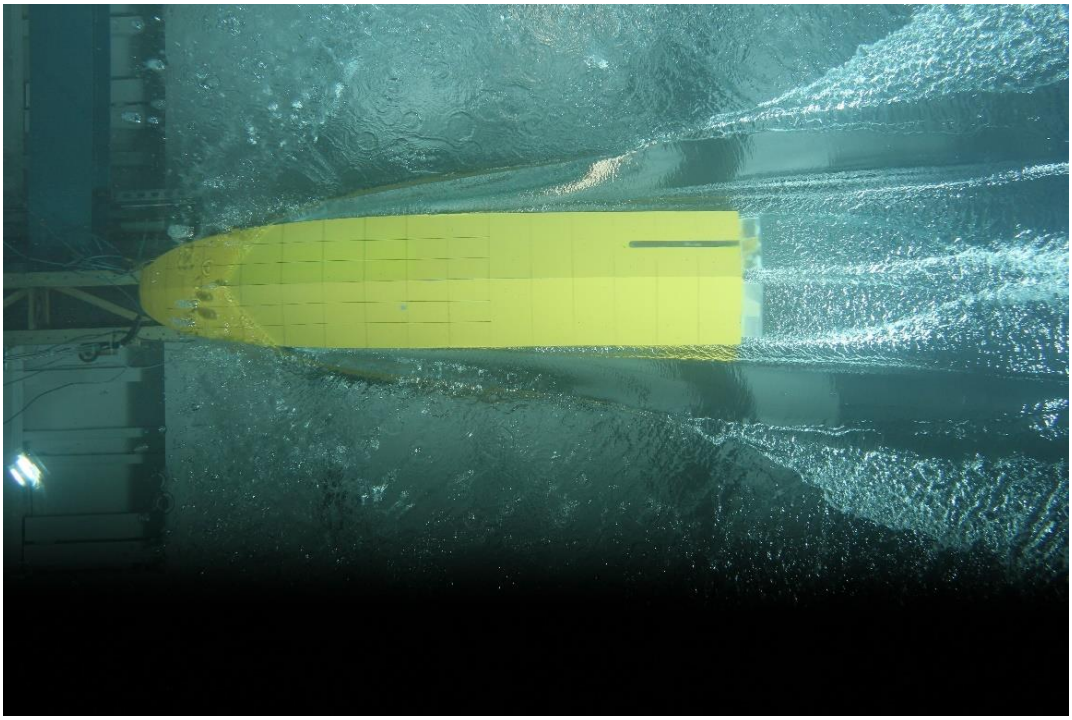

Figure 12. Underside Photo – Trim Tab C at DL ($F_\nabla = 2.77$)

The surface area of the transom lift devices was not included in surface area calculations, as the devices are appendages. Note that for this testing the effect of air resistance was ignored. The total resistance coefficient and residuary resistance coefficient are defined as follows:

$$C_T = \frac{R_T}{\frac{1}{2}\rho S_0 V^2} \tag{18}$$

$$C_R = \frac{R_R}{\frac{1}{2}\rho S_0 V^2} \tag{19}$$

R_T is the total resistance of the model, R_R is the residuary resistance of the model, ρ is the water density, and V is the model velocity.

The frictional resistance coefficient is calculated using the Schoenherr correlation line shown in Equation 20. The Schoenherr line is used to calculate the frictional resistance

coefficient rather than the ITTC 1957 line because the Schoenherr line is suggested by Savitsky (1964).

$$\frac{0.242}{\sqrt{C_F}} = \log_{10}(R_N \times C_F) \tag{20}$$

R_N is the Reynold's number of the model. Reynold's number for high-speed model testing is based on the mean wetted length of the model.

$$R_N = \frac{VL_m}{\nu} \tag{21}$$

ν is the kinematic viscosity of water, V is the model velocity and L_m is the mean wetted length or the average of the wetted chine and keel lengths. L_m is calculated from the underside photo taken for each run. As with surface area, the appendages are not included when calculating L_m.

PRESSURE COEFFICIENT

When discussing the pressure acting on a planing surface, it is advantageous to quantify the pressure in terms of a non-dimensional value. This value is known as the pressure coefficient, C_p,

$$C_p = \frac{P_T}{\frac{1}{2}\rho V^2} \tag{22}$$

where ρ is the density of the fluid, V is the vessel velocity, and P_T is the total gauge pressure acting on the surface of the model. The total pressure at a point on the surface of the hull is a summation of the hydrostatic pressure and the dynamic pressure. The setup of the pressure sensors in this testing measured only dynamic pressure, so hydrostatic pressure had to be calculated and added to the dynamic pressure to find the total pressure at any location on the surface of the hull.

$$P_T = P_D + \rho g z_n \tag{23}$$

P_D is the measured dynamic pressure and z_n is the running draft at that specific point on the surface of the hull.

To examine the pressure that is a direct effect of an appendage, an appendage-induced pressure coefficient, ΔC_p, is used. This coefficient is the difference in the appended C_p at a specific location and speed and the C_p at the same location and speed observed in bare-hull testing.

$$\Delta C_p = C_{p\_appended} - C_{p\_bare\ hull} \tag{24}$$

APPENDAGE EFFECTIVENESS

When comparing interceptors and trim tabs, it is important to define characteristics of effectiveness that can be used as modes of comparison. The first characteristic is each appendage's ability to reduce running trim at a given speed. Decreasing running trim is the direct effect of a transom lift device. To determine effectiveness, the running trim with the transom lift device is compared to the running trim of the vessel at the same speed without the transom lift device.

The second characteristic of effectiveness evaluates the intended effect of transom lift devices, resistance reduction. The residuary resistance coefficient with the transom lift device is compared to the residuary resistance coefficient without the transom lift device. The devices also influence frictional resistance, as they change the dynamic wetted surface area; however, frictional resistance scales differently from other forms of resistance. Residuary resistance, which excludes frictional resistance is used for comparison rather than total resistance.

UNCERTAINTY

Some tests and measurements were repeated multiple times so that the uncertainty associated with the results could be quantified. For uncertainty to be calculated, at least three separate measurements had to be taken. In the case of model tests, this involved running the same speed three times spaced out in the testing to attempt to capture any uncertainty dependent on time. The method to calculate uncertainty is shown below.

The average of the measurements, $\overline{x}$, was calculated by dividing the sum of the measurements by the number of measurements, n.

$$\overline{x} = \frac{\sum x_i}{n} \tag{25}$$

The sample standard deviation, s_x, was then calculated as shown in Equation 26.

$$s_x = \sqrt{\frac{\sum (x_i - \overline{x})^2}{n-1}} \tag{26}$$

The standard error, S, is defined by Equation 27.

$$S = s_x / n \tag{27}$$

Finally, the uncertainty, U, is determined.

$$U = 3\,S \tag{28}$$

DESIGN AND CONSTRUCTION

HULL MODEL

The hull form used in this thesis is part of the Leshnover Group C series of models. The models all had a constant deadrise angle of $\beta = 20°$, with varying buttock curvatures at the bow. The after-part of the models is prismatic with a transom stern. The Leshnover series was specifically designed for flying boats, and in 1953 Leshnover published data to

study the effects of the diving angle on the hull's hydrodynamic performance (Blount, 2014). The specific model used for this thesis, the C-1, was one of two previously used in the Webb Institute thesis by Gavel (2016). This model has an unusual bow, but the bow should have a minimal effect on the relative performance of the transom lift devices at the hump speeds this thesis focuses on.

The original C-1 hull form was slightly modified by Gavel to aid in model testing. The freeboard was increased with the anticipation of increased spray as well as an expected rooster tail at the stern. Figure 13 shows the model, as modified by Gavel.

Figure 13. Modified Leshnover C-1 Model
Source: Gavel (2016)

The principal geometric characteristics of the model used in this thesis are shown in Table 1.

Table 1. Principal Geometric Characteristics of Model

Characteristic	Value	Units
L_{OA}	5.00	ft
L_{WL}	4.48	ft
B_{OA}	1.00	ft
B_p	1.00	ft
β	20	deg

When performing low-speed model tests, it is standard practice to add turbulence stimulators near the bow to create a boundary layer that better matches the full-scale craft. However, with high-speed testing, it is not always feasible to add the stimulators to the

model. Because the trim and sinkage of the model change significantly at high speeds, it is not possible to choose one location for the stimulators that will work for all speeds. Furthermore, the speeds this thesis focuses on are high enough that the effect of turbulence stimulators would be small, as the smallest Reynold's numbers from testing were about two million. For this thesis, no turbulence stimulators were used.

The properties of the model as tested in the bare-hull condition are shown in Table 2. The LCG location as well as displacement were targeted to match LCG% and loading coefficient values recommended for model testing by Blount (2014).

Table 2. Characteristics of Model as Tested

Characteristic	**Value**	**Units**
Draft, T	0.30	ft
Δ	47.0	lbf
∇	0.76	ft^3
Projected Area, A_p	4.58	ft^2
Planing Length, L_p	5.00	ft
Center of Projected Area, C_{AP}	2.32	ft
Loading Coeff., $A_p/V^{2/3}$	5.5	
LCG	25.5	in
LCG%, $(C_{AP}\text{-LCG})/L_p$	4%	
Waterplane Area, A_{WP}	4.21	ft^2
Waterplane Coeff., C_{WP}	0.94	
Static Wetted Surface, S_0	5.42	ft^2

PRESSURE TAPS

A pressure manifold with eight pressure taps was 3D printed and then epoxied into a cutout made in the starboard side of the model. The spacing of the taps was designed to give a high density of measurement points near the transom. Each tap is $^1/_{16}$-inch diameter, and there are two rows of pressure taps spaced ¼-inch apart. The alternating pattern between the two rows was chosen to minimize the effect of a tap on the pressure observed

at the next downstream tap. Figure 14 shows the location and arrangement of the pressure taps. The longitudinal location of each tap, measured from the transom, is shown in Table 3.

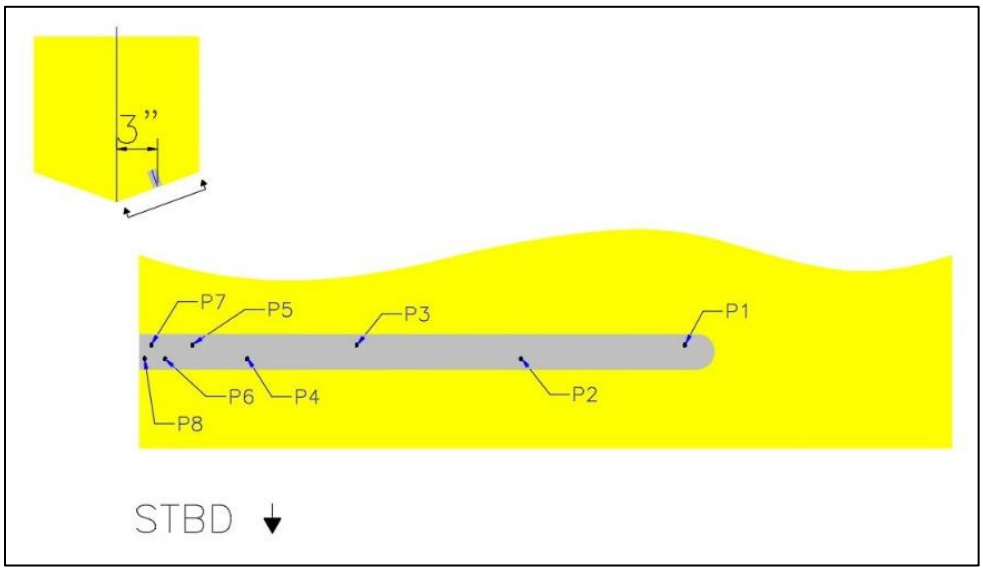

Figure 14. Pressure Manifold Layout

Table 3. Pressure Tap Locations – Manifold

Pressure Tap	Longitudinal Distance from Transom, Inches
P1	9 31/32
P2	6 31/32
P3	3 31/32
P4	1 31/32
P5	31/32
P6	15/32
P7	7/32
P8	3/32

TRIM TABS

Three different sets of trim tabs were created for testing with varying angles of deployment. The other principal dimensions, span and cord, were chosen using an analysis of publicly available industry sizing recommendations. For sizing purposes, the dimensions of the model were scaled up to a 25-ft vessel. For this notional vessel, a trim tab was

chosen that fell within the recommended area and had a typical aspect ratio. Converting these dimensions back to model scale, resulted in a span of five inches and a chord of two inches.

Blount suggests that transom lift devices should be sized to decrease the largest running trim of the vessel by about 1 to 1.5° (2014). When the trim tabs were being designed, there were no test data to determine at what speed the largest running trim occurred. The Savitsky method predicted that $F_\nabla = 2.77$ (15.0 ft/s) would be the speed with the largest running trim, so this speed was selected as the design speed. The Savitsky method, as modified by Brown, for the trim tab span and chord dimensions chosen, was used to determine that an attack angle of 4.2° would decrease the running trim at $F_\nabla = 2.77$ by 1.5°, meeting Blount's suggested size. To cover a range of deployments around and less than 4.2°, the deployment angles of 1°, 3°, and 5° were chosen. The principal dimensions for the trim tabs chosen are shown in Table 4.

Table 4. Trim Tab Geometry

Characteristic	**Tab A**	**Tab B**	**Tab C**
Angle of Attack, deg	1.00	3.00	5.00
Span, in	5.00		
Chord, in	2.00		

These trim tabs were 3D printed and were attached to the model by four screws (Figure 15). In addition to measuring pressure along the hull, pressure along the trim tabs was also measured. To do this, the starboard trim tabs were designed with three pressure taps along their bottom, as shown in Figure 16. The longitudinal location of each tap, measured from the transom along the bottom face of the tab, is shown in Table 5.

Figure 15. Trim Tabs as Mounted

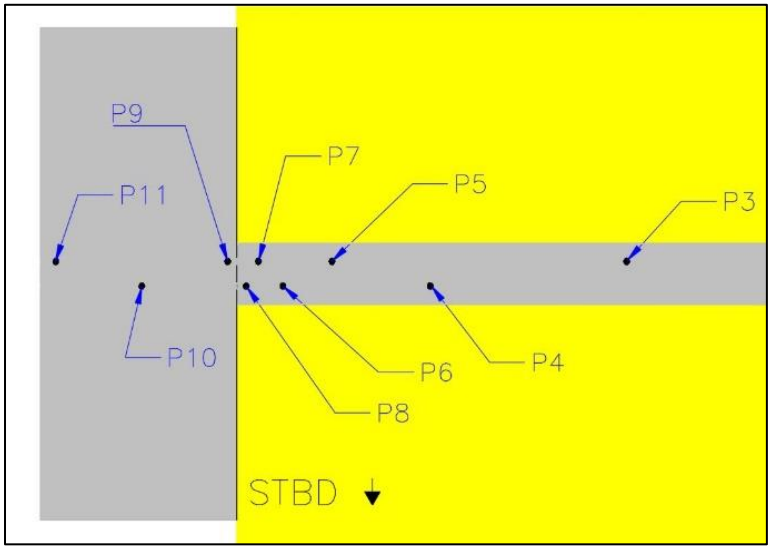

Figure 16. Starboard Trim Tab Pressure Tap Layout
Note: looking from above

Table 5. Pressure Tap Locations – Trim Tabs

Pressure Tap	**Distance from Transom, Inches**
P9	-3/32
P10	- 31/32
P11	-1 27/32

When the trim tabs were first tested on the model, an unexpected longitudinal distribution of pressure was observed. Additionally, large uncertainty was observed in the pressure measurements. It seemed that the gap between the trim tabs and the model was large enough to allow a relief of pressure and thus a discontinuity in the pressure distribution. To prevent this pressure relief, narrow pieces of tape were applied at the interface of the model and each of the trim tabs for all trim-tab testing. A comparison of the pressure distributions with and without the tape is shown in Figure 17.

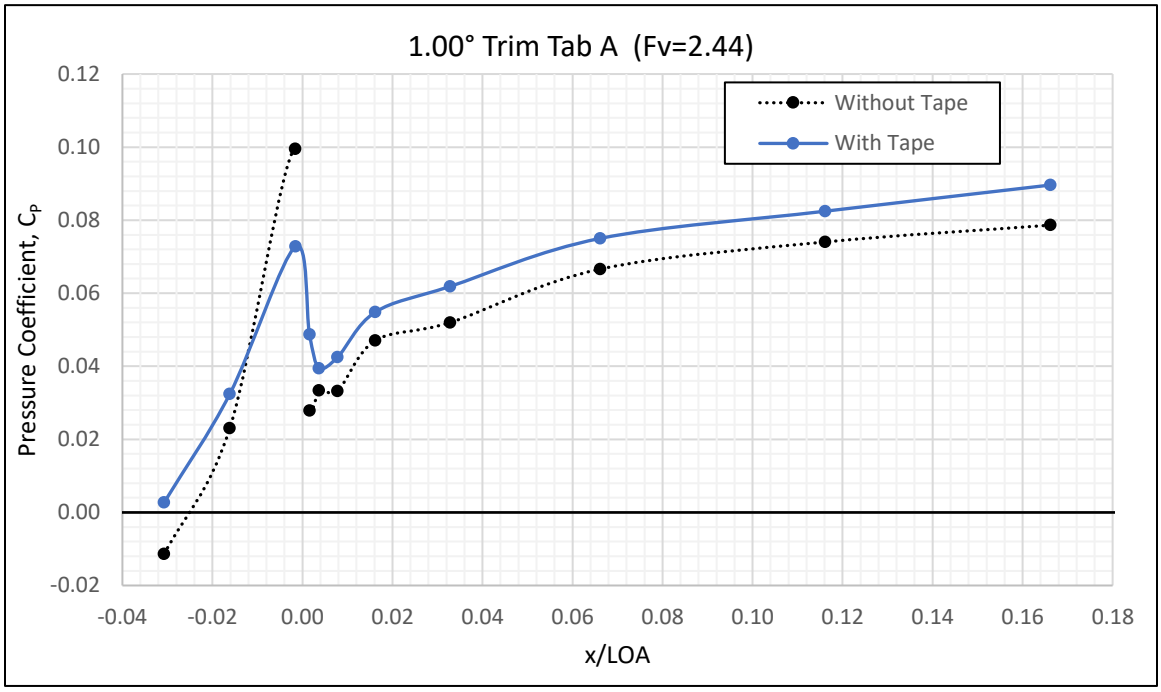

Figure 17. Effect of Pressure Relief on Trim Tab Pressure Distribution

INTERCEPTOR PLATE

The interceptor plate (Figure 18) was constructed from an ¼-inch acrylic plate. The span of the interceptors was the same as the trim tabs, five inches. The interceptor plate could slide vertically and be tested at multiple deployments ranging from 0 to 0.5 inches. This was accomplished using six screws placed in slots on the interceptor plate and screwed into the transom of the model.

Figure 18. Interceptor Plate

As with trim tabs, the interceptor deployments were selected based on a design speed corresponding to $F_\nabla = 2.77$. Three interceptor deployments were chosen such that the change in trim of each of the deployments would be equal to that of each of the trim tab deployments. To do this, preliminary testing was done at $F_\nabla = 2.77$ to determine the running trim with each of the three trim tabs attached, the interceptor plate's deployment was varied, and then tested at the same speed until three deployments were found that caused the same running trim as each of the three trim tabs. Once a deployment was found, a hole was drilled into the model through the interceptor plate, which allowed a set pin to keep the interceptor at this deployment. Appendix A discusses measuring the deployment of the interceptors and the uncertainty analysis performed. The deployments chosen are shown in Table 6.

Table 6. Interceptor Geometry and Uncertainty

Characteristic	**Deployment A**	**Deployment B**	**Deployment C**
Deployment, in	0.023±0.005	0.036±0.005	0.045±0.004
Span, in	5.00		

Because of multiple differences in the model setup between this preliminary testing and later testing, the running trim measured during the preliminary testing does not

precisely match later testing, which included $F_\nabla = 2.77$. Rather, the preliminary testing acted as a method to choose reasonable interceptor deployments that would be closely comparable to the trim tab deployment angles chosen.

PROCEDURE

TEST MATRIX

The model was tested at a displacement of approximately 47.0 lbs. and an LCG of 25.5" from the transom. To reach this displacement, ballast was added to the model. First, the model was weighed out of the water with all the equipment connected during bare hull testing as well as two extra weights on the transom, one equal to the weight of the interceptor plate and connecting hardware and the other equal to the weight of the trim tabs and connecting hardware. The two equivalent weights are shown in Figure 19. The results of the ballasting are shown in Table 7 and Table 8 for the two tow tanks the model was tested in, RMB and DL. Details of the condition of the model as tested are provided in Appendix B.

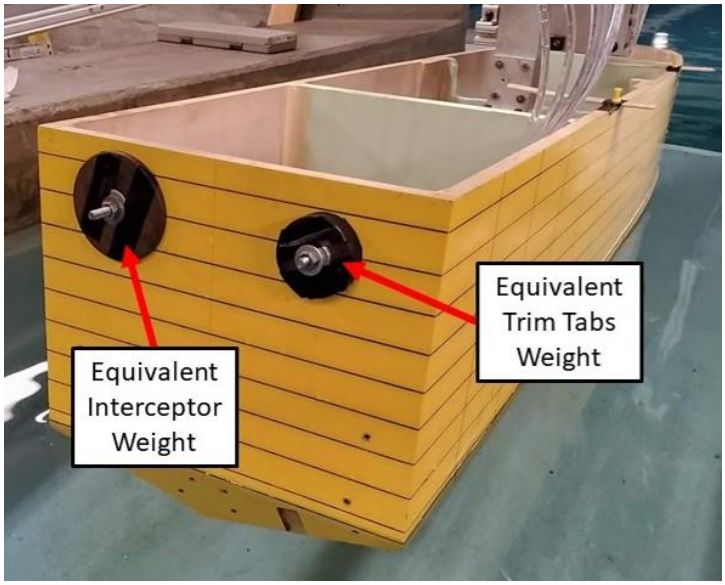

Figure 19. Equivalent Appendage Weights

Table 7. Bare Hull Ballasting – RMB

Item	Weight (lbs.)
Free to Heave Apparatus	1.080
Bare Hull, Fixed Fwd. Weight, Water Tubing, Ballast Pegs, and Extra Equipment	35.650
Equivalent Trim Tab Weight	0.525
Equivalent Interceptor Weight	0.520
Ballast	
Fwd. Peg	2.625
Aft Peg	6.585
TOTAL	**46.985**

Table 8. Bare Hull Ballasting – DL

Item	Weight (lbs.)
Free to Heave Apparatus	8.020
Bare Hull, Water Tubing, Ballast Pegs, and Extra Equipment	34.365
Equivalent Trim Tab Weight	0.525
Equivalent Interceptor Weight	0.520
Ballast	
Fwd. Peg	2.790
Aft Peg	0.810
TOTAL	**47.030**

When testing the hull in an appended configuration, removal of the respective equivalent appendage weight accounted for the additional weight of the appendage added to the model; however, it did not account for the additional buoyancy the appendage added. When running, the transom of the model would be ventilated, so the additional buoyancy of the appendage would no longer act on the hull. However, the added buoyancy of the appendages affects the "zero" measured before each run and subtracted from the run data. A correction factor was calculated to remove this effect on measured running trim and sinkage. The calculations for the buoyancy correction for each appendage are provided in Appendix C.

The model was tested at a range of speeds from 6 ft/s to 17 ft/s ($F_\nabla = 1.11$ to 3.14) in seven different configurations. RMB is only capable of speeds up to 15 ft/s, so testing at higher speeds was performed at DL. Some tests at speeds slower than 15 ft/s were performed at DL to confirm that the results between the two model basins were comparable. At DL, interceptor deployments were adjusted within the fit of the set pin to attempt to match earlier RMB trim data. The seven configurations tested, with their associated run name abbreviations, are as follows:

- BH The model with no appendages (bare hull)
- TA The model with trim tab A connected (1° deployment angle)
- TB The model with trim tab B connected (3° deployment angle)
- TC The model with trim tab C connected (5° deployment angle)
- IA The model with interceptor plate at deployment A (0.023")
- IB The model with interceptor plate at deployment B (0.036")
- IC The model with interceptor plate at deployment C (0.045")

For every run, trim, sinkage, resistance, and pressure at each manifold pressure tap were recorded. Additionally, for the trim tab runs, the pressure at the three additional taps on the starboard tab were recorded. To facilitate uncertainty analysis, certain speeds were tested three times.

TANK TESTING EQUIPMENT

Testing for this thesis was conducted at RMB and DL. Although much of the procedure for model testing is consistent, there are several differences that are highlighted.

Pressure Sensors

At both model basins, a series of eleven Motorola MPX5010DP pressure sensors were mounted to the tank carriage to measure dynamic pressure at each of the pressure taps. The sensors have a pressure and a vacuum port, and the sensors measure the differential pressure between these two ports. The pressure ports were connected to the pressure manifold and starboard trim tab through 0.175" diameter vinyl tubes, which were filled with water. Care was taken to avoid bubbles of air in the tubes. The vacuum ports were connected to a common manifold filled with air.

After calibration and before testing, a vacuum was pulled on the vacuum manifold that was enough to offset the head of the water in the tubes connected to the pressure ports. This ensured that the differential pressure acting on the sensors was always greater than zero. The vacuum leaked during testing, so it was occasionally re-pulled. Subtracting a zero-speed run taken before each actual run sufficiently accounted for the changing vacuum pressure, as the change during the run itself was inconsequential.

For calibration, a series of valves allowed the pressure ports of all the sensors to be isolated from their sensing tubes and connected to a common manifold, thus allowing all sensors to be calibrated at once.

Camera

To capture the dynamic wetted surface area and wetted lengths, a camera and a mirror were used to take photos of the model as it passed by. At RMB, the mirror was placed at a 45˚ angle and positioned on the bottom of the tank on centerline. The camera was oriented in view of the mirror through an acrylic window in the side of the tank and was wired to take a photo the instant the model passed over the mirror. At DL, the camera was placed

within a glass box that was partially submerged at the side of the tank, and the mirror was inclined such that it gave a view straight up at the centerline of the model.

Trim and Sinkage Measurement

At RMB, two Micro-Epsilon optoNCDT 1302 laser extensometers were used to record both the trim and sinkage of the model. They have a percentage uncertainty between 0.12 and 0.2 percent (Gavel, 2016). The lasers were attached to the carriage, one forward and one aft of the mounting point. Wood strips were mounted on the edge of the model in way of the laser. The lasers are a known distance apart, allowing calculation of trim as well as sinkage.

At DL, an inclinometer was connected to the model, which was used to measure trim. For sinkage, the heave staff was connected by a string to a rotational variable differential transformer, which rotated as the model translated up and down.

Force Block

The model was connected to the carriage through a force block. This block allowed measuring the resistance of the model. At RMB, the signal from the force block, made by Hydronautics, was run through a signal conditioner, made by Validyne Engineering. A similar setup was used at DL.

CALIBRATION

Pressure Sensor Calibration

The pressure sensors were calibrated both before and after each set of tests, and the combined calibration values were used to convert the output voltage of each sensor into a pressure. To calibrate the sensors, a calibration stand was created that allowed for known pressures to be placed on the pressure sensors. Figure 20 shows a simplified schematic of

the pressure-sensor calibration stand. The stand consists of a vertical mast measuring six-feet in height, with set-point holes at one-foot increments. One end of a tube, filled with water, was connected vertically to a cross piece that moved up and down on the mast. The other end of the tube was attached to a stationary vertical piece with a ruler. For calibration, the stand was leveled before it was used.

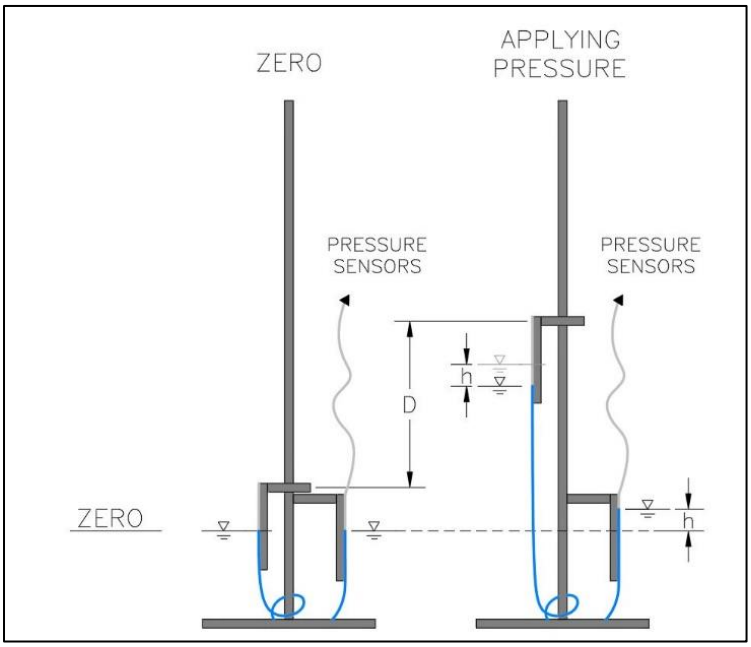

Figure 20. Pressure Calibration Stand

The line connecting the calibration stand to the pressure sensor manifold was filled with air; *h* was measured at each calibration step to account for the air's compression. The pressure applied to the sensors, $P_{calibration}$ was calculated as follows:

$$P_{calibration} = \rho g(D - 2h) \tag{29}$$

D is the distance the movable cross piece is above its original condition, ρ is the density of the water taken from the tank, and g is gravity. As the amount of air in the tube varied slightly, the actual range of pressure the sensors was calibrated for varied slightly for each calibration; however, all calibrations covered at least 0 psi to 1.45 psi with increments of about 0.36 psi.

Force Block Calibration

To calibrate the force block, known weights were attached to the model via a string and pulley system. For calibration, weights from zero to ten pounds were applied to the model at increments of two pounds. The angle from vertical of the string connecting the weight to the model was accounted for. The output voltage at each weight increment was used to create a slope and offset relating horizontal force to sensor voltage. The force block was calibrated both before and after each group of tests.

Trim and Sinkage Calibration

Before installation at RMB, the lasers were calibrated using a Bridgeport milling machine. The distance between the laser and the pivot point was measured so that sinkage could be calculated about the pivot point. Tare values were taken before each series of tests, and these reference values were then used to calculate sinkage and trim.

The inclinometer used at DL was calibrated before being attached to the model using plates of known inclination and a level. The rotational variable differential transformer used to measure sinkage was calibrated by propping up the sinkage staff with blocks of known thickness.

RESULTS

The data for all runs and the associated coefficient calculations are attached in Appendix D. A summary of the data collected is attached in Appendix E for resistance, trim, and sinkage and Appendix F for pressure. Unless otherwise noted, data for speeds less than and including $F_{\nabla} = 2.77$ (15.00 ft/s) are based on tests at RMB, and higher speeds are based on tests at DL.

ERROR ANALYSIS

The calculations for uncertainty in measured resistance, trim, sinkage, surface area, and each of the pressure sensors are attached in Appendix G. The average uncertainty in absolute units and percentages for all measurements excluding pressure is shown in Table 9.

Table 9. Average Uncertainty

	R_t lbf	**Trim** deg	**Sinkage** in	**S** ft^2
Average Uncertainty	0.052	0.023	0.013	0.01
Average %Uncertainty	0.59%	0.48%	2.09%	0.14%

Resistance, trim, and surface area all have very small uncertainties. Sinkage has a higher uncertainty, especially for tests at DL; however, the effect of this higher uncertainty on the results is negligible. Total pressure is the only result affected by errors in measuring sinkage, as sinkage is used in conjunction with trim to calculate hydrostatic pressure, which is added to the measured dynamic pressure to calculate total pressure. Assuming a water density of 1.93 slugs per cubic-foot, an error of 0.013 inches of sinkage would only lead to an error in calculated total pressure of 0.0005 psi, which is significantly less than the uncertainty observed in total pressure (see Table 10). Therefore, the two percent uncertainty of sinkage can be considered negligible.

Although trim has a low average uncertainty, there were several speeds at which a higher uncertainty was observed. The highest uncertainty in trim as a percentage was associated with F_∇ = 1.48 in the bare hull condition, with an uncertainty of 0.125 degrees, or 3.3% of the average. The rest of the bare-hull trims have low uncertainty, so the high uncertainty at F_∇ = 1.48 is not a major concern, especially as it is in a slower speed range that was not investigated in detail.

The second highest uncertainty is of more concern. F_∇ = 2.45 with an interceptor deployment of 0.036" had a trim uncertainty of 0.097°, or 2.4% of the average. Additionally, the next highest and lowest speeds on which uncertainty was calculated for this configuration both have elevated uncertainties, with 1.5% for F_∇ = 2.31 and 0.9% for F_∇ = 2.68. It is possible there is some sort of instability at these speeds for the 0.036" interceptor deployment. Unusual pressure distributions discussed in the *Pressure* section of results support this theory.

Table 10. Average Uncertainty – Pressure

	Total Pressure (psi)										
	P1	**P2**	**P3**	**P4**	**P5**	**P6**	**P7**	**P8**	**P9**	**P10**	**P11**
Average Uncertainty	0.002	0.003	0.003	0.004	0.003	0.003	0.003	0.004	0.004	0.004	0.005

Table 10 shows the average uncertainty of pressure. Percent uncertainty is not reported for pressure, as pressure is relative and many pressures readings approach zero, which artificially inflates the percent error.

TRIM REDUCTION

The trim recoded for the bare-hull configuration is shown in Figure 21. It was expected that trim would transition from increasing to decreasing somewhere within the speed range tested, defining the hump region; however, through all speeds tested, the bare-hull running trim increased with speed. Based on how trim seems to begin to level out after F_∇ = 2.4, it would seem the point of max trim would be near F_∇ = 3.3 at a running trim of about 6.8°, but this is an extrapolation.

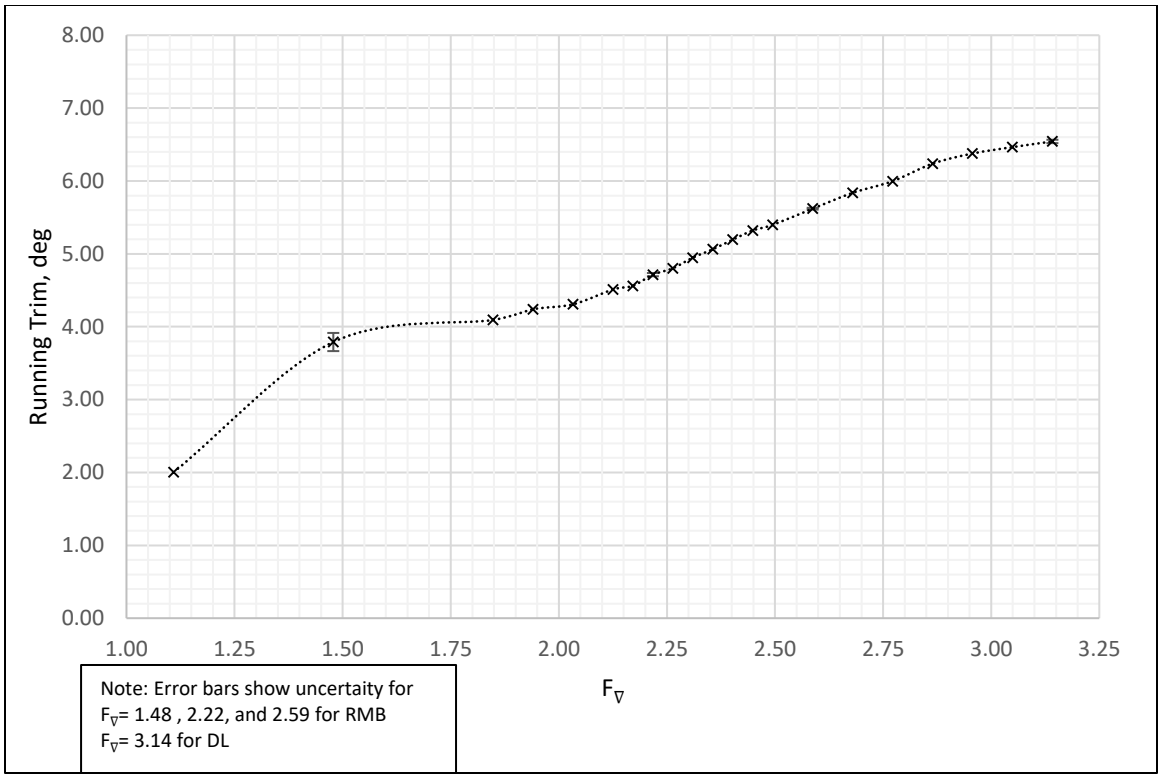

Figure 21. Running Trim - Bare Hull

The direct effect of trim tabs and interceptors is to decrease running trim compared to bare hull, so the reduction in running trim was calculated by subtracting the running trim of each appendage configuration from the bare hull running trim shown in Figure 21. Thus, Figure 22 and Figure 23 show the ***reduction*** in running trim due the trim tab deployments and the interceptor deployments respectively.

For trim tabs, reduction in running trim increases with speed to a point, after which it remains constant for a range, then begins to decrease, though for the speeds tested this decrease was observed for only the smallest deployment. For the smallest deployment, 1.00°, the plateau begins around F_∇ = 1.75 and continues until 2.75, and the trim tabs are unable to reduce trim by more than 0.8°. For the highest angle of attack, 5.00°, the plateau begins around F_∇ = 2.65 and remains relatively constant at the fastest speed tested. The deployments tested could not reduce trim by more than 2.3°.

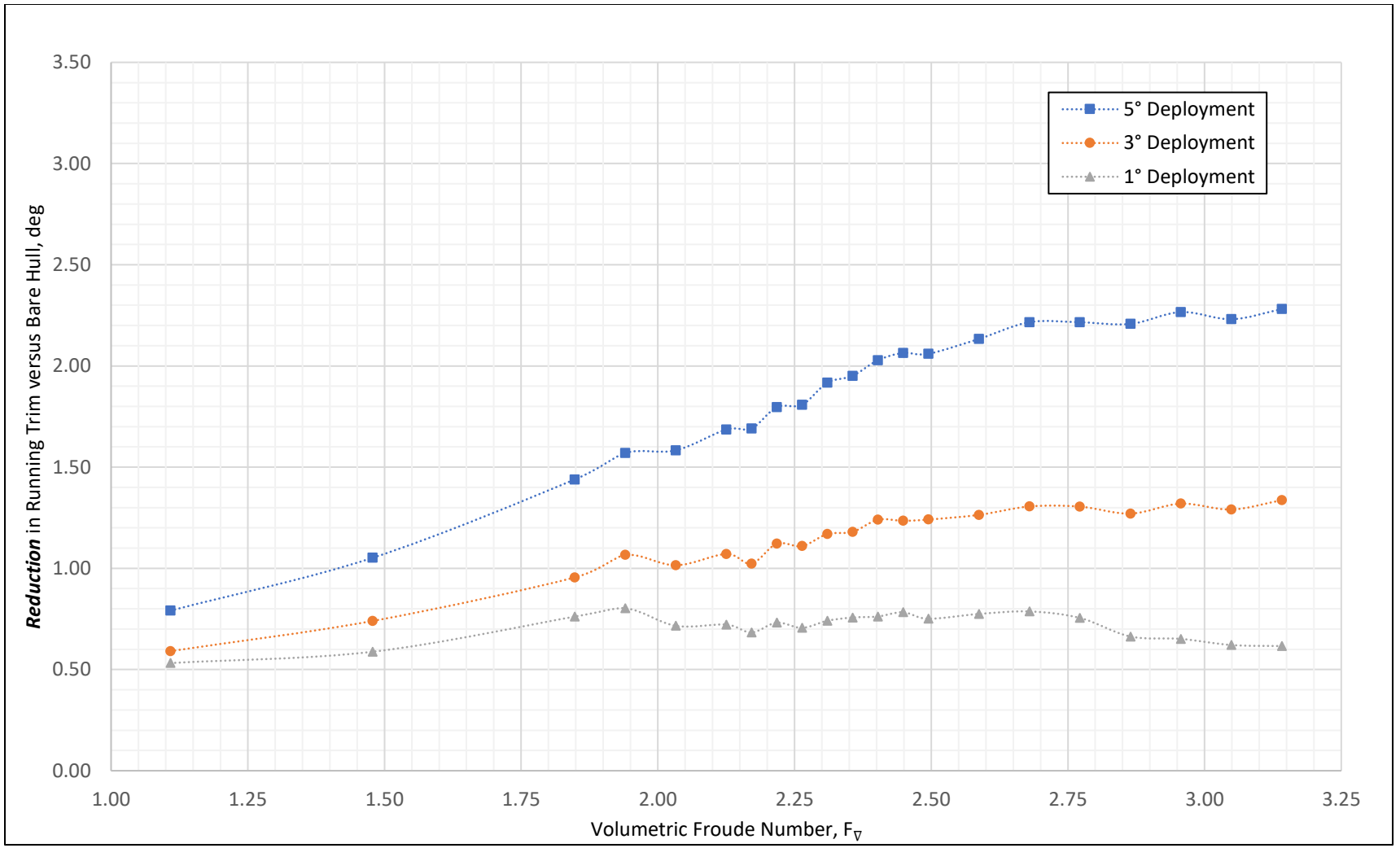

Figure 22. Reduction in Running Trim - Trim Tabs

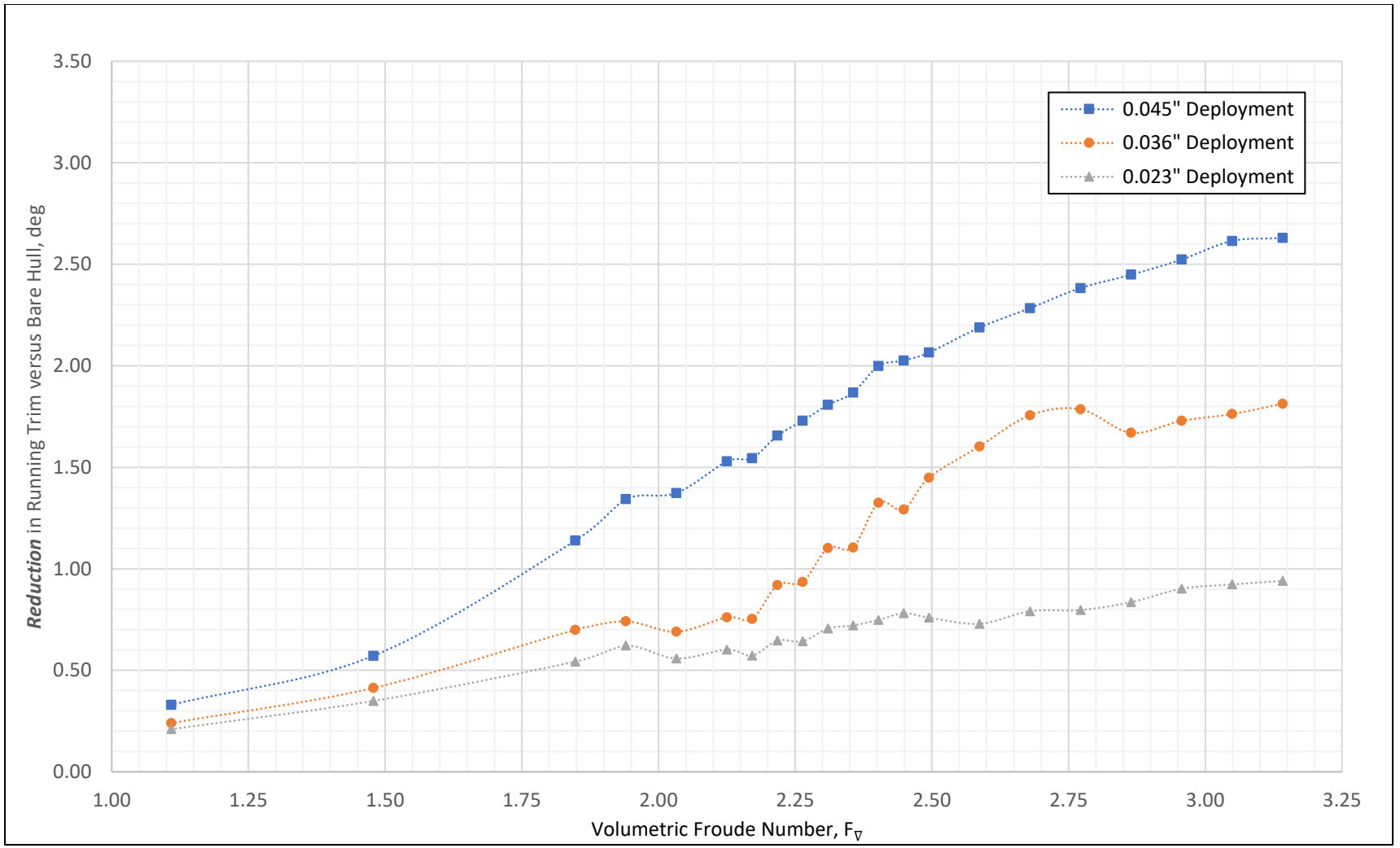

Figure 23. Reduction in Running Trim - Interceptors

The same plateau shape is not observed for interceptors over the speeds tested. Rather, the reduction in running trim caused by the interceptors generally increases with speed. The slope of the reduction in running trim versus speed increases with the larger interceptor deployments. As there is no plateau observed, the reduction caused by each of the deployments will likely continue to increase at higher speeds. At the speeds tested, the interceptors were able to cause a larger trim reduction than the trim tabs.

The trim reduction caused by the 0.036" interceptor deployment shows large variation compared to the other two deployments between F_∇ = 2.15 and 2.80, and had larger uncertainties, as discussed in the *Error Analysis* section. This anomaly is investigated in detail in the *Pressure* section of the *Results*.

RESISTANCE

The residuary resistance for the bare-hull configuration is shown in Figure 24. As expected for these speeds, the residuary resistance coefficient decreases with speed.

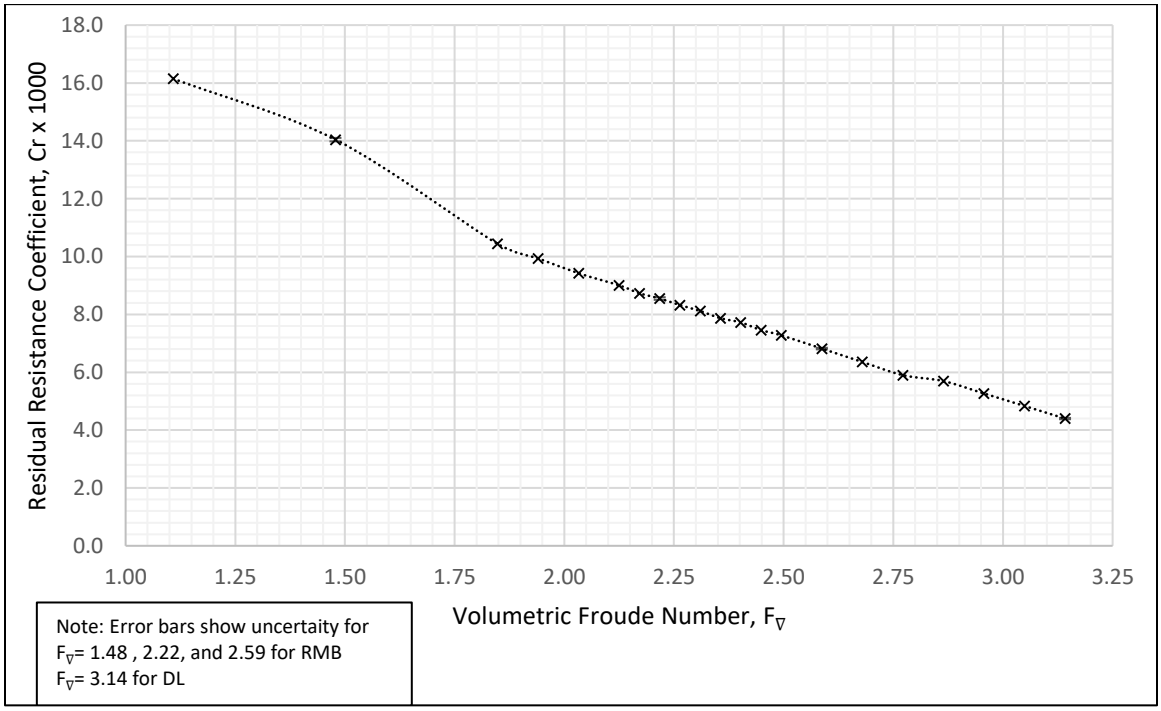

Figure 24. Resistance - Bare Hull

The effectiveness of interceptors and trim tabs can be judged on their ability to reduce the resistance from bare hull trim. Figure 25 and Figure 26 show the ***reduction*** in resistance observed for trim tabs and interceptors, respectively. There is some noise in the resistance reduction, as percent uncertainty increases when looking at the difference in resistance rather than the absolute resistance. To highlight the trend in resistance reduction, a cubic regression has been fit to the data.

Increasing the deployment angle of the trim tabs increases the magnitude of the resistance reduction, but the peak and zero crossing speeds remain the same. Presumably, there is a limit at which increasing the deployment no longer decreases resistance; however, the deployments tested were not large enough to observe this limit.

The plot of interceptor resistance reduction is similar to the trim tabs; however, there are differences. The most significant difference is that the largest percent resistance reduction is observed at around $F_{\nabla} = 2.0$ rather than 1.7 observed for trim tabs. After this peak, the decline in resistance reduction is more pronounced than was observed for the trim tabs. The point of zero resistance reduction is shifted to slightly higher speeds, approximately $F_{\nabla} = 2.7$.

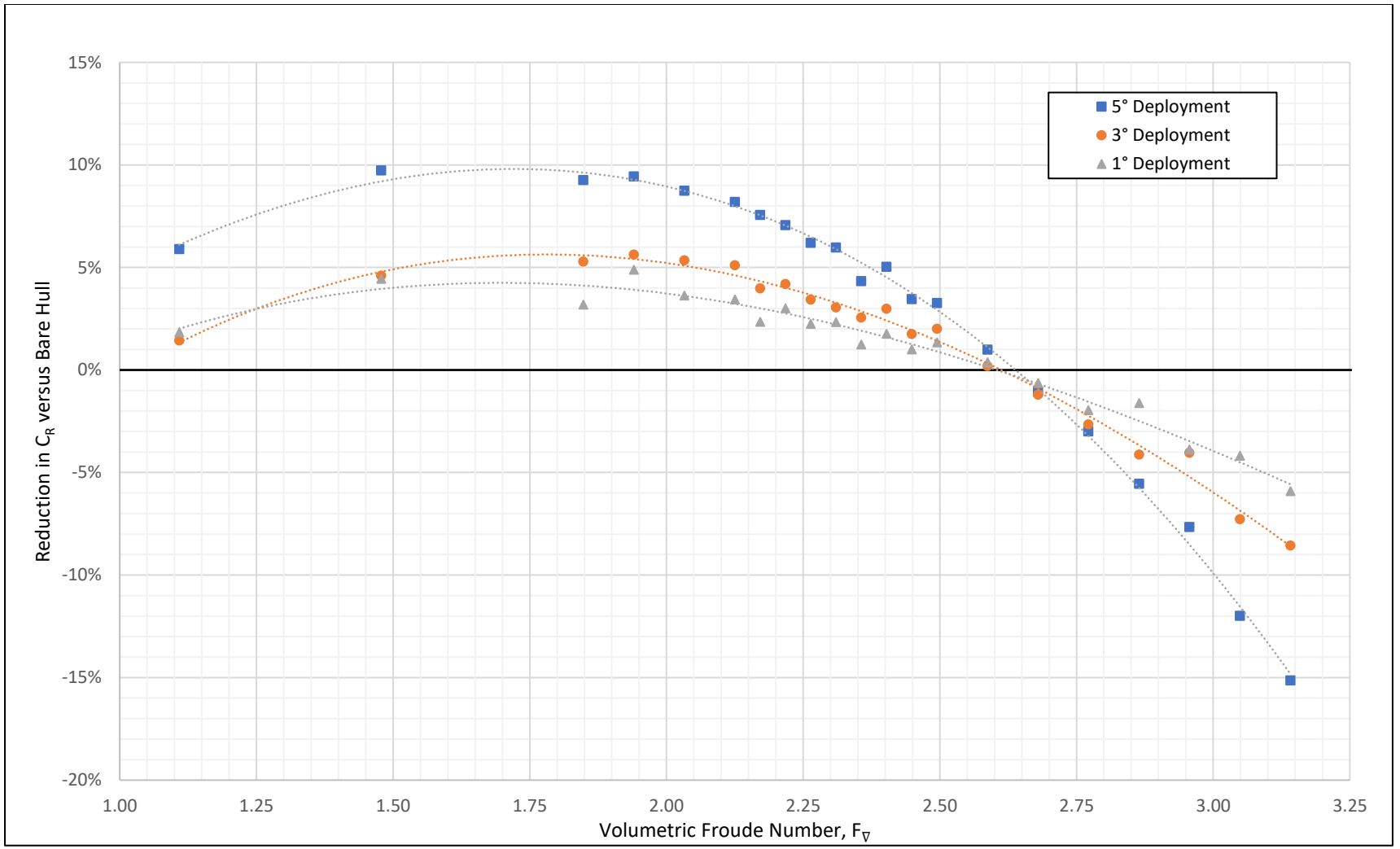

Figure 25. Reduction in Resistance - Trim Tabs

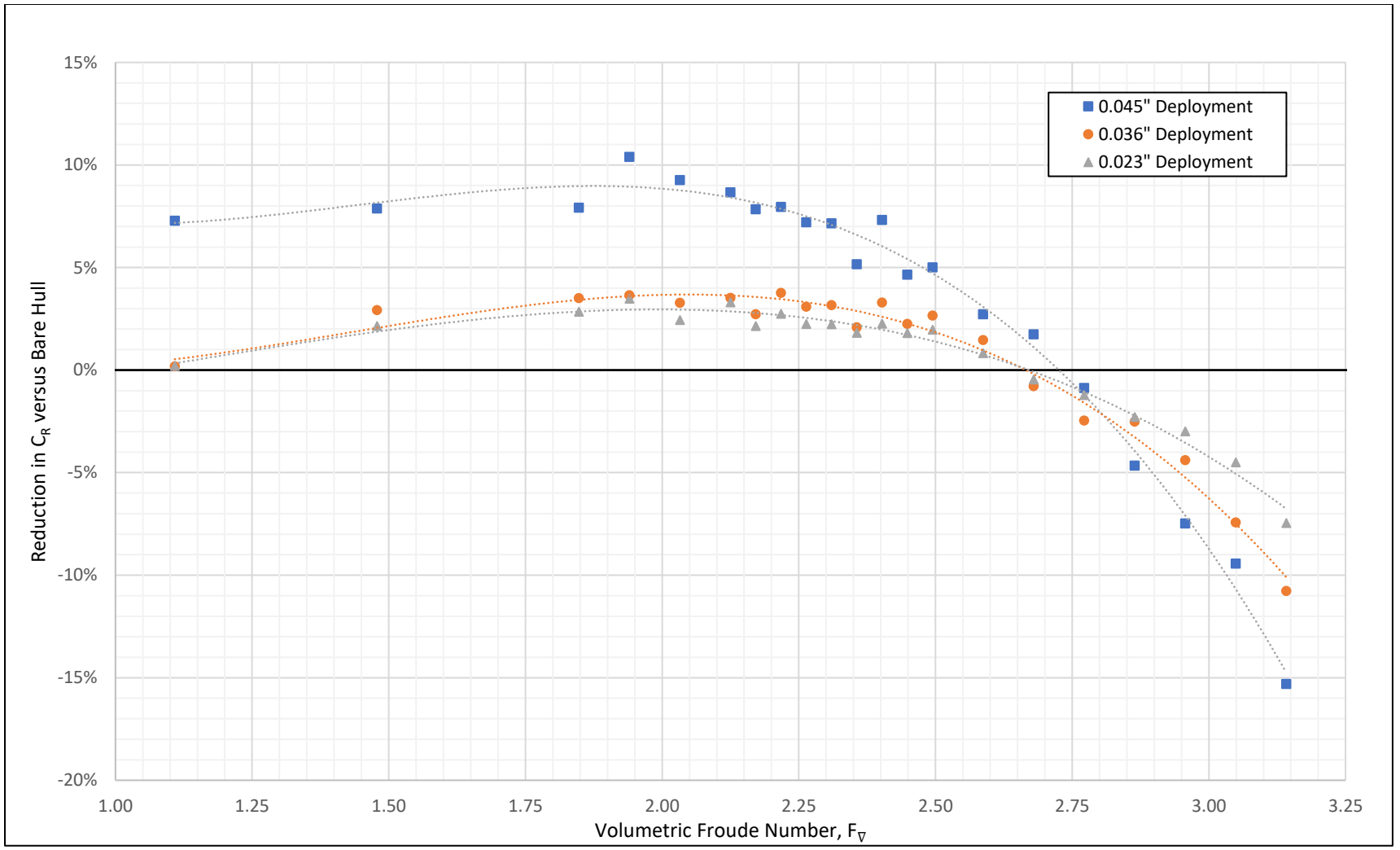

Figure 26. Reduction in Resistance - Interceptors

The trim reduction effects of trim tab A and interceptor A as well as trim tab C and interceptor C were near identical (within 0.01 degrees) respectively at F_∇ = 2.49, so the magnitude of the resistance reduction could be directly compared at this speed (Table 11).

Table 11. Direct Comparison of Resistance Reduction ($F_\nabla = 2.49$)

Configuration	Resistance Reduction, %Cr	Configuration	Resistance Reduction, %Cr
1.00° Trim Tab A	1.01%	5.00° Trim Tab C	3.45%
0.023" Interceptor A	1.80%	0.045" Interceptor C	4.65%

For the same amount of trim change, the interceptors decreased resistance significantly more than the trim tabs, meaning they were producing the same amount of lift while producing significantly less drag.

PRESSURE

Trim Tabs

Appendix F contains pressure distributions for all pressure taps over the speeds tested. Example distributions and pressure taps are chosen below to highlight the trends that were seen throughout the results.

Figure 27 shows typical pressure distributions for the three trim tab deployments as well as bare hull. The specific distributions shown are those recorded at $F_\nabla = 2.77$, the speed at which interceptor deployments were originally determined. The y-axis shows the total pressure coefficient, C_p, and the x-axis shows the longitudinal distance forward of the transom divided by LOA.

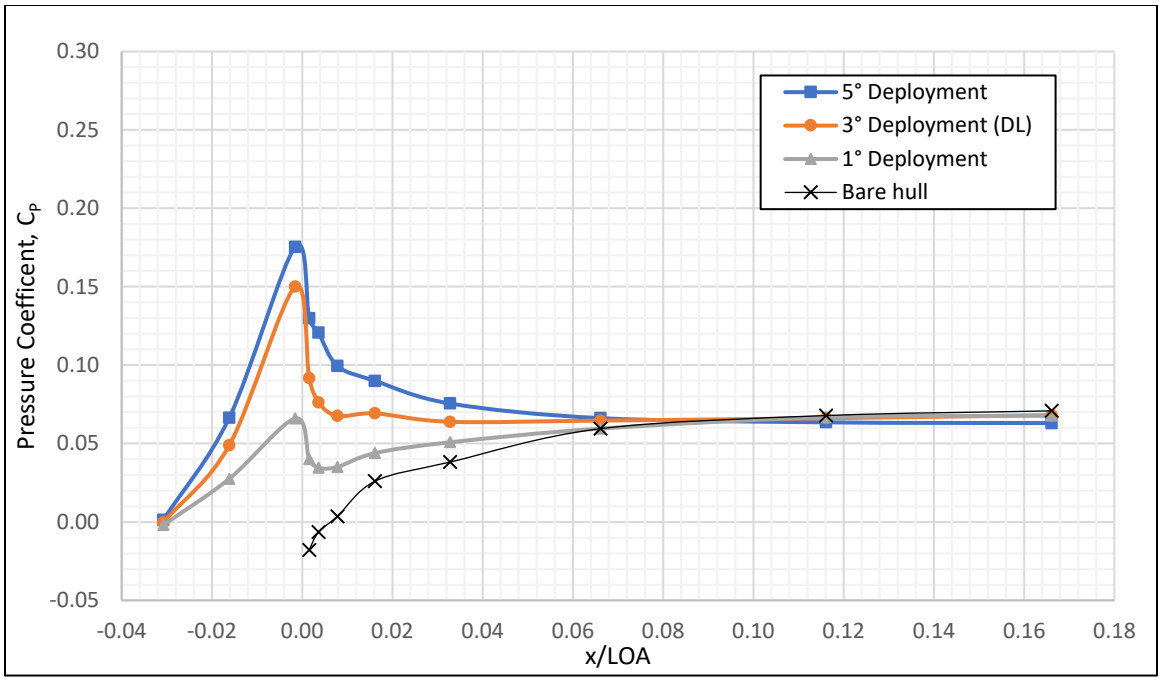

Figure 27. Typical Trim Tab Pressure Distribution ($F_\nabla = 2.77$)

This set of example pressure distributions illustrates key features that are of importance when characterizing the lift of the trim tab. The first notable feature is the significant increase in pressure far aft compared to bare hull. At 1.00° deployment, there is only a minor spike in pressure at the transom, but there is still a significant area of pressure created aft of the transom. At low deployment angles, trim tabs still produce meaningful lift as they act as an extension of the hull. This effect is not seen on interceptors.

The second notable feature is the location forward of the transom where the hull pressure returns to the approximate bare-hull magnitude. This location represents the forward extent of the induced pressures created by the trim tab and establishes the longitudinal region in which the trim tab has a pressure effect. For $F_\nabla = 2.77$ shown in Figure 27, all trim tabs converge to the bare hull pressure at about x/L = 0.09. The contour plots for trim tab induced pressure in Appendix F show that this distance is generally independent of deployment.

The third notable feature is the magnitude of the peak induced pressure at the transom. For all speeds, there is a measured local maximum located at x/L=-0.002, corresponding to P9. The magnitude increases with increased trim tab deployment, shifting from approximately 0.06 for the 1.00° deployment up to about 0.175 for the 5.00° deployment at $F_\nabla = 2.77$. A greater peak pressure is synonymous with greater lift produced.

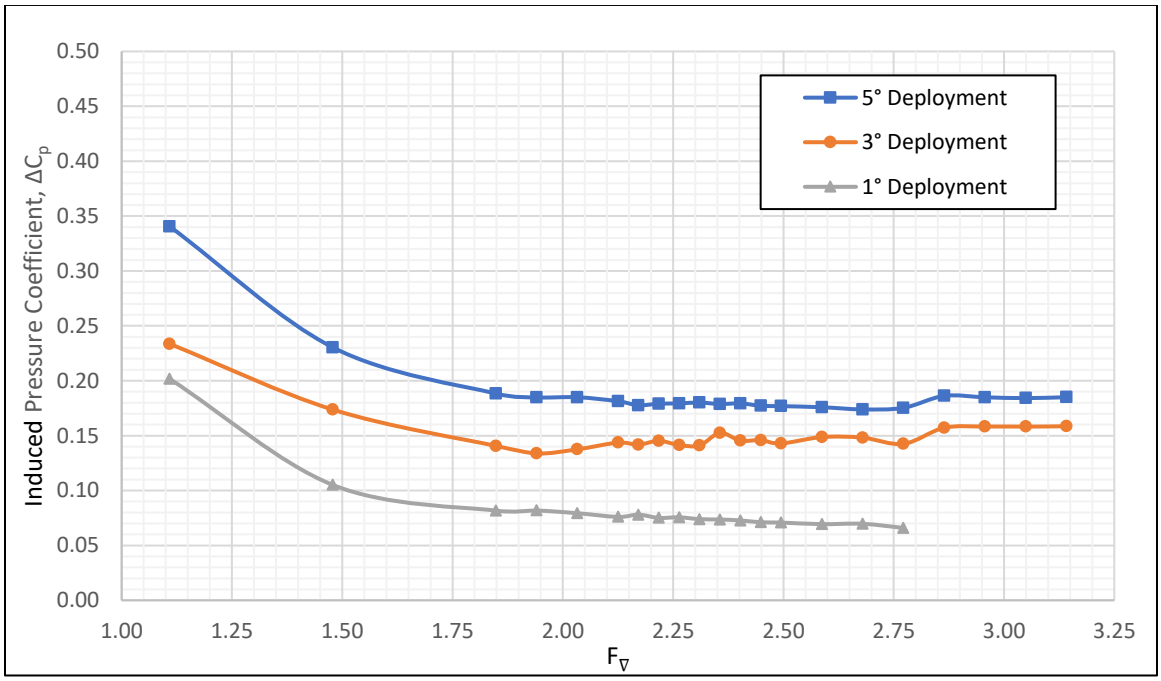

Figure 28. Trim Tab Peak Induced Pressure
Note: Peak pressure occurs at P9 (x/L=-0.002)

The last feature is how the distribution of the induced pressure distribution changes with speed, as shown in Figure 28[1]. At $F_\nabla > 1.85$, ΔC_p at x/L=-0.002 is near independent of velocity for all trim tabs. Figure 29 demonstrates that the entire induced pressure distribution for longitudinal extent affected by the trim tab remains constant at $F_\nabla > 1.85$. The variation further forward is due to speed and trim effects on the planing surface, which

[1] When testing at DL, pressure tap P9 was clogged on the 1.00° trim tab, so peak pressure is not reported for these runs.

although partially caused by the trim tabs, is direct evidence of the lift generated by the trim tabs.

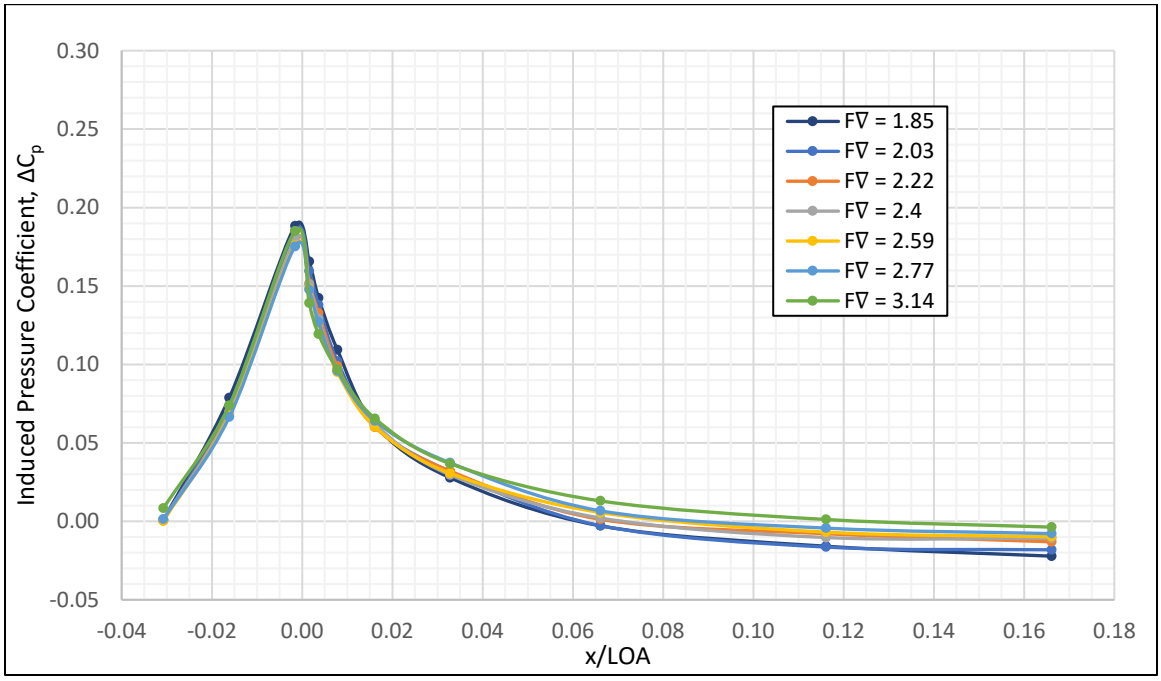

Figure 29. Selected 5.00° Trim Tab C Induced Pressure Distributions

The contour plots attached in Appendix F show that the constant C_p trends apply to the three trim tabs. This trend is significant, as it suggests the lift generated by a trim tab is proportional to model velocity squared.

Interceptors

Appendix F contains pressure distributions for all interceptors over the speeds tested. Example distributions and pressure taps are chosen below to highlight the trends that are seen throughout the data. Figure 30 shows typical pressure distributions for the three interceptor deployments as well as bare hull. The specific distributions shown are for $F_{\nabla} = 2.77$.

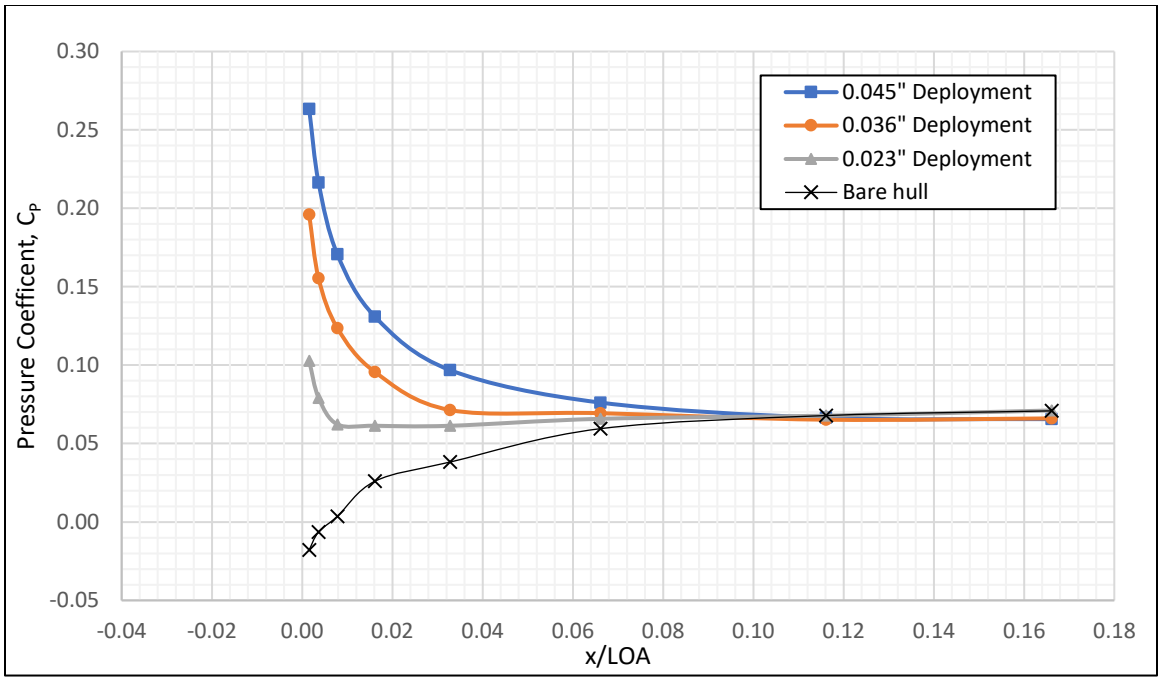

Figure 30. Example Interceptor Pressure Distribution ($F_\nabla = 2.77$)

The first notable feature is the forward extent of the interceptor's induced pressure. For this F_∇ the forward extent for all deployments appears to be around x/L = 0.09, a slightly larger extent than 0.08 observed for the trim tab forward extents at $F_\nabla = 2.77$. The contour plots of induced C_p in Appendix F show that the forward extent of the induced pressure increases with speed for all interceptors, and this trend is consistent for all deployments. This effect is most likely caused by the large peak pressures created by the interceptor at the transom. This shift in forward extent means that as speed increases, more area is affected by the interceptor, meaning more lift is generated.

The second notable feature is the change in the magnitude of the induced pressure at the transom with changing speed, as shown in Figure 31. For all interceptor configurations, the local maximum near the transom is located at x/L = 0.002, corresponding to P8.

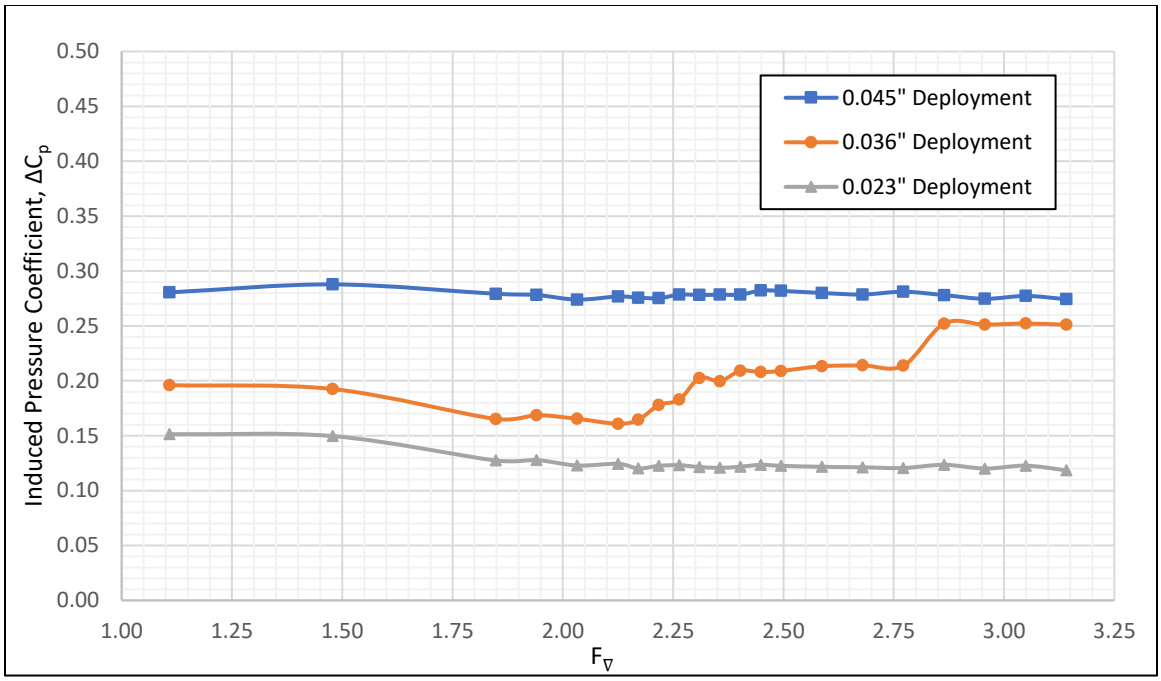

Figure 31. Interceptor Peak Induced Pressure
Note: Peak pressure occurs at P8 (x/L = 0.002)

The trend shows that for both the 0.023" and 0.045" interceptor deployment, the induced C_p at the transom remains near constant at $F_\nabla > 1.85$, the same speed as trim tabs. The magnitude of the peak C_p for the 0.036" does not follow the same trend, but rather increases in magnitude for $F_\nabla > 2.13$. At $F_\nabla > 2.86$, the induced lift appears to plateau around 0.25. At this deployment, the interceptor seemed to be operating in an unstable region, transitioning between effects like that of the lower deployment and that of the higher deployment. The exact cause of this behavior is unknown; however, it is evident that it yields significant uncertainty in running trim as discussed in the *Error Analysis* section.

The last key feature of the interceptor pressure distributions is how the shape of the induced pressure distribution varies with speed. Figure 32 shows that the induced pressure distribution for the 0.045" interceptor deployment remains constant for $F_\nabla > 1.85$ near the interceptor, meaning lift in this area is quadratically related to model velocity. However,

further forward of the interceptor, induced C_p increases with speed, meaning lift in this area has a relationship to model velocity that is above quadratic. The contour plots within Appendix F, show that a similar trend is also found for the 0.023" interceptor deployment.

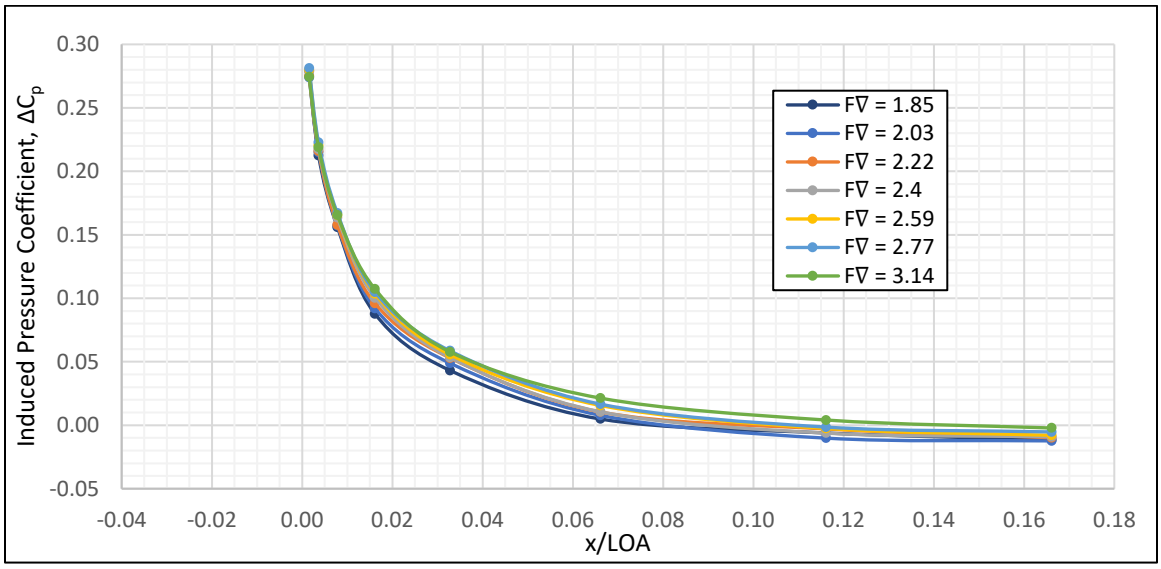

Figure 32. Selected 0.045" Interceptor C Induced Pressure Distributions

As opposed to the 0.045" and 0.023" deployments, Figure 33 shows that the unstable nature observed at the peak induced C_p for the 0.036" deployment affects all forward pressures up to x/L = 0.12.

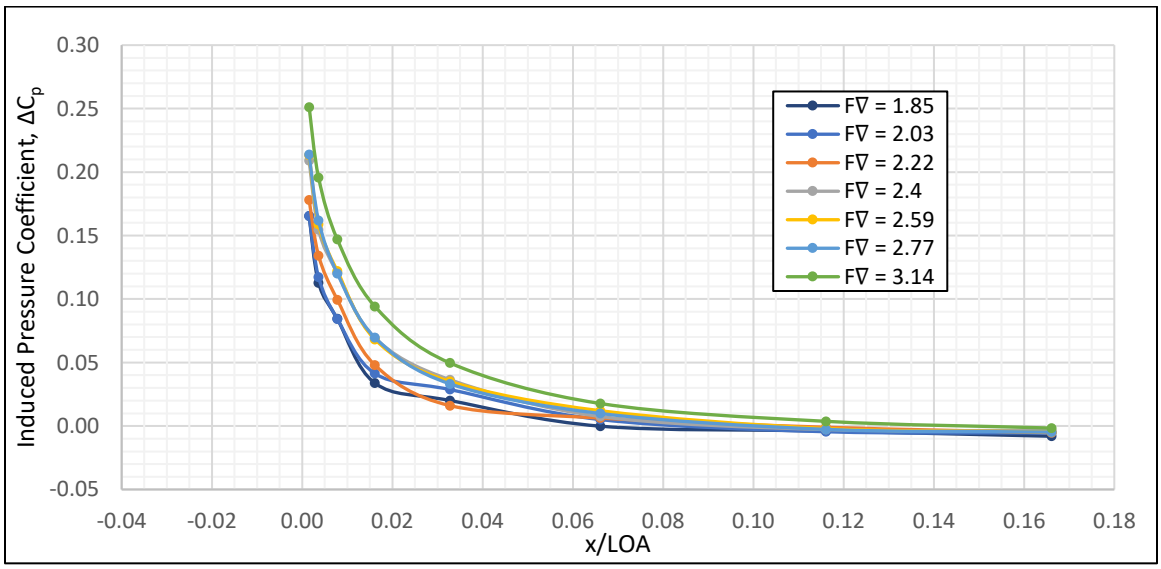

Figure 33. Selected 0.036" Interceptor B Induced Pressure Distributions

ANALYSIS

TRIM TAB PREDICTION METHODS

As discussed in the *Background* section, Brown (1971) proposed a method for predicting the lift generated by trim tabs. In this section the accuracy of Brown's method to the experimental results is examined.

Validity of Savitsky's Method

The prediction method for trim tabs proposed by Brown (1971) is an extension of the Savitsky method (1964). Therefore, before the results of the model tests can be compared to those predicted using Brown's method, it must be confirmed that the bare-hull results are similar to predictions made using the Savitsky method.

Figure 34 shows measured trim with the trim predicted by Savitsky's method overlaid. A summary of the calculated values from Savitsky's method is attached in Appendix H. There was less running trim observed than predicted using Savitsky's method for all speeds; however, the actual running trim of the model seems to approach that predicted by Savitsky's method at higher speeds.

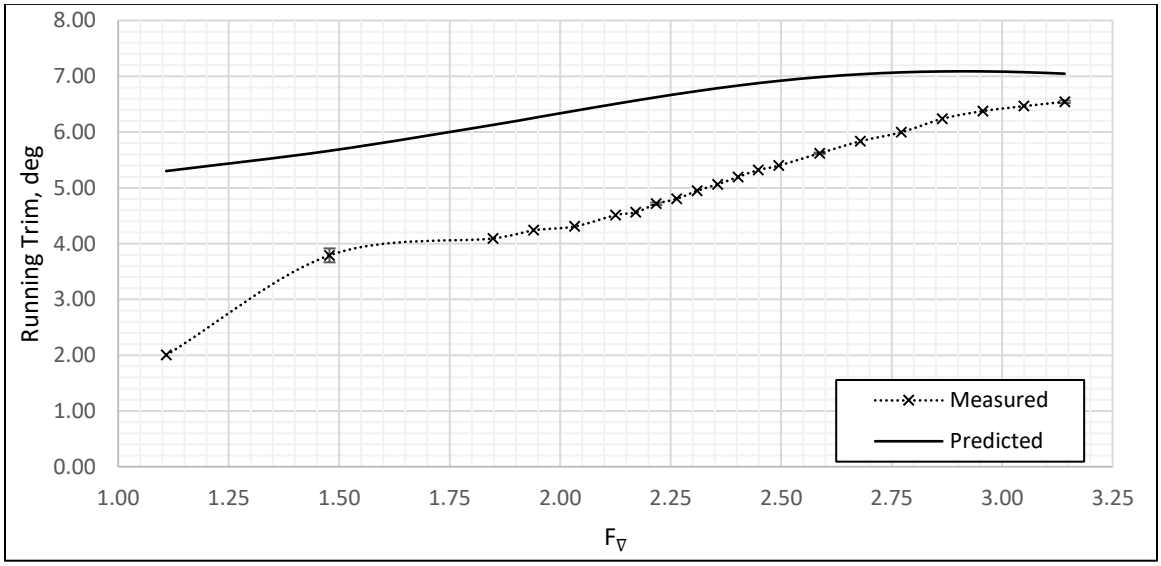

Figure 34. Bare Hull Trim Compared to Savitsky's Prediction Method

One reason for the disagreement between the measured results and Savitsky's method could be the unusual bow of the model, which has significant buttock curvature. Buttock curvature could be pulling the bow down at lower speeds, at which a significant portion of the curvature is submerged.

Because of the offset between the measured bare hull running trims and those predicted by Savitsky's method, the magnitude of the running trims predicted using the Brown method will likely be different than observed in the model tests; however, the Savitsky method does provide a reasonable approximation of the trend in running trim, so it could be expected that the Brown method will provide reasonable approximations of the ***change*** in running trim due to trim tabs.

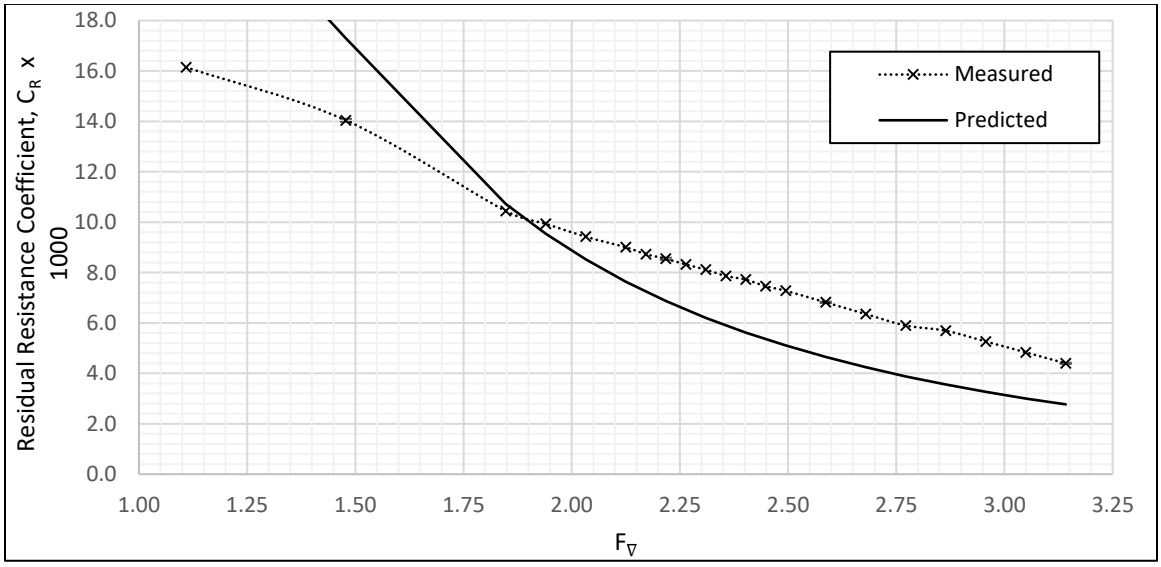

Figure 35. Bare Hull Resistance Compared to Savitsky's Prediction Method

In terms of resistance comparison, there is much less agreement between the experimental results and the Savitsky method, including the Blount and Fox correction (1976), prediction and model results, as shown in Figure 35. A reason for this disagreement could be that the model tested was not fitted with chine strips. It was observed that the flow re-attached to the sides of the model, which is unrealistic for a full-scale hull. The surface

area calculations assumed no reattachment, so the dynamic wetted surface area calculated was smaller than actuality, causing the frictional resistance of the model to be underestimated, leading to an overestimated residuary resistance. This could explain part of the disagreement between the measured results and Savitsky's method at higher speeds.

As the observed model resistance is not in close agreement with the Savitsky method, the Brown method would not be expected to provide any accurate predictions of how resistance would change with the addition of trim tabs.

Change in Trim Prediction Comparison

Because the differences between the bare hull results and those predicted by the Savitsky method, the only measure that the accuracy of Brown's method can be compared against is the predicted trim reduction due to the trim tabs. This is a significant measure of trim tab effectiveness, and Blount suggests that this is the measure that naval architects should use to size trim tabs. (Blount, 2014) Figure 36 shows how the predicted reduction in trim change using Brown's method compares to that of the model tests.

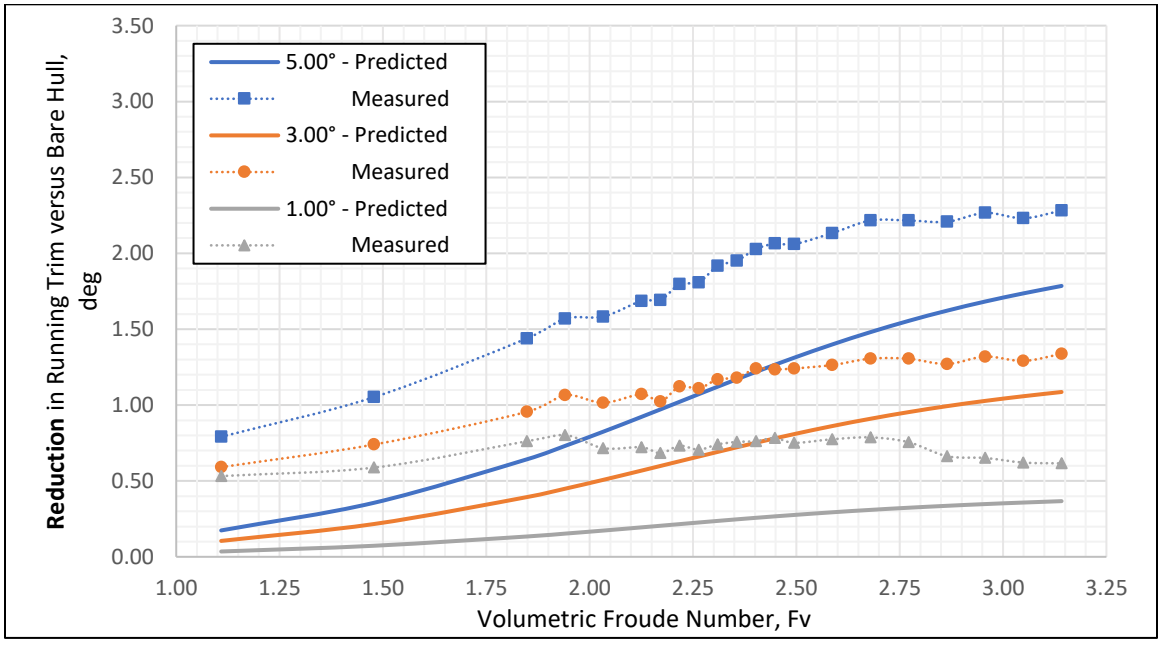

Figure 36. Reduction in Running Trim - Measured versus Predicted

The equation Brown uses for lift created by trim tabs, Δ_T, is repeated here for convenience.

$$\Delta_T = 0.046\, L_T\, \alpha_t \sigma B_{PX} \left[\frac{\rho}{2} V^2\right] \tag{6}$$

A noticeable difference between the prediction and the model test data is the vertical offset. Brown's method predicts that a trim tab with zero deployment, α_t, would create zero lift. However, this prediction neglects the hull extension effect a trim tab would create, even at zero deployment angle. Although a zero-deployment angle was not tested, the trend in pressure distributions suggest that it would still have pressure acting on it. A more accurate version of Equation 6 would include a term independent of deployment angle, perhaps replacing the deployment angle with the actual attack angle of the trim tab relative to the free surface.

Apart from the offset, the general trend shown in Figure 36 matches the results quite well for a preliminary prediction method, especially for higher trim tab angles. Ignoring the vertical offset, the matching of the trend is the best for the highest deployment of 5.00°, between $F_\nabla < 2.75$. The trends observed in the induced pressure distributions support the assumption that the lift generated by a trim tab is related to the velocity squared, as modeled by Brown.

INTERCEPTOR PREDICTION METHODS

As mentioned in *Design and Construction* section, the interceptor deployments were selected by adjusting the interceptor plate deployment and testing at $F_\nabla = 2.77$ until deployments were found that matched the running trim of each of the three trim tabs. Because of differences in model setup between these preliminary tests and later testing, the initial trim results do match those reported in this research. However, as discussed in the

Results section, at $F_\nabla = 2.49$ it was observed that the running trim of the interceptor A configuration and the trim tab A configuration were within 0.01°. The same was true for interceptor C and trim tab C at this speed. This means that at this speed the interceptors and trim tabs can be directly compared, as their trim reduction effect is equivalent.

Both Dawson and Blount (2002) and Villa and Brizzolara (2009) proposed similar equations predicting interceptor deployments that would give equivalent effects as a trim tab geometry, as was observed at $F_\nabla = 2.49$. Appendix I contains calculations of theoretical interceptor deployment determined from both equations as well as the actual interceptor deployment determined during preliminary testing. The comparison is shown in Figure 37.

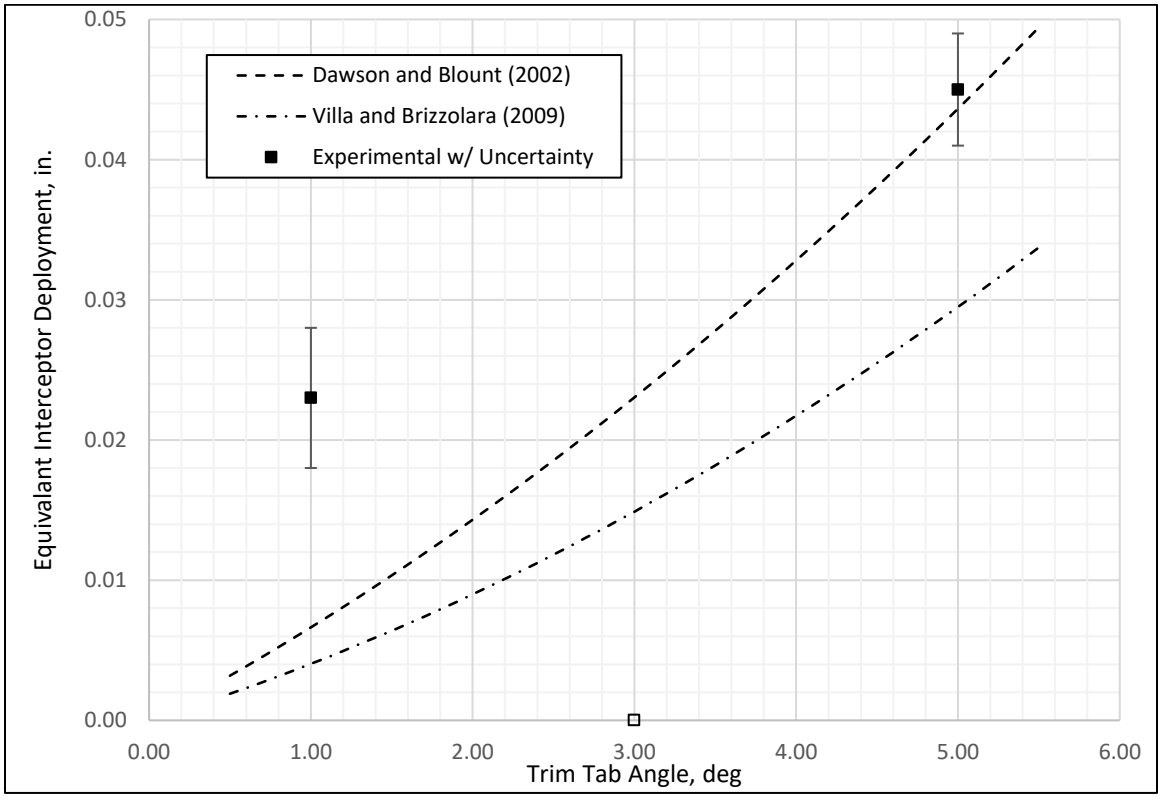

Figure 37. Equivalence Prediction Models versus Experimental Values

The equivalent interceptor deployment determined for the 1.00° trim tab was significantly larger than the predicted value of both models. However, the experimentally determined equivalent interceptor deployment of 0.045” for the 5.00° trim tab was found to be extremely close to Dawson and Blount’s predicted deployment of 0.044”. The large discrepancy in predicted versus actual equivalent interceptor deployment for the 1.00° trim tab is most likely the result of the point’s being outside the region of validity for both equations. Although it is unknown how Dawson and Blount collected data for their prediction model, Villa and Brizzolara tested multiple trim tab deployments ranging from 0 to 30°. Most of the deployments examined were over 5.00° and therefore well outside the range of trim tab deployments explored in this thesis.

While the trim effects were found to be equivalent for $F_\nabla = 2.49$, they quickly diverge at higher and lower speeds (Figure 38). The trim tabs have large plateaus in their trim reduction at various speeds while the interceptors show a constant increasing trim reduction.

The relative trim effect of an interceptor versus a trim tab is speed dependent, so any equivalence model would have to take this into account. This speed dependence is created by the differences in how the different appendages produce lift. A portion of the added lift created by a trim tab comes about because it creates an effective extension of the planing surface. This extension increases the pressure aft of the transom, even at slower speeds for which interceptors create little additional lift for the hull.

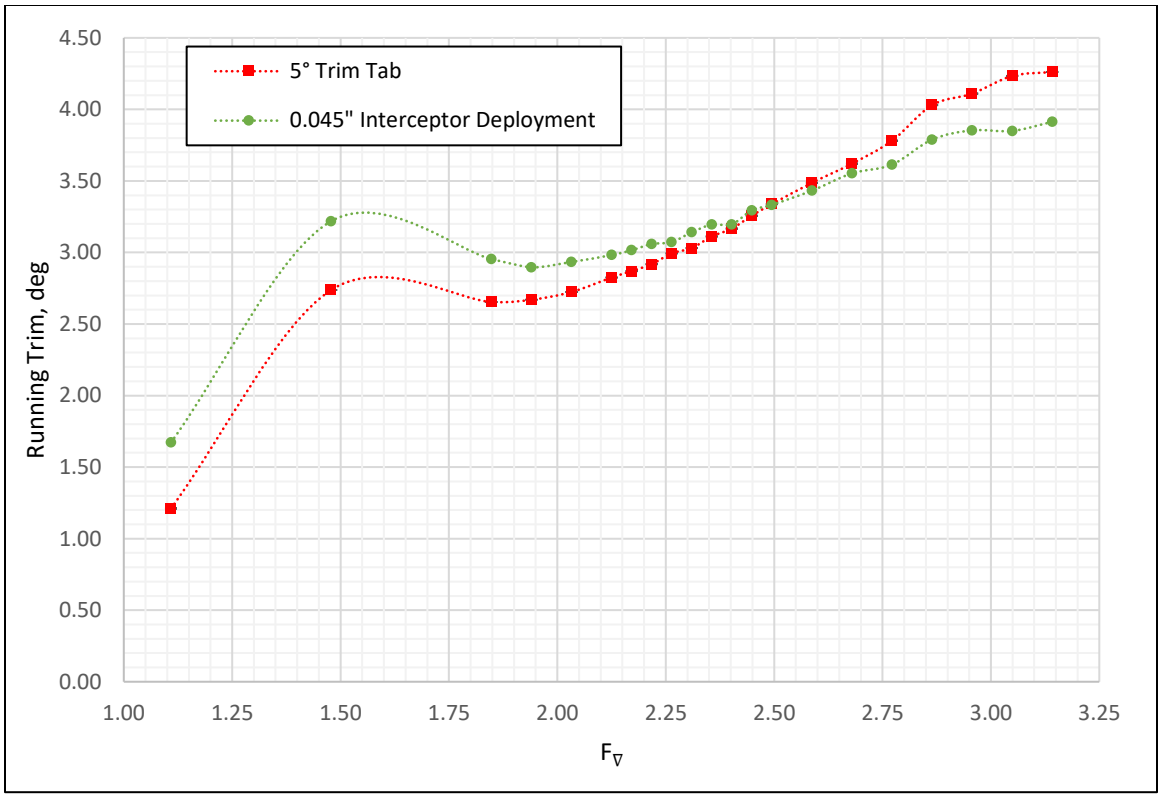

Figure 38. Comparison of Interceptor C and Trim Tab C

Another reason for the difference is related to higher speeds. As discussed in the *Pressure* section of the *Results* section, there is a forward shift in the longitudinal extent of the induced pressure of interceptors with increasing speed. This increased region of induced pressure creates additional lift, which implies that at high enough speeds the relationship between lift and velocity is greater than quadratic.

The lift generated by each appendage may be equivalent at a single speed, but a more sophisticated relationship between interceptors, trim tabs, and velocity must be created to properly equate the two transom lift devices for a range of speeds. Rather than try to predict interceptor performance by modeling an equivalent trim tab, further research should be performed to create independent models for interceptor performance.

CONCLUSION

TRANSOM LIFT DEVICE EFFECTIVENESS

When looking at effectiveness of the devices from the standpoint of decreasing the running trim of the vessel, both trim tabs and interceptors, at all deployments tested, created sufficient lift near the transom to create a reduction in running trim. Based on the trends observed, it seems that both devices will produce a running trim reduction at all speeds. At the speeds tested, trim tabs reached a peak in running trim reduction at speeds that varied with deployment. After this peak, the trim reduction stayed constant or even decreased as speed increased. For all speeds tested, interceptors created more trim reduction as speed increased; however, an unexplained unstable region of speeds was observed with the middle deployment that caused significant variation in running trim reduction.

Both trim tabs and interceptors decrease residuary resistance up to a speed, after which they were ineffective and caused an increase in residuary resistance. For trim tabs this cross-over speed was $F_{\nabla} = 2.65$, and for interceptors it was 2.70. Interceptors created their greatest resistance reductions at higher speeds ($F_{\nabla} = 2.0$) than trim tabs ($F_{\nabla} = 1.7$). Because of the deployments chosen, resistance reduction between the two devices could only be directly compared at $F_{\nabla} = 2.49$. At this speed, interceptors performed better than trim tabs, creating the same amount of trim reduction with significantly less resistance.

For planing craft operating at $F_{\nabla} < 2.70$, there is an advantage to having transom lift devices. Although there is insufficient data to make recommendations across a range of speeds, for speeds near $F_{\nabla} = 2.49$, an interceptor would decrease residuary resistance more than an equivalent trim tab.

TRIM TAB PERFORMANCE PREDICTIONS

The trim tab performance prediction method recommended by Brown (1971) provides a prediction for the lift produced by a trim tab, and this lift can be incorporated into Savitsky's method. Brown's method reasonably predicted the trends in running trim reduction; however, it was shown to under predict running trim reduction at all speeds. It is hypothesized that the reason for this is that the effective extension of the planing surface created by a trim tab is not considered in Brown's equation for trim tab lift. Experimental pressure distributions show that this effective extension of the planing surface is a significant portion of the lift generated by trim tabs, especially at low trim tab deployment angles. The authors suggest that Brown's equation for predicting trim tab lift be changed to include the lift because of the effective extension of the planing surface.

INTERCEPTOR PERFORMANCE PREDICTIONS

Current practice is to predict interceptor performance by modeling a trim tab that would theoretically create the same running trim reduction, then to use Brown's method on this equivalent trim tab. Dawson and Blount (2002) and Villa and Brizzolara (2009) provide two similar equations for calculating the equivalent trim tab deployment. The lower angle trim tabs used in this thesis are believed to be outside the deployment angle range for which these equivalence models are based; however, a broader problem was observed.

The equivalence between the interceptor and trim tab deployments was satisfied for one speed, but running trim quickly diverged at any speed higher or lower. Pressure distributions for both interceptors and trim tabs generally have a quadratic relationship between induced lift and velocity; however, smaller lift effects are not quadratic. For interceptors at higher speeds, the forward extent of the induced pressure increases with

speed, causing an increase in lift. Therefore, at higher speeds, the relationship between induced interceptor lift and velocity is greater than quadratic. For trim tabs at lower speeds, the effective planing surface extension is significant and create a non-quadratic effect on lift. The sum of these two effects causes the equivalence of an interceptor and a trim tab to be speed dependent. This means the current equivalence models are inadequate to predict the performance of an interceptor beyond the one speed the specific equivalence model was created around.

RECOMMENDATIONS FOR FUTURE WORK

For this thesis, lift was indirectly observed by measuring change in running trim as well as pressure along one longitudinal line. Future work could attempt to isolate and directly measure the induced lift of trim tabs and interceptors. These measurements could be used to generate lift coefficients, which would allow development of more accurate prediction methods. Ways to do this include measuring pressure at various transverse locations along the hull surface near the transom, or running the model fixed in trim and sinkage and measuring forces and moments to deduce lift.

LIST OF REFERENCES

Blount, D. L. (2014). *Performance by Design: Hydrodynamics for High-Speed Vessels.* Virginia Beach.

Blount, D. L., & Fox, D. L. (1976, January). Small-Craft Power Prediction. *Marine Technology, 13*(1), pp. 14-45.

Brown, P. W. (1971). *An Experimental and Theoretical Study of Planing Surfaces with Trim Flaps.* Stevens Institute of Technology, Davidson Laboratory, Hoboken.

Dawson, D., & Blount, D. L. (2002, February/March). Trim Control. *Professional Boatbuilder*, pp. 140-149.

Gavel, K. (2016). *Planing Craft Seakeeping: The Effect of Different Convex Buttock Curvatures at the Bow.* Undergraduate Thesis, Webb Institute.

International Towing Tank Conference. (2008). High Speed Marine Vehicles Resistance Test. *Recommended Procedures and Guidelines.*

Mansoori, M., & Fernandes, A. C. (2017, April). Hydrodynamics of the Interceptor Analysis Via Both Ultrareduced Model Test and Dynamic Computational Fluid Dynamics Simulation. *Journal of Offshore Mechanics and Arctic Engineering, 139*.

Molini, A., & Brizzolara, S. (2005). Hydrodynamics of Interceptors: A Fundamental Study. *ICMRT.* Naples.

Savitsky, D. (1964, October). Hydrodynamic Design of Planing Hulls. *Marine Technology, 1*, 71-95.

Savitsky, D., & Brown, P. W. (1976, October). Procedures for Hydrodynamic Evaluation of Planing Hulls in Smooth and Rough Water. *Marine Technology*, 381-400.

Steen, S. (2007). Experimental Investigation of Interceptor Performance. *9th International Conference on Fast Sea Transportation*, (pp. 238-245). Shanghai.

Villa, D., & Brizzolara, S. (2009). A Systematic CFD Analysis of Flaps/Interceptors Hydrodynamic Performance. *10th International Conference on Fast Sea Transportation.* Athens.

APPENDIX A. INTERCEPTOR DEPLOYMENT UNCERTAINTY

For each deployment, a total of twelve measurements were taken with a caliper. First, with the plate attached to the transom of the model and the set pin in the appropriate hole, the interceptor plate was firmly tapped upward with a mallet. then deployment was measured three times on the starboard side and three times on the port side. Next, the plate was tapped in a similar fashion downward, and six more measurements were taken. From these twelve measurements, an average and an uncertainty for each deployment was calculated, as described in the *Uncertainty* section of *Theory*.

Table A-1. Interceptor Deployment A Measurements and Uncertainty Calculations

Deployment Measurements (in)			
Stbd.		Port	
Up	Down	Up	Down
0.0185	0.0195	0.0255	0.0315
0.0150	0.0210	0.0270	0.0295
0.0155	0.0175	0.0250	0.0305

Uncertainty		
Average	0.0230	in
Std Dev	0.0059	in
Standard Error	0.0017	in
Uncertainty	0.0051	in
%Uncertainty	22%	

Table A-2. Interceptor Deployment B Measurements and Uncertainty Calculations

Deployment Measurements (in)			
Stbd.		Port	
Up	Down	Up	Down
0.0280	0.0335	0.0465	0.0425
0.0325	0.0305	0.0380	0.0435
0.0285	0.0330	0.0385	0.0420

Uncertainty		
Average	0.0364	in
Std Dev	0.0063	in
Standard Error	0.0018	in
Uncertainty	0.0054	in
%Uncertainty	15%	

Table A-2. Interceptor Deployment C Measurements and Uncertainty Calculations

Deployment Measurements (in)			
Stbd.		Port	
Up	Down	Up	Down
0.0415	0.0420	0.0500	0.0500
0.0405	0.0390	0.0500	0.0480
0.0405	0.0410	0.0500	0.0495

Uncertainty		
Average	0.0452	in
Std Dev	0.0047	in
Standard Error	0.0014	in
Uncertainty	0.0041	in
%Uncertainty	9%	

APPENDIX B. MOUNTING LAYOUT

This appendix contains the mounting layout of the model, which shows the tow point location as well as the implied thrust line. A thrust angle of 10 degrees was assumed for this model. The model is drawn at the draft and trim at which it was tested.

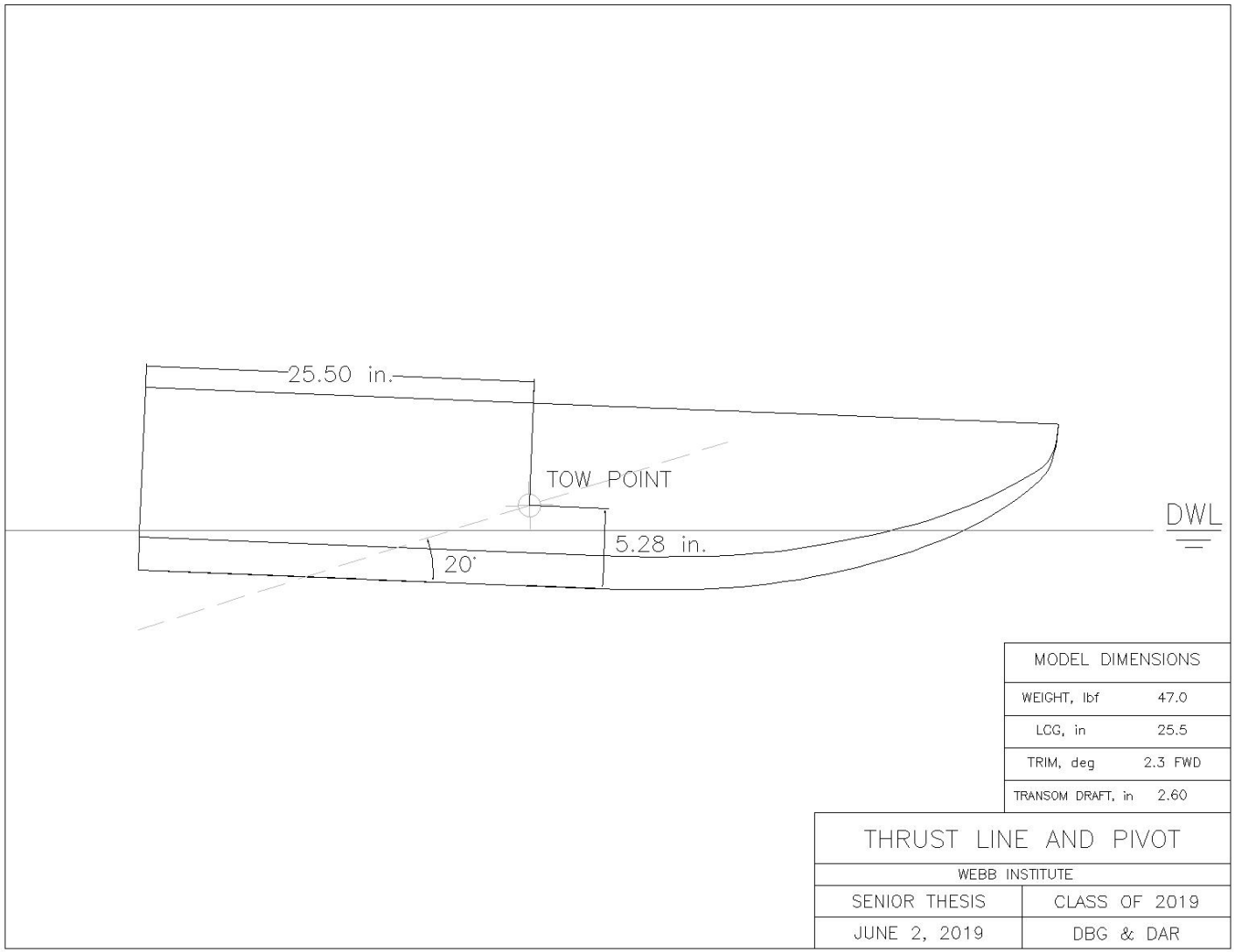

Figure B-1. Thrust line and Pivot Point

APPENDIX C. APPENDAGE BUOYANCY CORRECTION

Before testing each configuration at RMB, the change in trim and heave after adding the appendage and removing the equivalent weight was recorded. Note that during testing heave was measured, which for calm water testing is simply the negative of sinkage. After testing the configuration, the change in trim and heave after removing the appendage and replacing the equivalent weight was recorded. For trim, the correction was calculated and applied as follows,

$$\tau_{DIFF} = \tau_{appended\_static} - \tau_{bare\_static} \quad \text{(C1)}$$

where τ_{DIFF} is the correction factor, τ_{apend_static} is the measured static trim in the appended condition, and τ_{bare_static} is the measured static trim in the appended condition.

The measured running trim of the model, $\tau_{measured}$, was calculated by subtracting a "zero run" trim, which is equivalent to $\tau_{appended\_static}$.

$$\tau_{measured} = \tau_{running} - \tau_{appended\_static} \quad \text{(C2)}$$

However, this measured trim includes the buoyant effect of the appendage on appended static trim. Combining Equation 1 and 2, the corrected trim, $\tau_{corrected}$, is given by the following equation.

$$\tau_{corrected} = \tau_{running} + \tau_{DIFF} \quad \text{(C3)}$$

The heave correction was calculated the same way.

This appendix contains the calculations used to determine the correction for each appendage.

Table C-1. Buoyancy Correction Calculations for Trim Tab A

Configuration:	Trim Tab A	**Date:**	5/9/2019
Deployment:	1.00 °		

Before Testing		
	Trim (°)	**Heave (in)**
Appended	0.000	0.000
Bare Hull	-0.083	0.012
DIFF	-0.083	0.012

After Testing		
	Trim (°)	**Heave (in)**
Appended	-0.005	-0.011
Bare Hull	-0.088	0.002
DIFF	-0.083	0.013

Combined Correction		
	Trim (°)	**Heave (in)**
DIFF	-0.083	0.013

Table C-2. Buoyancy Correction Calculations for Trim Tab B

Configuration:	Trim Tab B	**Date:**	5/10/2019
Deployment:	3.00 °		

Before Testing		
	Trim (°)	**Heave (in)**
Appended	-0.002	-0.001
Bare Hull	-0.083	0.033
DIFF	-0.081	0.034

After Testing		
	Trim (°)	**Heave (in)**
Appended	-0.009	0.028
Bare Hull	-0.088	0.041
DIFF	-0.079	0.013

Combined Correction		
	Trim (°)	**Heave (in)**
DIFF	-0.080	0.024

Table C-3. Buoyancy Correction Calculations for Trim Tab C

Configuration:	Trim Tab C	**Date:**	5/10/2019
Deployment:	5.00 °		

Before Testing		
	Trim (°)	**Heave (in)**
Appended	-0.004	0.001
Bare Hull	-0.072	0.012
DIFF	-0.068	0.011

After Testing		
	Trim (°)	**Heave (in)**
Appended	0.084	-0.017
Bare Hull	0.016	-0.002
DIFF	-0.068	0.015

Combined Correction		
	Trim (°)	**Heave (in)**
DIFF	-0.068	0.013

Table C-4. Buoyancy Correction Calculations for Interceptor A

Configuration:	Interceptor A	**Date:**	5/7/2019
Deployment:	0.023 in		

Before Testing		
	Trim (°)	**Heave (in)**
Appended	0.001	0.000
Bare Hull	-0.023	-0.005
DIFF	-0.024	-0.005

After Testing		
	Trim (°)	**Heave (in)**
Appended	0.036	-0.024
Bare Hull	0.008	-0.020
DIFF	-0.028	0.004

Combined Correction		
	Trim (°)	**Heave (in)**
DIFF	-0.026	-0.001

Table C-5. Buoyancy Correction Calculations for Interceptor B

Configuration:	Interceptor B	**Date:**	5/7/2019
Deployment:	0.036 in		

Before Testing		
	Trim (°)	**Heave (in)**
Appended	-0.001	0.000
Bare Hull	-0.031	0.003
DIFF	-0.030	0.003

After Testing		
	Trim (°)	**Heave (in)**
Appended	0.011	-0.011
Bare Hull	-0.020	-0.009
DIFF	-0.031	0.002

Combined Correction		
	Trim (°)	**Heave (in)**
DIFF	-0.031	0.003

Table C-6. Buoyancy Correction Calculations for Interceptor C

Configuration:	Interceptor C	**Date:**	5/9/2019
Deployment:	0.045 in		

Before Testing		
	Trim (°)	**Heave (in)**
Appended	0.004	0.000
Bare Hull	-0.038	-0.003
DIFF	-0.042	-0.003

After Testing		
	Trim (°)	**Heave (in)**
Appended	0.022	-0.008
Bare Hull	-0.007	-0.003
DIFF	-0.029	0.005

Combined Correction		
	Trim (°)	**Heave (in)**
DIFF	-0.036	0.001

APPENDIX D. RUN DATA AND COEFFICIENT CALCULATIONS

This appendix, located on the attached CD, contains the calibrated data for all runs as well as the coefficient calculations associated with each run. The underside photographs used to calculate dynamic surface area and wetted lengths for each run are also included. The calculations for non-dimensionalizing are explained in the *Theory* section. Note that during testing heave was measured, which for calm water testing is simply the negative of sinkage. The trim and sinkage correction method is explained in Appendix C. To calculate the hydrostatic pressure, trim and sinkage were used along with the geometry of the model to calculate the height of the pressure taps compared to the static waterline. These geometric calculations are not included.

APPENDIX E. RESISTANCE, TRIM, AND SINKAGE RESULTS

In this appendix, the non-dimensional resistance is reported for each speed in terms of total resistance coefficient, and residual resistance coefficient, as calculated in Appendix D. Running trim and sinkage are also reported. Speeds of 15.00 ft/s and below are based on tests at RMB, and speeds above are from tests at DL. This data is also available on the attached CD.

BARE HULL

Speed *(ft/s)*	**F_∇**	**C_T**	**C_R**	**Trim** deg	**Sinkage** in	
6.00	1.11	0.0194	0.0161	2.002	0.433	From RMB
8.00	1.48	0.0170	0.0140	3.790	0.189	
10.00	1.85	0.0132	0.0104	4.093	-0.202	
10.50	1.94	0.0127	0.0099	4.240	-0.258	
11.00	2.03	0.0122	0.0094	4.307	-0.343	
11.50	2.13	0.0117	0.0090	4.511	-0.421	
11.75	2.17	0.0114	0.0087	4.561	-0.456	
12.00	2.22	0.0112	0.0085	4.715	-0.505	
12.25	2.26	0.0109	0.0083	4.802	-0.526	
12.50	2.31	0.0107	0.0081	4.948	-0.559	
12.75	2.36	0.0105	0.0079	5.063	-0.615	
13.00	2.40	0.0103	0.0077	5.195	-0.662	
13.25	2.45	0.0100	0.0075	5.321	-0.701	
13.50	2.49	0.0098	0.0073	5.398	-0.746	
14.00	2.59	0.0093	0.0068	5.620	-0.829	
14.50	2.68	0.0088	0.0064	5.837	-0.914	
15.00	2.77	0.0083	0.0059	5.997	-1.008	
15.50	2.86	0.0080	0.0057	6.238	-0.991	From DL
16.00	2.96	0.0076	0.0053	6.377	-1.089	
16.50	3.05	0.0071	0.0048	6.465	-1.150	
17.00	3.14	0.0066	0.0044	6.543	-1.242	

TRIM TAB A

Deployment: 1.00 deg

Speed *(ft/s)*	**F_∇**	**C_T**	**C_R**	**Trim** deg	**Sinkage** in	
6.00	1.11	0.0191	0.0159	1.470	0.423	From RMB
8.00	1.48	0.0164	0.0134	3.202	0.195	
10.00	1.85	0.0130	0.0101	3.332	-0.182	
10.50	1.94	0.0123	0.0095	3.437	-0.260	
11.00	2.03	0.0119	0.0091	3.591	-0.321	
11.50	2.13	0.0114	0.0087	3.789	-0.365	
11.75	2.17	0.0112	0.0085	3.878	-0.402	
12.00	2.22	0.0110	0.0083	3.983	-0.423	
12.25	2.26	0.0108	0.0081	4.096	-0.452	
12.50	2.31	0.0106	0.0079	4.207	-0.493	
12.75	2.36	0.0104	0.0078	4.306	-0.531	
13.00	2.40	0.0102	0.0076	4.433	-0.545	
13.25	2.45	0.0100	0.0074	4.538	-0.598	
13.50	2.49	0.0098	0.0072	4.647	-0.627	
14.00	2.59	0.0093	0.0068	4.845	-0.707	
14.50	2.68	0.0089	0.0064	5.050	-0.792	
15.00	2.77	0.0085	0.0060	5.242	-0.863	
15.50	2.86	0.0082	0.0058	5.575	-0.939	From DL
16.00	2.96	0.0078	0.0055	5.726	-0.976	
16.50	3.05	0.0074	0.0050	5.844	-1.061	
17.00	3.14	0.0070	0.0047	5.927	-1.134	

TRIM TAB B

Deployment: 3.00 deg

Speed *(ft/s)*	**F_∇**	**C_T**	**C_R**	**Trim** deg	**Sinkage** in	
6.00	1.11	0.0192	0.0159	1.411	0.376	From RMB
8.00	1.48	0.0164	0.0134	3.050	0.159	
10.00	1.85	0.0127	0.0099	3.138	-0.217	
10.50	1.94	0.0122	0.0094	3.174	-0.280	
11.00	2.03	0.0117	0.0089	3.292	-0.339	
11.50	2.13	0.0113	0.0085	3.440	-0.398	
11.75	2.17	0.0111	0.0084	3.538	-0.424	
12.00	2.22	0.0109	0.0082	3.593	-0.450	
12.25	2.26	0.0107	0.0080	3.692	-0.468	
12.50	2.31	0.0105	0.0079	3.779	-0.497	
12.75	2.36	0.0103	0.0077	3.883	-0.521	
13.00	2.40	0.0101	0.0075	3.955	-0.541	
13.25	2.45	0.0100	0.0073	4.086	-0.578	
13.50	2.49	0.0097	0.0071	4.157	-0.601	
14.00	2.59	0.0094	0.0068	4.356	-0.684	
14.50	2.68	0.0090	0.0064	4.531	-0.747	
15.00	2.77	0.0086	0.0061	4.692	-0.831	
15.50	2.86	0.0084	0.0059	4.967	-0.770	From DL
16.00	2.96	0.0079	0.0055	5.057	-0.889	
16.50	3.05	0.0076	0.0052	5.174	-0.918	
17.00	3.14	0.0071	0.0048	5.206	-1.006	

TRIM TAB C

Deployment: 5.00 deg

Speed *(ft/s)*	**F_∇**	**C_T**	**C_R**	**Trim** deg	**Sinkage** in	
6.00	1.11	0.0185	0.0152	1.211	0.387	From RMB
8.00	1.48	0.0157	0.0127	2.738	0.168	
10.00	1.85	0.0123	0.0095	2.654	-0.188	
10.50	1.94	0.0118	0.0090	2.670	-0.243	
11.00	2.03	0.0114	0.0086	2.724	-0.302	
11.50	2.13	0.0110	0.0083	2.825	-0.349	
11.75	2.17	0.0108	0.0081	2.870	-0.359	
12.00	2.22	0.0107	0.0079	2.918	-0.379	
12.25	2.26	0.0105	0.0078	2.994	-0.396	
12.50	2.31	0.0103	0.0076	3.031	-0.415	
12.75	2.36	0.0102	0.0075	3.112	-0.442	
13.00	2.40	0.0100	0.0073	3.167	-0.467	
13.25	2.45	0.0099	0.0072	3.257	-0.480	
13.50	2.49	0.0097	0.0070	3.338	-0.510	
14.00	2.59	0.0094	0.0068	3.487	-0.565	
14.50	2.68	0.0090	0.0064	3.621	-0.630	
15.00	2.77	0.0086	0.0061	3.781	-0.691	
15.50	2.86	0.0085	0.0060	4.030	-0.716	From DL
16.00	2.96	0.0082	0.0057	4.110	-0.769	
16.50	3.05	0.0079	0.0054	4.234	-0.825	
17.00	3.14	0.0075	0.0051	4.262	-0.905	

INTERCEPTOR A

Deployment: 0.023 in

Speed *(ft/s)*	**F_∇**	**C_T**	**C_R**	**Trim** deg	**Sinkage** in	
6.00	1.11	0.01937	0.0161	1.792	0.420	From RMB
8.00	1.48	0.01673	0.0137	3.441	0.185	
10.00	1.85	0.01297	0.0101	3.550	-0.184	
10.50	1.94	0.01239	0.0096	3.618	-0.259	
11.00	2.03	0.01189	0.0092	3.749	-0.319	
11.50	2.13	0.01143	0.0087	3.909	-0.371	
11.75	2.17	0.01124	0.0085	3.989	-0.419	
12.00	2.22	0.01100	0.0083	4.068	-0.443	
12.25	2.26	0.01080	0.0081	4.159	-0.470	
12.50	2.31	0.01059	0.0079	4.242	-0.505	
12.75	2.36	0.01036	0.0077	4.342	-0.544	
13.00	2.40	0.01016	0.0075	4.447	-0.565	
13.25	2.45	0.00992	0.0073	4.540	-0.597	
13.50	2.49	0.00971	0.0071	4.639	-0.648	
13.75	2.54	0.00952	0.0070	4.810	-0.693	
14.00	2.59	0.00930	0.0068	4.891	-0.733	
14.50	2.68	0.00888	0.0064	5.046	-0.817	
15.00	2.77	0.00844	0.0060	5.200	-0.886	
15.50	2.86	0.00825	0.0058	5.402	-0.875	From DL
16.00	2.96	0.00781	0.0054	5.475	-0.969	
16.50	3.05	0.00742	0.0051	5.541	-1.003	
17.00	3.14	0.00706	0.0047	5.602	-1.061	

INTERCEPTOR B

Deployment: 0.036 in

Speed *(ft/s)*	**F_∇**	**C_T**	**C_R**	**Trim** deg	**Sinkage** in	
6.00	1.11	0.0194	0.0161	1.762	0.416	From RMB
8.00	1.48	0.0166	0.0136	3.377	0.182	
10.00	1.85	0.0129	0.0101	3.394	-0.182	
10.50	1.94	0.0124	0.0096	3.499	-0.252	
11.00	2.03	0.0119	0.0091	3.617	-0.322	
11.50	2.13	0.0114	0.0087	3.750	-0.378	
11.75	2.17	0.0112	0.0085	3.808	-0.411	
12.00	2.22	0.0109	0.0082	3.795	-0.423	
12.25	2.26	0.0108	0.0081	3.867	-0.463	
12.50	2.31	0.0105	0.0079	3.847	-0.490	
12.75	2.36	0.0104	0.0077	3.958	-0.510	
13.00	2.40	0.0101	0.0075	3.870	-0.527	
13.25	2.45	0.0099	0.0073	4.029	-0.568	
13.50	2.49	0.0097	0.0071	3.949	-0.573	
14.00	2.59	0.0093	0.0067	4.017	-0.626	
14.50	2.68	0.0090	0.0064	4.081	-0.687	
15.00	2.77	0.0086	0.0060	4.211	-0.750	
15.50	2.86	0.0083	0.0058	4.568	-0.739	From DL
16.00	2.96	0.0080	0.0055	4.648	-0.776	
16.50	3.05	0.0076	0.0052	4.702	-0.889	
17.00	3.14	0.0073	0.0049	4.729	-0.936	

INTERCEPTOR C

Deployment: 0.045 in

Speed *(ft/s)*	**F_∇**	**C_T**	**C_R**	**Trim** deg	**Sinkage** in	
6.00	1.11	0.0182	0.0150	1.672	0.426	From RMB
8.00	1.48	0.0159	0.0129	3.219	0.178	
10.00	1.85	0.0125	0.0096	2.954	-0.192	
10.50	1.94	0.0117	0.0089	2.897	-0.255	
11.00	2.03	0.0113	0.0085	2.934	-0.301	
11.50	2.13	0.0110	0.0082	2.982	-0.349	
11.75	2.17	0.0108	0.0080	3.016	-0.376	
12.00	2.22	0.0106	0.0079	3.059	-0.399	
12.25	2.26	0.0104	0.0077	3.073	-0.415	
12.50	2.31	0.0102	0.0075	3.141	-0.444	
12.75	2.36	0.0102	0.0075	3.195	-0.451	
13.00	2.40	0.0098	0.0072	3.197	-0.477	
13.25	2.45	0.0098	0.0071	3.295	-0.494	
13.50	2.49	0.0096	0.0069	3.333	-0.531	
14.00	2.59	0.0093	0.0066	3.432	-0.586	
14.50	2.68	0.0088	0.0062	3.553	-0.629	
15.00	2.77	0.0085	0.0060	3.614	-0.686	
15.50	2.86	0.0085	0.0060	3.789	-0.623	From DL
16.00	2.96	0.0082	0.0057	3.854	-0.671	
16.50	3.05	0.0078	0.0053	3.850	-0.713	
17.00	3.14	0.0075	0.0051	3.913	-0.772	

APPENDIX F. PRESSURE RESULTS

This appendix contains the non-dimensionalized pressure results for each configuration. This data is also available on the attached CD. Speeds of 15.00 ft/s and below are based on tests at RMB, and speeds above are from tests at DL. The distance of pressure taps from the transom, in absolute distance and relative to LOA, are shown in Table F-1 for reference.

Table F-1. Longitudinal Location of Pressure Taps

Ta	x, inches	x/LOA
P1	9.9688	0.166
P2	6.9688	0.116
P3	3.9688	0.066
P4	1.9688	0.033
P5	0.9688	0.016
P6	0.4688	0.008
P7	0.2188	0.004
P8	0.0938	0.002
P9	-0.0938	-0.002
P10	-0.9688	-0.016
P11	-1.8438	-0.031

For each configuration, two contour plots are included after the raw data. The one on the left shows the variation in C_p with longitudinal location relative to LOA on the x-axis, and non-dimensionalized speed on the y-axis. The graph to the right shows the difference between the C_p with the respective appendage and the C_p at the same point at the same speed in the bare-hull configuration (ΔC_p). This induced pressure coefficient shows the pressure caused directly by the appendage.

BARE HULL

Speed *(ft/s)*	F_∇	C_P P1	P2	P3	P4	P5	P6	P7	P8	P9	P10	P11	
6.000	1.11	0.351	0.333	0.319	0.236	0.213	0.125	0.096	0.057	-	-	-	From RMB
8.000	1.48	0.202	0.179	0.159	0.107	0.092	0.032	0.005	-0.019	-	-	-	
10.000	1.85	0.144	0.128	0.114	0.077	0.056	0.017	0.001	-0.017	-	-	-	
10.500	1.94	0.133	0.119	0.103	0.073	0.051	0.017	0.001	-0.022	-	-	-	
11.000	2.03	0.124	0.114	0.097	0.064	0.047	0.014	-0.004	-0.018	-	-	-	
11.500	2.13	0.115	0.101	0.092	0.062	0.042	0.014	0.001	-0.017	-	-	-	
11.750	2.17	0.112	0.102	0.088	0.060	0.042	0.013	-0.001	-0.017	-	-	-	
12.000	2.22	0.107	0.095	0.085	0.055	0.040	0.011	-0.002	-0.015	-	-	-	
12.250	2.26	0.106	0.098	0.083	0.056	0.038	0.010	-0.003	-0.016	-	-	-	
12.500	2.31	0.100	0.094	0.083	0.053	0.034	0.009	-0.004	-0.017	-	-	-	
12.750	2.36	0.098	0.089	0.078	0.053	0.037	0.009	-0.003	-0.018	-	-	-	
13.000	2.40	0.094	0.088	0.078	0.051	0.033	0.007	-0.004	-0.018	-	-	-	
13.250	2.45	0.092	0.083	0.075	0.049	0.033	0.006	-0.002	-0.019	-	-	-	
13.500	2.49	0.089	0.082	0.070	0.049	0.031	0.005	-0.003	-0.019	-	-	-	
14.000	2.59	0.082	0.077	0.067	0.045	0.030	0.005	-0.005	-0.018	-	-	-	
14.500	2.68	0.077	0.073	0.064	0.043	0.027	0.006	-0.006	-0.018	-	-	-	
15.000	2.77	0.071	0.068	0.060	0.038	0.026	0.004	-0.006	-0.018	-	-	-	
15.500	2.86	0.062	0.057	0.049	0.033	0.016	-0.001	-0.007	-0.021	-	-	-	From DL
16.000	2.96	0.061	0.056	0.049	0.035	0.018	0.001	-0.005	-0.017	-	-	-	
16.500	3.05	0.055	0.051	0.044	0.030	0.014	-0.002	-0.009	-0.020	-	-	-	
17.000	3.14	0.053	0.049	0.043	0.030	0.016	0.000	-0.005	-0.017	-	-	-	

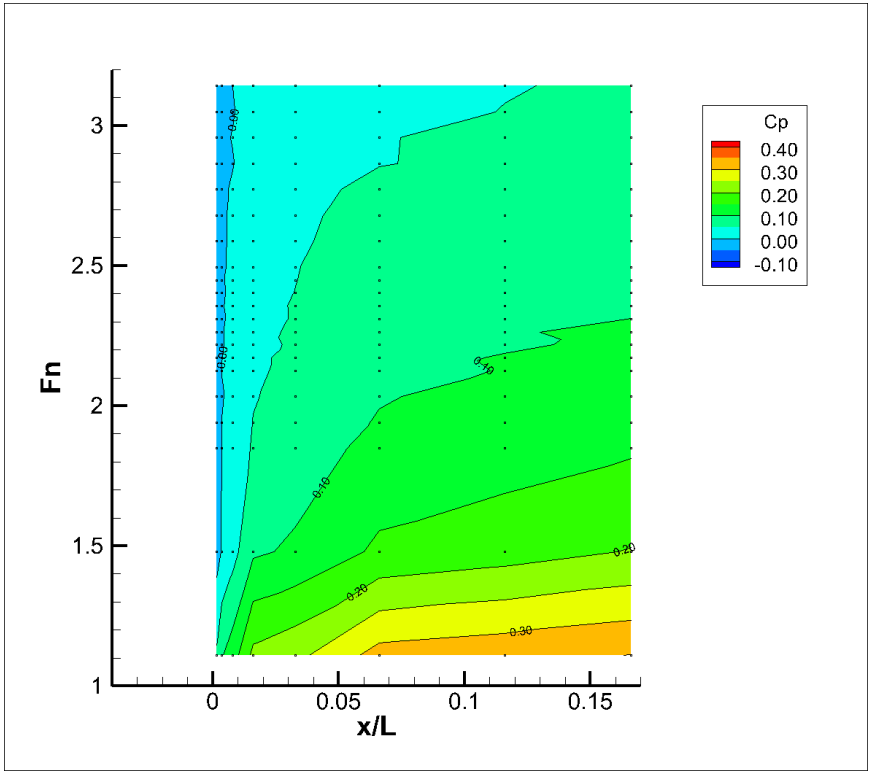

Figure F-1. Bare Hull Pressure Plot

TRIM TAB A

Deployment: 1 deg

Speed (ft/s)	F_∇	C_P P1	P2	P3	P4	P5	P6	P7	P8	P9	P10	P11	
6.000	1.11	0.340	0.322	0.304	0.257	0.238	0.208	0.207	0.206	0.202	0.147	0.037	From RMB
8.000	1.48	0.191	0.169	0.158	0.125	0.118	0.097	0.096	0.105	0.105	0.072	0.007	
10.000	1.85	0.133	0.121	0.110	0.089	0.078	0.064	0.062	0.069	0.082	0.044	0.001	
10.500	1.94	0.126	0.116	0.105	0.081	0.072	0.061	0.059	0.064	0.082	0.041	-0.001	
11.000	2.03	0.116	0.107	0.098	0.078	0.068	0.056	0.058	0.062	0.079	0.039	0.002	
11.500	2.13	0.110	0.101	0.091	0.073	0.063	0.052	0.051	0.057	0.076	0.038	0.003	
11.750	2.17	0.107	0.099	0.088	0.071	0.063	0.053	0.051	0.054	0.078	0.037	0.003	
12.000	2.22	0.104	0.095	0.085	0.069	0.060	0.049	0.048	0.054	0.075	0.034	0.001	
12.250	2.26	0.101	0.093	0.085	0.066	0.058	0.048	0.047	0.051	0.076	0.035	0.001	
12.500	2.31	0.098	0.092	0.081	0.065	0.055	0.045	0.047	0.052	0.074	0.035	0.003	
12.750	2.36	0.093	0.086	0.079	0.063	0.054	0.042	0.043	0.049	0.074	0.034	-0.001	
13.000	2.40	0.090	0.082	0.075	0.062	0.055	0.043	0.039	0.049	0.073	0.032	0.003	
13.250	2.45	0.089	0.082	0.074	0.061	0.052	0.042	0.041	0.047	0.071	0.033	0.000	
13.500	2.49	0.083	0.079	0.072	0.058	0.051	0.041	0.040	0.047	0.071	0.030	0.000	
14.000	2.59	0.079	0.075	0.068	0.055	0.049	0.038	0.037	0.044	0.069	0.030	0.001	
14.500	2.68	0.072	0.069	0.063	0.051	0.046	0.035	0.036	0.041	0.070	0.027	-0.001	
15.000	2.77	0.068	0.067	0.060	0.051	0.044	0.035	0.035	0.040	0.066	0.028	-0.002	
15.500	2.86	0.064	0.061	0.056	0.047	0.042	0.032	0.031	0.045	-	0.023	-0.003	From DL
16.000	2.96	0.062	0.059	0.054	0.046	0.041	0.031	0.031	0.045	-	0.024	-0.001	
16.500	3.05	0.058	0.055	0.051	0.044	0.039	0.029	0.029	0.043	-	0.023	-0.002	
17.000	3.14	0.054	0.051	0.047	0.040	0.036	0.027	0.027	0.041	-	0.022	-0.001	

Note: Pressure tap 9 was not working during testing at DL.

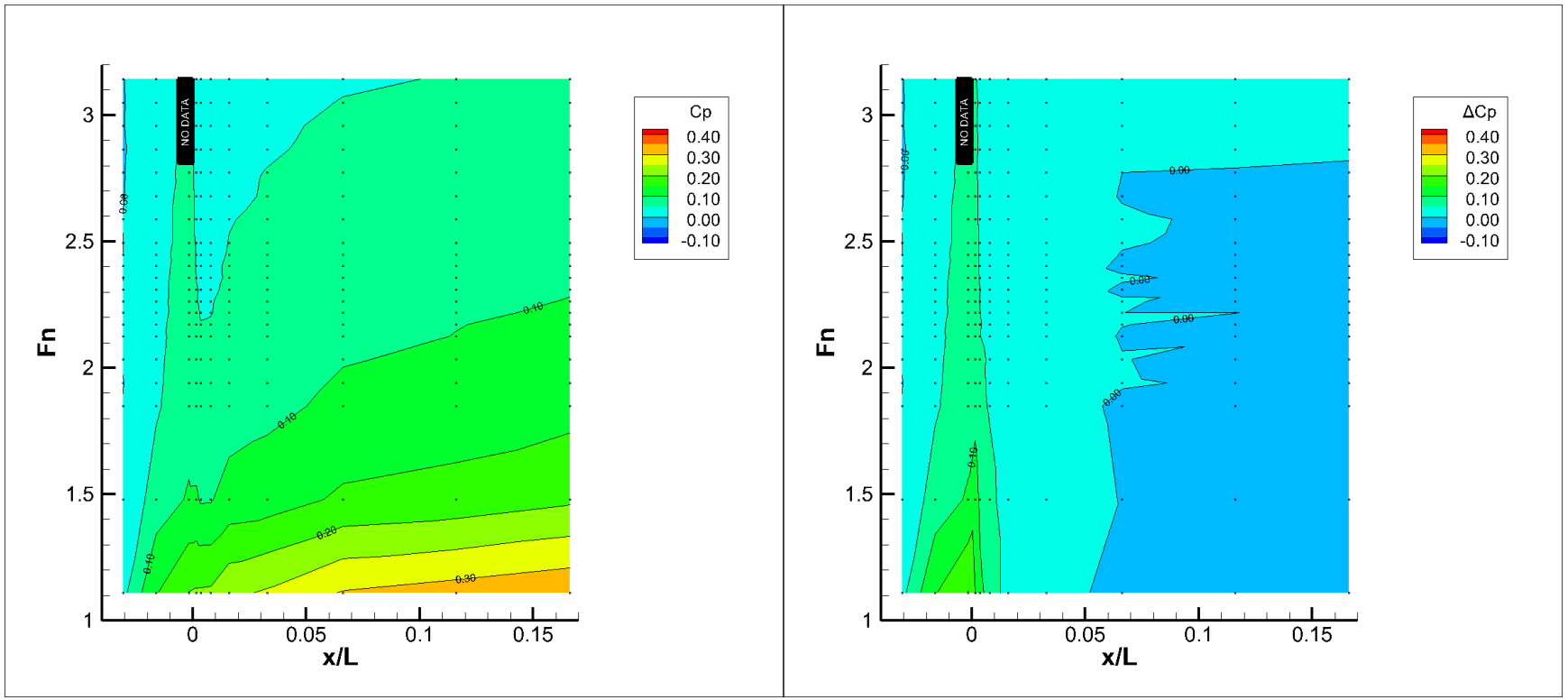

Figure F-2. 1.00° Trim Tab A Pressure and Induced Pressure Plot

TRIM TAB B

Deployment: 3 deg

Speed (ft/s)	F_∇	C_P P1	P2	P3	P4	P5	P6	P7	P8	P9	P10	P11	
6.000	1.11	0.261	0.273	0.234	0.191	0.189	0.157	0.173	0.183	0.234	0.099	-0.052	From RMB
8.000	1.48	0.171	0.175	0.146	0.122	0.124	0.109	0.122	0.128	0.174	0.073	-0.014	
10.000	1.85	0.105	0.085	0.093	0.076	0.074	0.073	0.077	0.083	0.141	0.042	-0.023	
10.500	1.94	0.094	0.090	0.078	0.064	0.069	0.062	0.068	0.076	0.134	0.033	-0.031	
11.000	2.03	0.091	0.091	0.077	0.064	0.068	0.063	0.071	0.079	0.138	0.037	-0.026	
11.500	2.13	0.094	0.093	0.081	0.069	0.074	0.069	0.075	0.080	0.144	0.044	-0.019	
11.750	2.17	0.090	0.091	0.079	0.067	0.069	0.068	0.073	0.080	0.142	0.042	-0.017	
12.000	2.22	0.083	0.082	0.071	0.064	0.065	0.063	0.067	0.074	0.145	0.040	-0.021	
12.250	2.26	0.080	0.081	0.070	0.061	0.057	0.062	0.067	0.075	0.141	0.038	-0.022	
12.500	2.31	0.076	0.076	0.066	0.057	0.060	0.058	0.065	0.071	0.141	0.035	-0.022	
12.750	2.36	0.082	0.082	0.074	0.066	0.069	0.068	0.073	0.081	0.152	0.044	-0.011	
13.000	2.40	0.077	0.078	0.069	0.061	0.064	0.063	0.069	0.074	0.145	0.040	-0.015	
13.250	2.45	0.075	0.074	0.067	0.060	0.057	0.063	0.068	0.076	0.146	0.045	-0.015	
13.500	2.49	0.068	0.067	0.061	0.056	0.054	0.058	0.064	0.071	0.143	0.038	-0.018	
14.000	2.59	0.069	0.067	0.064	0.058	0.056	0.061	0.068	0.075	0.149	0.042	-0.013	
14.500	2.68	0.065	0.065	0.061	0.057	0.060	0.060	0.068	0.073	0.148	0.043	-0.011	
15.000	2.77	0.055	0.054	0.052	0.049	0.052	0.054	0.060	0.067	0.143	0.036	-0.016	
15.500	2.86	0.065	0.062	0.062	0.061	0.065	0.066	0.075	0.092	0.157	0.052	0.010	From DL
16.000	2.96	0.060	0.058	0.058	0.058	0.062	0.064	0.073	0.089	0.158	0.050	0.008	
16.500	3.05	0.056	0.055	0.055	0.056	0.061	0.062	0.072	0.088	0.158	0.050	0.008	
17.000	3.14	0.053	0.051	0.052	0.053	0.058	0.061	0.070	0.087	0.159	0.049	0.007	

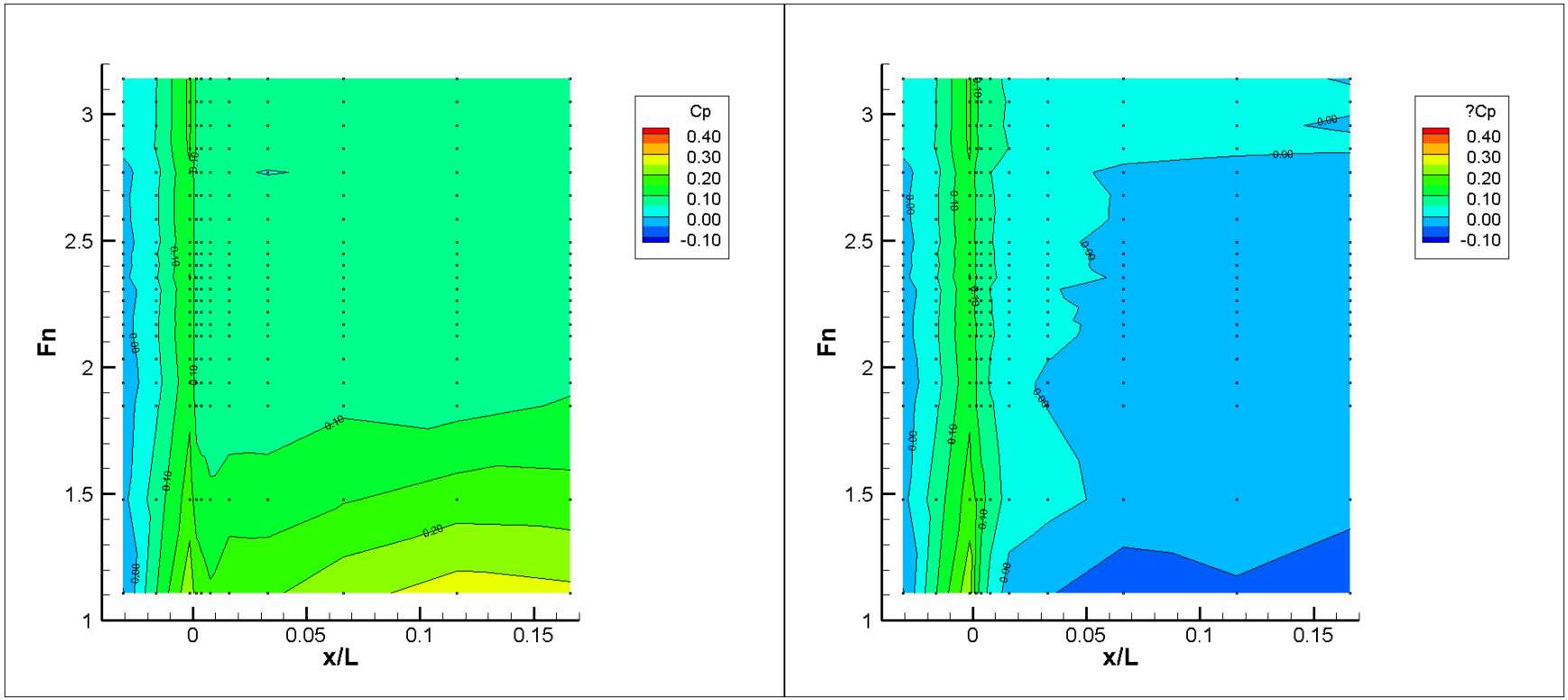

Figure F-3. 3.00° Trim Tab B Pressure and Induced Pressure Plot

TRIM TAB C

Deployment: 5 deg

Speed (ft/s)	F_∇	C_P P1	P2	P3	P4	P5	P6	P7	P8	P9	P10	P11	
6.000	1.11	0.323	0.300	0.297	0.273	0.277	0.274	0.290	0.293	0.341	0.183	0.036	From RMB
8.000	1.48	0.172	0.158	0.156	0.141	0.156	0.162	0.180	0.188	0.230	0.102	0.003	
10.000	1.85	0.122	0.112	0.111	0.105	0.118	0.127	0.144	0.148	0.188	0.079	0.001	
10.500	1.94	0.114	0.105	0.105	0.102	0.112	0.120	0.139	0.146	0.185	0.078	0.000	
11.000	2.03	0.106	0.097	0.094	0.096	0.108	0.116	0.134	0.142	0.185	0.074	0.000	
11.500	2.13	0.101	0.093	0.092	0.093	0.104	0.113	0.131	0.142	0.181	0.072	0.000	
11.750	2.17	0.097	0.091	0.089	0.090	0.102	0.111	0.131	0.138	0.178	0.072	0.001	
12.000	2.22	0.094	0.087	0.086	0.087	0.100	0.109	0.130	0.137	0.179	0.070	0.001	
12.250	2.26	0.092	0.086	0.085	0.087	0.100	0.109	0.129	0.135	0.179	0.071	0.002	
12.500	2.31	0.088	0.082	0.083	0.085	0.095	0.105	0.127	0.133	0.180	0.069	0.000	
12.750	2.36	0.086	0.079	0.080	0.083	0.095	0.105	0.125	0.134	0.179	0.068	0.001	
13.000	2.40	0.083	0.078	0.080	0.080	0.095	0.103	0.125	0.133	0.179	0.069	0.001	
13.250	2.45	0.080	0.076	0.078	0.081	0.093	0.107	0.125	0.133	0.177	0.069	0.000	
13.500	2.49	0.077	0.075	0.076	0.082	0.092	0.105	0.123	0.130	0.177	0.068	0.002	
14.000	2.59	0.072	0.070	0.072	0.076	0.090	0.100	0.122	0.130	0.176	0.067	0.000	
14.500	2.68	0.063	0.061	0.065	0.069	0.085	0.096	0.116	0.126	0.174	0.061	-0.005	
15.000	2.77	0.063	0.064	0.066	0.076	0.090	0.099	0.121	0.130	0.175	0.066	0.001	
15.500	2.86	0.061	0.060	0.064	0.073	0.087	0.101	0.118	0.126	0.186	0.070	0.008	From DL
16.000	2.96	0.057	0.057	0.061	0.071	0.084	0.099	0.116	0.125	0.185	0.069	0.008	
16.500	3.05	0.053	0.053	0.058	0.068	0.082	0.097	0.115	0.123	0.184	0.069	0.007	
17.000	3.14	0.049	0.050	0.056	0.067	0.081	0.096	0.114	0.122	0.185	0.074	0.008	

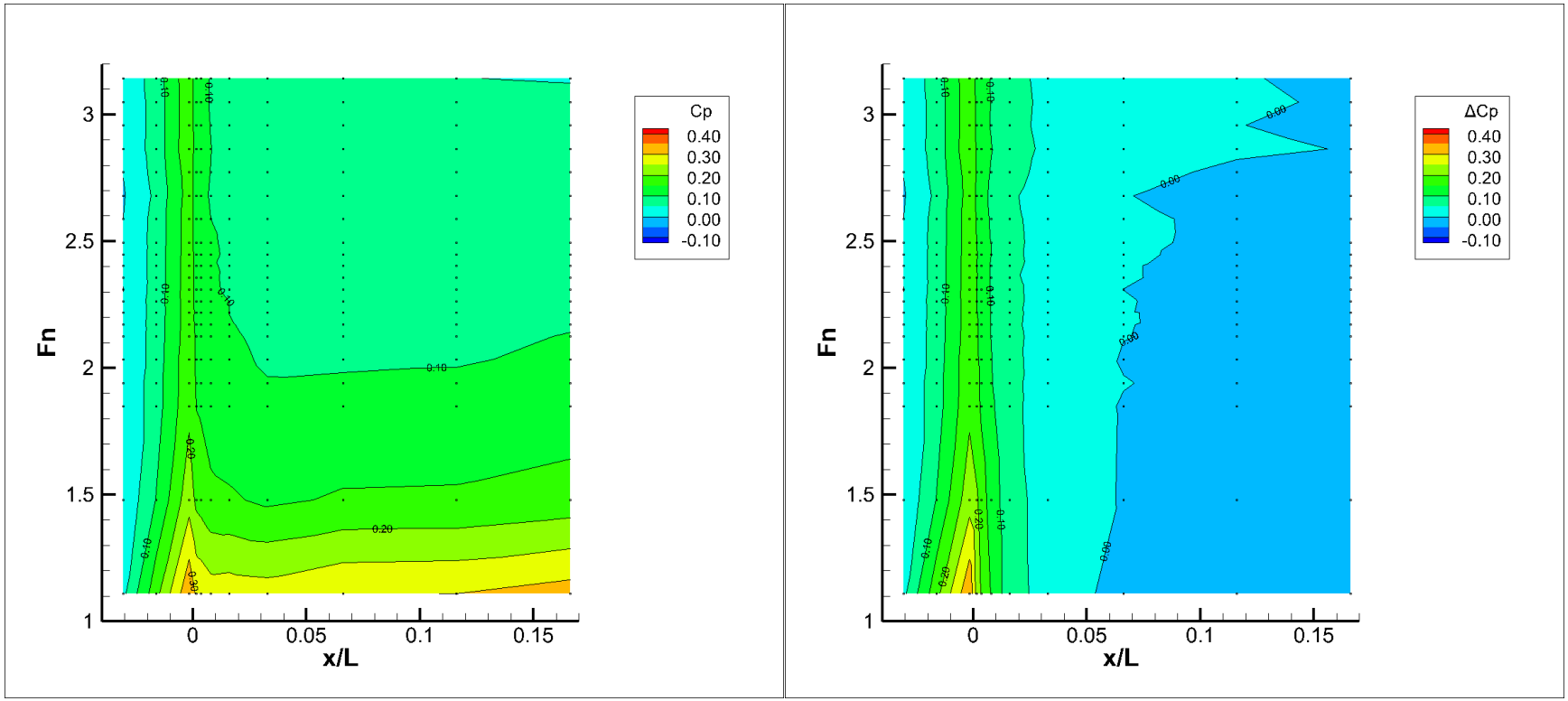

Figure F-4. 5.00° Trim Tab C Pressure and Induced Pressure Plot

INTERCEPTOR A

Deployment: 0.023 in

Speed (ft/s)	F_V	C_P P1	P2	P3	P4	P5	P6	P7	P8	P9	P10	P11	
6.000	1.11	0.352	0.329	0.315	0.275	0.235	0.199	0.201	0.208	-	-	-	From RMB
8.000	1.48	0.198	0.181	0.164	0.143	0.115	0.105	0.112	0.130	-	-	-	
10.000	1.85	0.138	0.126	0.115	0.099	0.087	0.080	0.088	0.110	-	-	-	
10.500	1.94	0.129	0.116	0.108	0.096	0.083	0.075	0.086	0.106	-	-	-	
11.000	2.03	0.120	0.108	0.100	0.086	0.078	0.072	0.083	0.105	-	-	-	
11.500	2.13	0.112	0.103	0.096	0.087	0.077	0.074	0.085	0.108	-	-	-	
11.750	2.17	0.108	0.100	0.091	0.086	0.076	0.071	0.081	0.103	-	-	-	
12.000	2.22	0.105	0.097	0.090	0.079	0.075	0.070	0.084	0.108	-	-	-	
12.250	2.26	0.101	0.093	0.087	0.075	0.072	0.073	0.083	0.107	-	-	-	
12.500	2.31	0.098	0.091	0.086	0.078	0.072	0.068	0.082	0.104	-	-	-	
12.750	2.36	0.095	0.088	0.082	0.074	0.074	0.070	0.079	0.103	-	-	-	
13.000	2.40	0.092	0.085	0.080	0.073	0.072	0.068	0.080	0.104	-	-	-	
13.250	2.45	0.089	0.084	0.079	0.068	0.068	0.068	0.081	0.104	-	-	-	
13.500	2.49	0.086	0.081	0.077	0.070	0.067	0.067	0.080	0.104	-	-	-	
13.750	2.54	0.083	0.079	0.076	0.069	0.067	0.067	0.080	0.095	-	-	-	
14.000	2.59	0.081	0.077	0.073	0.067	0.065	0.064	0.080	0.103	-	-	-	
14.500	2.68	0.074	0.071	0.068	0.063	0.062	0.064	0.078	0.103	-	-	-	
15.000	2.77	0.071	0.068	0.066	0.061	0.061	0.062	0.079	0.103	-	-	-	
15.500	2.86	0.063	0.061	0.059	0.055	0.057	0.061	0.081	0.103	-	-	-	From DL
16.000	2.96	0.059	0.056	0.055	0.053	0.055	0.061	0.080	0.103	-	-	-	
16.500	3.05	0.055	0.053	0.052	0.051	0.054	0.059	0.080	0.103	-	-	-	
17.000	3.14	0.051	0.048	0.048	0.048	0.052	0.058	0.079	0.101	-	-	-	

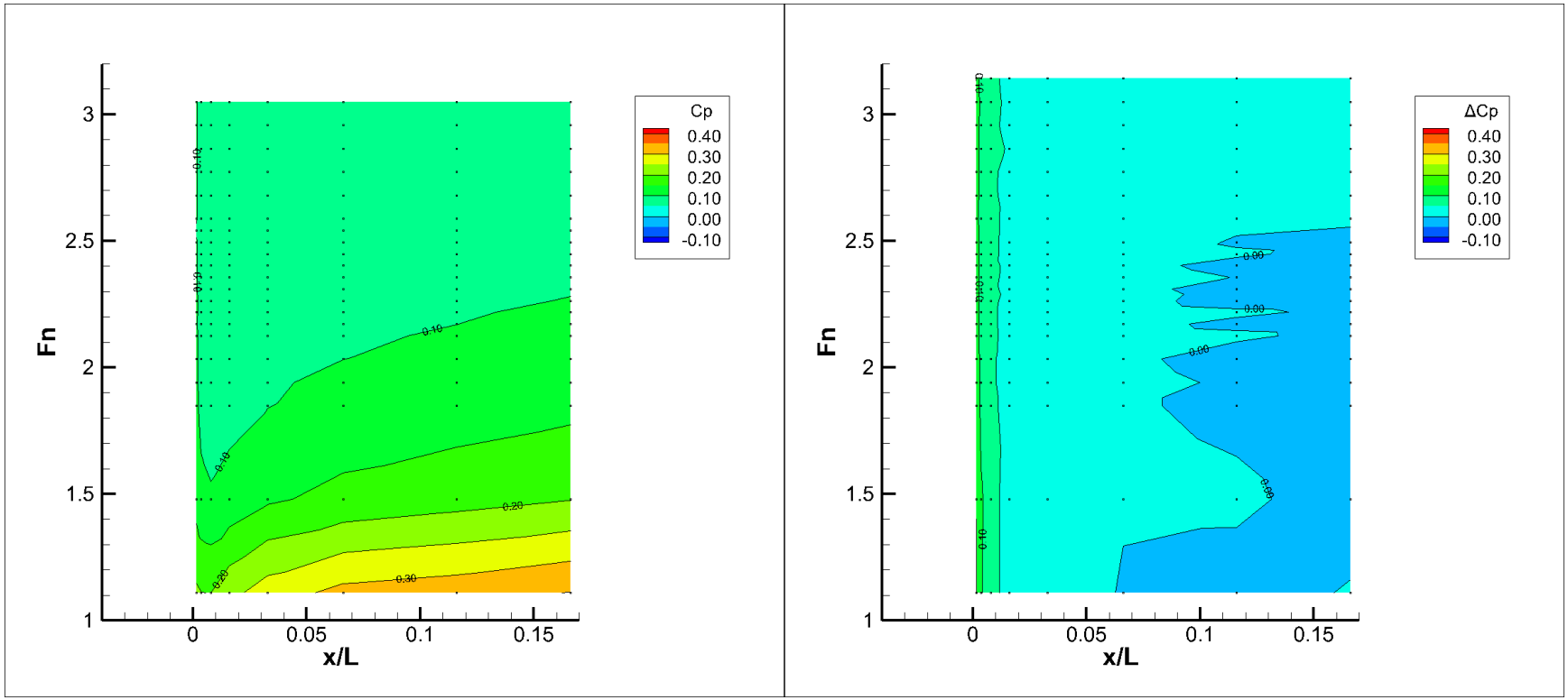

Figure F-5. 0.023” Interceptor A Pressure and Induced Pressure Plot

INTERCEPTOR B

Deployment: 0.036 in

Speed (ft/s)	F_V	C_P P1	P2	P3	P4	P5	P6	P7	P8	P9	P10	P11	
6.000	1.11	0.347	0.326	0.317	0.256	0.239	0.240	0.231	0.253	-	-	-	From RMB
8.000	1.48	0.199	0.177	0.165	0.139	0.122	0.134	0.140	0.173	-	-	-	
10.000	1.85	0.136	0.124	0.114	0.097	0.090	0.102	0.114	0.148	-	-	-	
10.500	1.94	0.127	0.116	0.108	0.090	0.093	0.103	0.113	0.147	-	-	-	
11.000	2.03	0.118	0.109	0.102	0.092	0.089	0.098	0.114	0.147	-	-	-	
11.500	2.13	0.111	0.103	0.098	0.085	0.086	0.096	0.113	0.144	-	-	-	
11.750	2.17	0.106	0.099	0.094	0.082	0.085	0.100	0.113	0.148	-	-	-	
12.000	2.22	0.102	0.094	0.091	0.071	0.088	0.110	0.132	0.163	-	-	-	
12.250	2.26	0.099	0.094	0.090	0.082	0.092	0.108	0.133	0.167	-	-	-	
12.500	2.31	0.096	0.090	0.090	0.086	0.101	0.124	0.148	0.186	-	-	-	
12.750	2.36	0.094	0.087	0.087	0.086	0.099	0.121	0.146	0.182	-	-	-	
13.000	2.40	0.090	0.085	0.085	0.087	0.102	0.128	0.151	0.191	-	-	-	
13.250	2.45	0.087	0.082	0.083	0.078	0.097	0.128	0.151	0.189	-	-	-	
13.500	2.49	0.083	0.079	0.081	0.083	0.099	0.128	0.151	0.190	-	-	-	
14.000	2.59	0.078	0.075	0.079	0.080	0.098	0.127	0.154	0.195	-	-	-	
14.500	2.68	0.072	0.070	0.073	0.080	0.098	0.126	0.155	0.196	-	-	-	
15.000	2.77	0.066	0.065	0.069	0.071	0.096	0.124	0.155	0.196	-	-	-	
15.500	2.86	0.063	0.063	0.069	0.085	0.111	0.145	0.187	0.231	-	-	-	From DL
16.000	2.96	0.058	0.059	0.066	0.083	0.111	0.146	0.190	0.234	-	-	-	
16.500	3.05	0.054	0.055	0.062	0.080	0.109	0.145	0.188	0.232	-	-	-	
17.000	3.14	0.051	0.053	0.060	0.080	0.110	0.146	0.190	0.234	-	-	-	

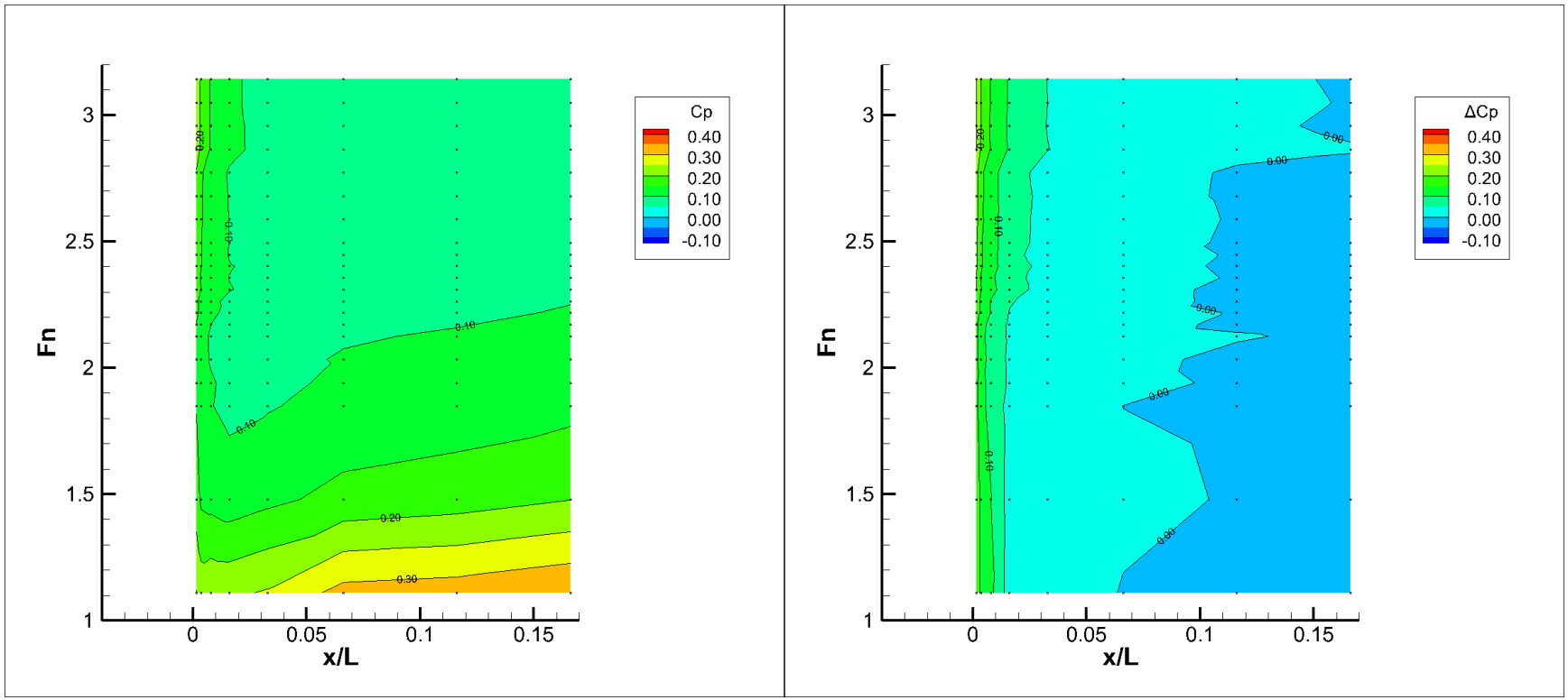

Figure F-6. 0.036” Interceptor B Pressure and Induced Pressure Plot

INTERCEPTOR C

Deployment: 0.045 in

Speed (ft/s)	F_V	C_P P1	P2	P3	P4	P5	P6	P7	P8	P9	P10	P11	
6.000	1.11	0.348	0.327	0.316	0.266	0.272	0.254	0.292	0.337	-	-	-	From RMB
8.000	1.48	0.189	0.177	0.166	0.151	0.167	0.186	0.221	0.269	-	-	-	
10.000	1.85	0.133	0.122	0.119	0.120	0.144	0.173	0.214	0.262	-	-	-	
10.500	1.94	0.120	0.112	0.113	0.116	0.141	0.171	0.213	0.257	-	-	-	
11.000	2.03	0.111	0.104	0.105	0.113	0.139	0.171	0.211	0.256	-	-	-	
11.500	2.13	0.102	0.098	0.098	0.110	0.138	0.170	0.213	0.260	-	-	-	
11.750	2.17	0.101	0.096	0.099	0.110	0.136	0.170	0.211	0.259	-	-	-	
12.000	2.22	0.098	0.092	0.095	0.107	0.136	0.168	0.214	0.261	-	-	-	
12.250	2.26	0.095	0.090	0.094	0.106	0.135	0.172	0.219	0.262	-	-	-	
12.500	2.31	0.090	0.088	0.093	0.107	0.134	0.170	0.215	0.261	-	-	-	
12.750	2.36	0.088	0.085	0.089	0.104	0.135	0.169	0.213	0.261	-	-	-	
13.000	2.40	0.085	0.082	0.088	0.104	0.133	0.171	0.214	0.260	-	-	-	
13.250	2.45	0.081	0.080	0.087	0.104	0.133	0.170	0.214	0.263	-	-	-	
13.500	2.49	0.080	0.078	0.085	0.101	0.134	0.170	0.214	0.263	-	-	-	
14.000	2.59	0.074	0.074	0.082	0.101	0.134	0.171	0.215	0.262	-	-	-	
14.500	2.68	0.070	0.070	0.079	0.099	0.133	0.171	0.216	0.261	-	-	-	
15.000	2.77	0.066	0.066	0.076	0.097	0.131	0.171	0.216	0.263	-	-	-	
15.500	2.86	0.063	0.064	0.073	0.093	0.125	0.165	0.212	0.257	-	-	-	From DL
16.000	2.96	0.059	0.060	0.070	0.091	0.125	0.165	0.213	0.257	-	-	-	
16.500	3.05	0.054	0.056	0.066	0.089	0.123	0.165	0.213	0.257	-	-	-	
17.000	3.14	0.051	0.053	0.064	0.088	0.123	0.165	0.214	0.257	-	-	-	

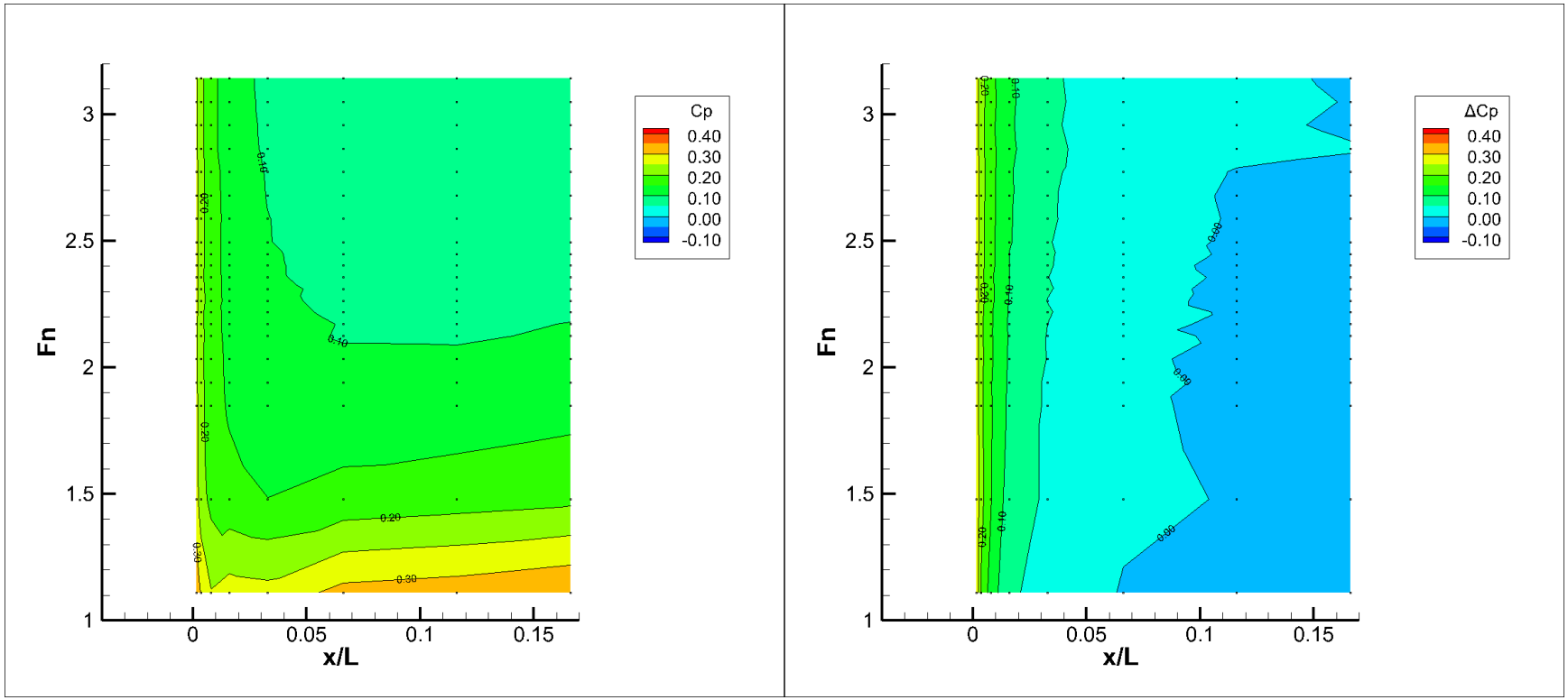

Figure F-7. 0.045” Interceptor B Pressure and Induced Pressure Plot

APPENDIX G. UNCERTAINTY ANALYSIS

This appendix contains the values measured for resistance, trim, heave, surface area, and pressure for the speeds that were repeated for each configuration (excluding those repeated for the purpose of comparing DL results to RMB results). From these repeated runs, uncertainty was calculated as described in the *Uncertainty* section of *Theory*. Percentage uncertainty is not calculated for pressures, as pressure is relative and is often near zero, so the percentage is artificially high.

Table G-1 shows the speeds for which configurations were used to calculate uncertainty and are included in this appendix.

Table G-1. Speeds Tested for Uncertainty

	Speed, ft/s																				
	6.00	8.00	10.00	10.50	11.00	11.50	11.75	12.00	12.25	12.50	12.75	13.00	13.25	13.50	14.00	14.50	15.00	15.50	16.00	16.50	17.00
BH		■						■							■						■
TA			■					■							■						■
TB				■					■							■				■	
TC					■			■							■			■			
IA	■					■								■						■	
IB			■							■			■			■					■
IC				■								■							■		

Table G-2. Uncertainty Analysis for Bare Hull (8.00 ft/s)

ID	Run Name	F_∇	R_t	Trim	Heave	S	Total Pressure (psi)										
			lbf	deg	in	ft^2	P1	P2	P3	P4	P5	P6	P7	P8	P9	P10	P11
5	BH-8.00	1.478	5.596	3.835	-0.190	4.37	0.086	0.079	0.070	0.047	0.041	0.014	0.002	-0.008	-	-	-
14	BH-8.00B	1.478	5.587	3.828	-0.188	4.41	0.088	0.075	0.068	0.047	0.041	0.015	0.003	-0.008	-	-	-
21	BH-8.00C	1.478	5.608	3.707	-0.190	4.41	0.087	0.077	0.068	0.044	0.037	0.012	0.001	-0.009	-	-	-
Average			5.597	3.790	-0.189	4.39	0.087	0.077	0.069	0.046	0.040	0.014	0.002	-0.008	-	-	-
Std Dev			0.010	0.072	0.001	0.02	0.001	0.002	0.001	0.002	0.003	0.001	0.001	0.001	-	-	-
Standard Error			0.006	0.042	0.001	0.01	0.000	0.001	0.001	0.001	0.002	0.001	0.001	0.000	-	-	-
Uncertainty			0.018	0.125	0.002	0.04	0.001	0.003	0.002	0.003	0.005	0.002	0.002	0.001	-	-	-
%Uncertainty			0.3%	3.3%	-1.1%	1.0%	not calculated for pressure										

Table G-3. Uncertainty Analysis for Bare Hull (12.00 ft/s)

ID	Run Name	F_∇	R_t	Trim	Heave	S	Total Pressure (psi)										
			lbf	deg	in	ft^2	P1	P2	P3	P4	P5	P6	P7	P8	P9	P10	P11
3	BH-12.00	2.218	8.273	4.702	0.508	4.17	0.102	0.094	0.080	0.051	0.037	0.009	-0.002	-0.015	-	-	-
11	BH-12.00B	2.218	8.311	4.728	0.503	4.17	0.105	0.092	0.085	0.053	0.039	0.010	-0.001	-0.013	-	-	-
15	BH-12.00C	2.218	8.291	4.714	0.504	4.16	0.105	0.090	0.082	0.054	0.039	0.012	-0.003	-0.015	-	-	-
Average			8.292	4.715	0.505	4.17	0.104	0.092	0.082	0.053	0.039	0.010	-0.002	-0.014	-	-	-
Std Dev			0.019	0.013	0.003	0.01	0.002	0.002	0.002	0.002	0.001	0.002	0.001	0.001	-	-	-
Standard Error			0.011	0.007	0.002	0.00	0.001	0.001	0.001	0.001	0.001	0.001	0.001	0.001	-	-	-
Uncertainty			0.033	0.022	0.005	0.01	0.003	0.003	0.004	0.003	0.002	0.003	0.002	0.002	-	-	-
%Uncertainty			0.4%	0.5%	0.9%	0.2%	not calculated for pressure										

Table G-4. Uncertainty Analysis for Bare Hull (14.00 ft/s)

ID	Run Name	F_∇	R_t	Trim	Heave	S	Total Pressure (psi)										
			lbf	deg	in	ft^2	P1	P2	P3	P4	P5	P6	P7	P8	P9	P10	P11
23	BH-14.00C	2.587	9.377	5.617	0.832	3.96	0.108	0.101	0.088	0.059	0.038	0.005	-0.008	-0.025	-	-	-
26	BH-14.00D	2.587	9.354	5.615	0.826	3.97	0.108	0.101	0.088	0.062	0.041	0.006	-0.007	-0.024	-	-	-
28	BH-14.00E	2.587	9.372	5.628	0.829	3.95	0.109	0.101	0.088	0.059	0.041	0.009	-0.004	-0.023	-	-	-
Average			9.368	5.620	0.829	3.96	0.108	0.101	0.088	0.060	0.040	0.007	-0.006	-0.024	-	-	-
Std Dev			0.012	0.007	0.003	0.01	0.001	0.000	0.000	0.002	0.002	0.002	0.002	0.001	-	-	-
Standard Error			0.007	0.004	0.002	0.00	0.000	0.000	0.000	0.001	0.001	0.001	0.001	0.001	-	-	-
Uncertainty			0.021	0.012	0.005	0.01	0.001	0.000	0.001	0.003	0.003	0.003	0.004	0.002	-	-	-
%Uncertainty			0.2%	0.2%	0.6%	0.3%	not calculated for pressure										

Table G-5. Uncertainty Analysis for Bare Hull (17.00 ft/s)

ID	Run Name	F_∇	R_t	Trim	Heave	S	Total Pressure (psi)										
			lbf	deg	in	ft^2	P1	P2	P3	P4	P5	P6	P7	P8	P9	P10	P11
204	BH_17.00_DL	3.142	9.869	6.531	1.240	3.65	0.104	0.095	0.083	0.059	0.031	0.000	-0.011	-0.033	-	-	-
205	BH_17.00B_DL	3.142	9.879	6.540	1.236	3.65	0.104	0.096	0.084	0.060	0.032	0.000	-0.009	-0.032	-	-	-
206	BH_17.00C_DL	3.142	9.903	6.557	1.251	3.65	0.102	0.094	0.082	0.058	0.029	-0.003	-0.011	-0.035	-	-	-
Average			9.884	6.543	1.242	3.65	0.103	0.095	0.083	0.059	0.031	-0.001	-0.010	-0.033	-	-	-
Std Dev			0.018	0.013	0.008	0.00	0.001	0.001	0.001	0.001	0.001	0.002	0.001	0.002	-	-	-
Standard Error			0.010	0.008	0.004	0.00	0.001	0.001	0.001	0.001	0.001	0.001	0.000	0.001	-	-	-
Uncertainty			0.031	0.023	0.013	0.00	0.002	0.002	0.002	0.002	0.002	0.003	0.001	0.003	-	-	-
%Uncertainty			0.3%	0.4%	1.0%	0.1%	not calculated for pressure										

Table G-6. Uncertainty Analysis for Trim Tab A (10.00 ft/s)

ID	Run Name	F_∇	R_t	Trim	Heave	S	Total Pressure (psi)										
			lbf	deg	in	ft^2	P1	P2	P3	P4	P5	P6	P7	P8	P9	P10	P11
174	TA_10.00	1.848	6.593	3.337	0.188	4.37	0.089	0.081	0.073	0.059	0.052	0.042	0.042	0.048	0.055	0.029	0.000
186	TA_10.00B	1.848	6.717	3.324	0.179	4.38	0.089	0.081	0.074	0.061	0.053	0.044	0.042	0.045	0.055	0.031	0.001
192	TA_10.00C	1.848	6.669	3.334	0.181	4.37	0.091	0.082	0.075	0.060	0.052	0.042	0.042	0.045	0.055	0.030	0.001
Average			6.660	3.332	0.182	4.37	0.090	0.081	0.074	0.060	0.052	0.043	0.042	0.046	0.055	0.030	0.001
Std Dev			0.062	0.007	0.005	0.00	0.001	0.001	0.001	0.001	0.000	0.001	0.000	0.002	0.000	0.001	0.001
Standard Error			0.036	0.004	0.003	0.00	0.000	0.000	0.000	0.000	0.000	0.001	0.000	0.001	0.000	0.000	0.000
Uncertainty			0.108	0.012	0.008	0.00	0.001	0.001	0.001	0.001	0.001	0.002	0.000	0.003	0.001	0.001	0.001
%Uncertainty			1.6%	0.4%	4.5%	0.1%	not calculated for pressure										

Table G-7. Uncertainty Analysis for Trim Tab A (12.00 ft/s)

ID	Run Name	F_∇	R_t	Trim	Heave	S	Total Pressure (psi)										
			lbf	deg	in	ft^2	P1	P2	P3	P4	P5	P6	P7	P8	P9	P10	P11
177	TA_12.00	2.218	8.119	3.993	0.431	4.26	0.101	0.092	0.082	0.065	0.058	0.048	0.046	0.054	0.074	0.031	0.005
180	TA_12.00B	2.218	8.127	3.979	0.416	4.25	0.101	0.093	0.082	0.067	0.058	0.048	0.046	0.052	0.071	0.033	-0.002
188	TA_12.00C	2.218	8.158	3.977	0.423	4.25	0.100	0.092	0.083	0.068	0.058	0.046	0.048	0.052	0.073	0.034	0.001
Average			8.135	3.983	0.423	4.25	0.101	0.092	0.083	0.067	0.058	0.047	0.047	0.053	0.073	0.033	0.001
Std Dev			0.020	0.009	0.008	0.00	0.000	0.000	0.001	0.002	0.000	0.001	0.001	0.001	0.001	0.001	0.003
Standard Error			0.012	0.005	0.004	0.00	0.000	0.000	0.000	0.001	0.000	0.001	0.001	0.001	0.001	0.001	0.002
Uncertainty			0.035	0.015	0.013	0.01	0.001	0.001	0.001	0.003	0.000	0.002	0.002	0.002	0.002	0.002	0.006
%Uncertainty			0.4%	0.4%	3.1%	0.1%	not calculated for pressure										

Table G-8. Uncertainty Analysis for Trim Tab A (14.00 ft/s)

ID	Run Name	F_∇	R_t	Trim	Heave	S	Total Pressure (psi)										
			lbf	deg	in	ft^2	P1	P2	P3	P4	P5	P6	P7	P8	P9	P10	P11
182	TA_14.00	2.587	9.402	4.851	0.708	4.08	0.104	0.099	0.090	0.073	0.063	0.048	0.049	0.057	0.092	0.040	0.002
185	TA_14.00B	2.587	9.402	4.847	0.709	4.08	0.104	0.097	0.090	0.073	0.066	0.051	0.047	0.058	0.091	0.040	0.001
195	TA_14.00C	2.587	9.407	4.838	0.704	4.08	0.103	0.100	0.090	0.073	0.065	0.051	0.050	0.058	0.092	0.040	0.000
Average			9.404	4.845	0.707	4.08	0.104	0.099	0.090	0.073	0.064	0.050	0.049	0.057	0.091	0.040	0.001
Std Dev			0.003	0.007	0.003	0.00	0.001	0.001	0.000	0.000	0.001	0.002	0.001	0.001	0.001	0.000	0.001
Standard Error			0.002	0.004	0.002	0.00	0.000	0.001	0.000	0.000	0.001	0.001	0.001	0.000	0.000	0.000	0.001
Uncertainty			0.006	0.012	0.005	0.01	0.001	0.002	0.001	0.001	0.002	0.003	0.002	0.001	0.001	0.001	0.002
%Uncertainty			0.1%	0.2%	0.6%	0.2%	not calculated for pressure										

Table G-9. Uncertainty Analysis for Trim Tab A (17.00 ft/s)

ID	Run Name	F_∇	R_t	Trim	Heave	S	Total Pressure (psi)										
			lbf	deg	in	ft^2	P1	P2	P3	P4	P5	P6	P7	P8	P9	P10	P11
233	TA_17.00_DL	3.142	10.320	5.915	1.164	3.75	0.106	0.101	0.093	0.079	0.071	0.053	0.053	0.080	0.057	0.042	-0.001
236	TA_17.00B_DL	3.142	10.373	5.919	1.130	3.76	0.105	0.100	0.092	0.078	0.069	0.051	0.052	0.079	0.057	0.043	-0.001
238	TA_17.00C_DL	3.142	10.366	5.927	1.134	3.77	0.104	0.099	0.091	0.077	0.068	0.051	0.052	0.079	0.056	0.041	-0.004
Average			10.353	5.920	1.143	3.76	0.105	0.100	0.092	0.078	0.069	0.052	0.052	0.079	0.057	0.042	-0.002
Std Dev			0.029	0.006	0.018	0.01	0.001	0.001	0.001	0.001	0.001	0.001	0.001	0.001	0.001	0.001	0.002
Standard Error			0.017	0.003	0.010	0.00	0.001	0.001	0.000	0.001	0.001	0.001	0.000	0.001	0.000	0.001	0.001
Uncertainty			0.050	0.010	0.031	0.01	0.002	0.002	0.001	0.002	0.002	0.002	0.001	0.002	0.001	0.002	0.003
%Uncertainty			0.5%	0.2%	2.8%	0.3%	not calculated for pressure										

Table G-10. Uncertainty Analysis for Trim Tab B (10.50 ft/s)

ID	Run Name	F_∇	R_t	Trim	Heave	S	Total Pressure (psi)										
			lbf	deg	in	ft^2	P1	P2	P3	P4	P5	P6	P7	P8	P9	P10	P11
130	TB_10.50	1.940	6.892	3.164	0.289	4.36	0.068	0.060	0.057	0.046	0.049	0.045	0.049	0.056	0.096	0.023	-0.026
141	TB_10.50B	1.940	6.924	3.173	0.276	4.37	0.072	0.072	0.060	0.050	0.053	0.048	0.052	0.059	0.101	0.026	-0.020
149	TB_10.50D	1.940	6.926	3.185	0.277	4.37	0.069	0.068	0.056	0.047	0.052	0.046	0.050	0.055	0.100	0.024	-0.023
Average			6.914	3.174	0.280	4.37	0.070	0.067	0.058	0.048	0.051	0.046	0.051	0.056	0.099	0.025	-0.023
Std Dev			0.019	0.011	0.007	0.01	0.002	0.006	0.002	0.002	0.002	0.002	0.001	0.002	0.003	0.001	0.003
Standard Error			0.011	0.006	0.004	0.00	0.001	0.003	0.001	0.001	0.001	0.001	0.001	0.001	0.002	0.001	0.002
Uncertainty			0.032	0.018	0.013	0.01	0.003	0.010	0.003	0.003	0.004	0.003	0.003	0.004	0.005	0.002	0.005
%Uncertainty			0.5%	0.6%	4.5%	0.3%	not calculated for pressure										

Table G-11. Uncertainty Analysis for Trim Tab B (12.50 ft/s)

ID	Run Name	F_∇	R_t	Trim	Heave	S	Total Pressure (psi)										
			lbf	deg	in	ft^2	P1	P2	P3	P4	P5	P6	P7	P8	P9	P10	P11
136	TB_12.50	2.310	8.463	3.782	0.495	4.25	0.088	0.089	0.078	0.067	0.071	0.069	0.076	0.082	0.155	0.044	-0.014
138	TB_12.50D	2.310	8.479	3.776	0.502	4.26	0.084	0.086	0.074	0.067	0.068	0.065	0.075	0.080	0.154	0.042	-0.019
150	TB_12.50E	2.310	8.483	3.778	0.495	4.26	0.066	0.065	0.056	0.046	0.051	0.047	0.055	0.061	0.136	0.023	-0.038
Average			8.475	3.779	0.497	4.26	0.079	0.080	0.069	0.060	0.063	0.060	0.069	0.074	0.148	0.036	-0.023
Std Dev			0.010	0.003	0.004	0.00	0.012	0.013	0.012	0.012	0.011	0.012	0.012	0.012	0.011	0.011	0.013
Standard Error			0.006	0.002	0.002	0.00	0.007	0.007	0.007	0.007	0.006	0.007	0.007	0.007	0.006	0.007	0.007
Uncertainty			0.018	0.005	0.007	0.01	0.021	0.022	0.021	0.021	0.019	0.020	0.021	0.020	0.019	0.020	0.022
%Uncertainty			0.2%	0.1%	1.4%	0.2%	not calculated for pressure										

Table G-12. Uncertainty Analysis for Trim Tab B (14.50 ft/s)

ID	Run Name	F_∇	R_t	Trim	Heave	S	Total Pressure (psi)										
			lbf	deg	in	ft^2	P1	P2	P3	P4	P5	P6	P7	P8	P9	P10	P11
135	TB_14.50	2.679	9.696	4.523	0.750	4.11	0.094	0.095	0.088	0.083	0.088	0.086	0.098	0.105	0.211	0.063	-0.014
144	TB_14.50B	2.679	9.684	4.547	0.740	4.11	0.090	0.092	0.085	0.081	0.084	0.085	0.096	0.103	0.207	0.060	-0.015
147	TB_14.50D	2.679	9.706	4.524	0.753	4.11	0.091	0.089	0.086	0.078	0.084	0.085	0.094	0.104	0.210	0.060	-0.016
Average			9.695	4.531	0.747	4.11	0.092	0.092	0.087	0.080	0.085	0.085	0.096	0.104	0.210	0.061	-0.015
Std Dev			0.011	0.014	0.007	0.00	0.002	0.003	0.002	0.002	0.002	0.001	0.002	0.001	0.002	0.002	0.001
Standard Error			0.006	0.008	0.004	0.00	0.001	0.002	0.001	0.001	0.001	0.000	0.001	0.001	0.001	0.001	0.000
Uncertainty			0.019	0.024	0.012	0.00	0.003	0.006	0.003	0.004	0.004	0.001	0.004	0.002	0.004	0.003	0.001
%Uncertainty			0.2%	0.5%	1.6%	0.0%	not calculated for pressure										

Table G-13. Uncertainty Analysis for Trim Tab B (16.50 ft/s)

ID	Run Name	F_∇	R_t	Trim	Heave	S	Total Pressure (psi)										
			lbf	deg	in	ft^2	P1	P2	P3	P4	P5	P6	P7	P8	P9	P10	P11
241	TB_16.50_DL	3.049	10.682	5.200	0.932	3.93	0.104	0.101	0.102	0.103	0.113	0.115	0.132	0.161	0.294	0.091	0.013
244	TB_16.50B_DL	3.049	10.621	5.168	0.918	3.92	0.103	0.100	0.101	0.102	0.111	0.114	0.131	0.162	0.287	0.092	0.014
246	TB_16.50C_DL	3.049	10.592	5.154	0.905	3.93	0.103	0.100	0.100	0.102	0.110	0.114	0.130	0.161	0.288	0.090	0.016
Average			10.632	5.174	0.918	3.93	0.103	0.101	0.101	0.102	0.112	0.114	0.131	0.161	0.290	0.091	0.015
Std Dev			0.046	0.023	0.013	0.01	0.000	0.001	0.001	0.001	0.002	0.001	0.001	0.000	0.004	0.001	0.001
Standard Error			0.027	0.013	0.008	0.00	0.000	0.000	0.000	0.001	0.001	0.000	0.001	0.000	0.002	0.000	0.001
Uncertainty			0.080	0.040	0.023	0.01	0.001	0.001	0.001	0.002	0.003	0.001	0.002	0.001	0.006	0.001	0.002
%Uncertainty			0.7%	0.8%	2.5%	0.3%	not calculated for pressure										

Table G-14. Uncertainty Analysis for Trim Tab C (11.00 ft/s)

ID	Run Name	F_∇	R_t	Trim	Heave	S	Total Pressure (psi)										
			lbf	deg	in	ft^2	P1	P2	P3	P4	P5	P6	P7	P8	P9	P10	P11
152	TC_11.00	2.033	7.093	2.710	0.304	4.40	0.084	0.078	0.070	0.075	0.087	0.093	0.106	0.113	0.151	0.058	-0.003
163	TC_11.00B	2.033	7.097	2.730	0.300	4.40	0.086	0.080	0.080	0.079	0.089	0.094	0.110	0.116	0.150	0.060	0.002
173	IC_11.00C	2.033	7.109	2.732	0.302	4.41	0.088	0.080	0.080	0.079	0.088	0.095	0.112	0.117	0.151	0.062	0.002
Average			7.100	2.724	0.302	4.40	0.086	0.079	0.077	0.078	0.088	0.094	0.109	0.115	0.151	0.060	0.000
Std Dev			0.008	0.012	0.002	0.00	0.002	0.001	0.006	0.002	0.001	0.001	0.003	0.002	0.001	0.002	0.003
Standard Error			0.005	0.007	0.001	0.00	0.001	0.001	0.003	0.001	0.000	0.001	0.002	0.001	0.000	0.001	0.001
Uncertainty			0.014	0.021	0.003	0.00	0.003	0.002	0.010	0.004	0.001	0.002	0.005	0.004	0.001	0.004	0.004
%Uncertainty			0.2%	0.8%	1.1%	0.1%	not calculated for pressure										

Table G-15. Uncertainty Analysis for Trim Tab C (12.00 ft/s)

ID	Run Name	F_∇	R_t	Trim	Heave	S	Total Pressure (psi)										
			lbf	deg	in	ft^2	P1	P2	P3	P4	P5	P6	P7	P8	P9	P10	P11
155	TC_12.00	2.218	7.934	2.884	0.382	4.37	0.089	0.082	0.082	0.083	0.096	0.105	0.124	0.131	0.174	0.068	-0.002
160	TC_12.00B	2.218	7.892	2.930	0.374	4.36	0.093	0.086	0.085	0.085	0.097	0.107	0.127	0.134	0.174	0.067	0.003
165	TC_12.00C	2.218	7.932	2.941	0.381	4.37	0.093	0.086	0.084	0.083	0.097	0.106	0.127	0.132	0.173	0.069	0.001
Average			7.920	2.918	0.379	4.36	0.091	0.085	0.084	0.084	0.097	0.106	0.126	0.132	0.173	0.068	0.001
Std Dev			0.024	0.030	0.004	0.00	0.002	0.002	0.001	0.001	0.001	0.001	0.002	0.001	0.001	0.001	0.002
Standard Error			0.014	0.017	0.003	0.00	0.001	0.001	0.001	0.000	0.001	0.001	0.001	0.001	0.000	0.001	0.001
Uncertainty			0.042	0.052	0.008	0.00	0.004	0.004	0.002	0.001	0.002	0.002	0.003	0.002	0.001	0.002	0.004
%Uncertainty			0.5%	1.8%	2.0%	0.1%	not calculated for pressure										

Table G-16. Uncertainty Analysis for Trim Tab C (14.00 ft/s)

ID	Run Name	F_∇	R_t	Trim	Heave	S	Total Pressure (psi)										
			lbf	deg	in	ft^2	P1	P2	P3	P4	P5	P6	P7	P8	P9	P10	P11
153	TC_14.00	2.587	9.477	3.483	0.559	4.25	0.094	0.091	0.093	0.098	0.119	0.132	0.159	0.170	0.233	0.087	-0.002
158	TC_14.00B	2.587	9.437	3.479	0.572	4.25	0.096	0.091	0.097	0.101	0.119	0.131	0.161	0.171	0.231	0.089	0.000
169	IC_14.00C	2.587	9.437	3.498	0.563	4.25	0.097	0.093	0.096	0.102	0.120	0.133	0.160	0.173	0.231	0.090	0.003
Average			9.450	3.487	0.565	4.25	0.095	0.092	0.095	0.100	0.119	0.132	0.160	0.172	0.232	0.089	0.000
Std Dev			0.023	0.010	0.007	0.00	0.001	0.001	0.002	0.002	0.001	0.001	0.001	0.002	0.001	0.002	0.002
Standard Error			0.014	0.006	0.004	0.00	0.001	0.001	0.001	0.001	0.000	0.001	0.001	0.001	0.001	0.001	0.001
Uncertainty			0.041	0.017	0.012	0.00	0.002	0.002	0.004	0.003	0.001	0.002	0.002	0.003	0.002	0.003	0.004
%Uncertainty			0.4%	0.5%	2.0%	0.0%	not calculated for pressure										

Table G-17. Uncertainty Analysis for Trim Tab C (15.50 ft/s)

ID	Run Name	F_∇	R_t	Trim	Heave	S	Total Pressure (psi)										
			lbf	deg	in	ft^2	P1	P2	P3	P4	P5	P6	P7	P8	P9	P10	P11
251	TC_15.50_DL	2.864	10.570	4.034	0.7252	4.14	0.096	0.096	0.103	0.118	0.139	0.161	0.189	0.203	0.301	0.112	0.012
253	TC_15.50B_DL	2.864	10.573	4.032	0.7168	4.14	0.099	0.098	0.105	0.119	0.141	0.163	0.191	0.205	0.300	0.115	0.014
255	TC_15.50C_DL	2.864	10.550	4.024	0.7068	4.14	0.098	0.098	0.105	0.119	0.141	0.164	0.191	0.204	0.302	0.114	0.014
Average			10.564	4.030	0.716	4.14	0.098	0.097	0.104	0.119	0.140	0.163	0.190	0.204	0.301	0.114	0.013
Std Dev			0.012	0.005	0.009	0.00	0.001	0.001	0.001	0.000	0.001	0.001	0.001	0.001	0.001	0.002	0.001
Standard Error			0.007	0.003	0.005	0.00	0.001	0.001	0.001	0.000	0.001	0.001	0.001	0.001	0.001	0.001	0.001
Uncertainty			0.021	0.009	0.016	0.00	0.002	0.002	0.002	0.000	0.002	0.002	0.002	0.002	0.002	0.003	0.002
%Uncertainty			0.2%	0.2%	2.2%	0.1%	not calculated for pressure										

Table G-18. Uncertainty Analysis for Interceptor A (6.00 ft/s)

ID	Run Name	F_∇	R_t	Trim	Heave	S	Total Pressure (psi)										
			lbf	deg	in	ft^2	P1	P2	P3	P4	P5	P6	P7	P8	P9	P10	P11
35	IA_6.00	1.109	3.584	1.794	-0.412	4.604	0.085	0.079	0.076	0.063	0.057	0.049	0.049	0.051	-	-	-
46	IA-6.00B	1.109	3.602	1.809	-0.423	4.626	0.086	0.080	0.077	0.068	0.056	0.047	0.047	0.049	-	-	-
53	IA-6.00C	1.109	3.569	1.773	-0.426	4.629	0.085	0.079	0.076	0.068	0.058	0.049	0.049	0.051	-	-	-
Average			3.585	1.792	-0.420	4.620	0.085	0.080	0.076	0.066	0.057	0.048	0.049	0.050	-	-	-
Std Dev			0.016	0.018	0.007	0.014	0.000	0.001	0.000	0.003	0.001	0.001	0.001	0.001	-	-	-
Standard Error			0.009	0.010	0.004	0.008	0.000	0.000	0.000	0.002	0.000	0.000	0.001	0.001	-	-	-
Uncertainty			0.028	0.031	0.013	0.024	0.001	0.001	0.001	0.005	0.001	0.001	0.002	0.002	-	-	-
%Uncertainty			0.8%	1.7%	-3.0%	0.5%	not calculated for pressure										

Table G-19. Uncertainty Analysis for Interceptor A (11.50 ft/s)

ID	Run Name	F_∇	R_t	Trim	Heave	S	Total Pressure (psi)										
			lbf	deg	in	ft^2	P1	P2	P3	P4	P5	P6	P7	P8	P9	P10	P11
33	IA_11.50	2.125	7.745	3.899	0.377	4.277	0.098	0.089	0.084	0.072	0.065	0.064	0.075	0.096	-	-	-
41	IA_11.50B	2.125	7.791	3.912	0.351	4.287	0.101	0.093	0.086	0.082	0.070	0.067	0.077	0.097	-	-	-
47	IA-11.50C	2.125	7.788	3.917	0.387	4.264	0.100	0.093	0.086	0.080	0.071	0.066	0.076	0.095	-	-	-
Average			7.775	3.909	0.371	4.276	0.100	0.092	0.085	0.078	0.068	0.066	0.076	0.096	-	-	-
Std Dev			0.026	0.009	0.019	0.011	0.001	0.002	0.001	0.005	0.003	0.002	0.001	0.001	-	-	-
Standard Error			0.015	0.005	0.011	0.006	0.001	0.001	0.001	0.003	0.002	0.001	0.001	0.001	-	-	-
Uncertainty			0.045	0.016	0.032	0.019	0.002	0.004	0.002	0.009	0.005	0.003	0.002	0.002	-	-	-
%Uncertainty			0.6%	0.4%	8.7%	0.5%	not calculated for pressure										

Table G-20. Uncertainty Analysis for Interceptor A (13.50 ft/s)

ID	Run Name	F_∇	R_t	Trim	Heave	S	Total Pressure (psi)										
			lbf	deg	in	ft^2	P1	P2	P3	P4	P5	P6	P7	P8	P9	P10	P11
37	IA_13.50	2.495	9.113	4.639	0.651	4.126	0.105	0.100	0.094	0.088	0.081	0.083	0.097	0.128	-	-	-
44	IA-13.50B	2.495	9.081	4.634	0.646	4.131	0.106	0.099	0.094	0.082	0.081	0.082	0.098	0.127	-	-	-
52	IA-13.50C	2.495	9.109	4.643	0.647	4.127	0.107	0.099	0.094	0.086	0.084	0.081	0.098	0.126	-	-	-
Average			9.101	4.639	0.648	4.128	0.106	0.099	0.094	0.085	0.082	0.082	0.098	0.127	-	-	-
Std Dev			0.018	0.005	0.003	0.002	0.001	0.001	0.000	0.003	0.002	0.001	0.001	0.001	-	-	-
Standard Error			0.010	0.003	0.002	0.001	0.001	0.000	0.000	0.002	0.001	0.001	0.000	0.001	-	-	-
Uncertainty			0.031	0.008	0.005	0.004	0.002	0.001	0.000	0.006	0.003	0.002	0.001	0.002	-	-	-
%Uncertainty			0.3%	0.2%	0.7%	0.1%	not calculated for pressure										

Table G-21. Uncertainty Analysis for Interceptor A (16.50 ft/s)

ID	Run Name	F_∇	R_t	Trim	Heave	S	Total Pressure (psi)										
			lbf	deg	in	ft^2	P1	P2	P3	P4	P5	P6	P7	P8	P9	P10	P11
211	IA_16.50_DL	3.049	10.378	5.5399	1.006	3.853	0.101	0.097	0.095	0.092	0.099	0.109	0.146	0.188	-	-	-
212	IA_16.50B_DL	3.049	10.419	5.557	1.010	3.856	0.103	0.099	0.097	0.094	0.100	0.110	0.146	0.190	-	-	-
213	IA_16.50C_DL	3.049	10.354	5.527	0.994	3.859	0.100	0.095	0.094	0.092	0.098	0.108	0.146	0.187	-	-	-
Average			10.383	5.541	1.003	3.856	0.101	0.097	0.095	0.093	0.099	0.109	0.146	0.188	-	-	-
Std Dev			0.033	0.015	0.009	0.003	0.001	0.002	0.001	0.001	0.001	0.001	0.000	0.002	-	-	-
Standard Error			0.019	0.009	0.005	0.002	0.001	0.001	0.001	0.001	0.001	0.001	0.000	0.001	-	-	-
Uncertainty			0.057	0.026	0.015	0.005	0.002	0.003	0.002	0.002	0.002	0.002	0.001	0.003	-	-	-
%Uncertainty			0.5%	0.5%	1.5%	0.1%	not calculated for pressure										

Table G-22. Uncertainty Analysis for Interceptor B (10.00 ft/s)

ID	Run Name	F_∇	R_t	Trim	Heave	S	Total Pressure (psi)										
			lbf	deg	in	ft^2	P1	P2	P3	P4	P5	P6	P7	P8	P9	P10	P11
56	IB_10.00	1.848	6.576	3.395	0.185	4.37	0.092	0.083	0.076	0.065	0.059	0.066	0.077	0.101	-	-	-
63	IB_10.00B	1.848	6.671	3.390	0.182	4.37	0.092	0.085	0.078	0.067	0.069	0.070	0.078	0.099	-	-	-
72	IB_10.00C	1.848	6.666	3.398	0.180	4.37	0.091	0.082	0.076	0.064	0.054	0.069	0.076	0.099	-	-	-
Average			6.638	3.394	0.182	4.37	0.092	0.083	0.077	0.065	0.060	0.068	0.077	0.100	-	-	-
Std Dev			0.053	0.004	0.003	0.00	0.001	0.001	0.001	0.002	0.008	0.002	0.001	0.001	-	-	-
Standard Error			0.031	0.002	0.001	0.00	0.000	0.001	0.001	0.001	0.004	0.001	0.001	0.001	-	-	-
Uncertainty			0.092	0.007	0.004	0.00	0.001	0.002	0.002	0.003	0.013	0.003	0.002	0.002	-	-	-
%Uncertainty			1.4%	0.2%	2.4%	0.1%	not calculated for pressure										

Table G-23. Uncertainty Analysis for Interceptor B (12.50 ft/s)

ID	Run Name	F_∇	R_t	Trim	Heave	S	Total Pressure (psi)										
			lbf	deg	in	ft^2	P1	P2	P3	P4	P5	P6	P7	P8	P9	P10	P11
59	IB_12.50	2.310	8.426	3.810	0.514	4.26	0.100	0.093	0.094	0.093	0.108	0.135	0.159	0.201	-	-	-
64	IB_12.50B	2.310	8.473	3.859	0.484	4.26	0.101	0.095	0.095	0.092	0.107	0.133	0.155	0.194	-	-	-
70	IB_12.50C	2.310	8.482	3.872	0.474	4.25	0.102	0.096	0.095	0.087	0.105	0.124	0.153	0.190	-	-	-
Average			8.460	3.847	0.490	4.26	0.101	0.095	0.095	0.091	0.107	0.131	0.156	0.195	-	-	-
Std Dev			0.030	0.033	0.021	0.01	0.001	0.002	0.001	0.003	0.002	0.006	0.003	0.005	-	-	-
Standard Error			0.017	0.019	0.012	0.00	0.001	0.001	0.000	0.002	0.001	0.003	0.002	0.003	-	-	-
Uncertainty			0.052	0.057	0.036	0.01	0.002	0.003	0.001	0.005	0.003	0.010	0.005	0.010	-	-	-
%Uncertainty			0.6%	1.5%	7.4%	0.3%	not calculated for pressure										

Table G-24. Uncertainty Analysis for Interceptor B (13.25 ft/s)

ID	Run Name	F_∇	R_t	Trim	Heave	S	Total Pressure (psi)										
			lbf	deg	in	ft^2	P1	P2	P3	P4	P5	P6	P7	P8	P9	P10	P11
73	IB_13.25	2.448	8.931	4.032	0.568	4.21	0.103	0.097	0.098	0.101	0.119	0.150	0.180	0.226	-	-	-
79	IB_13.25B	2.448	8.957	4.029	0.568	4.21	0.103	0.096	0.097	0.088	0.113	0.152	0.178	0.222	-	-	-
80	IB_13.25C	2.448	8.951	3.893	0.557	4.23	0.103	0.097	0.099	0.096	0.120	0.152	0.178	0.220	-	-	-
81	IB_13.25D	2.448	8.951	3.990	0.556	4.22	0.104	0.098	0.099	0.102	0.124	0.145	0.179	0.224	-	-	-
Average			8.947	3.986	0.562	4.22	0.103	0.097	0.098	0.097	0.119	0.150	0.179	0.223	-	-	-
Std Dev			0.011	0.065	0.007	0.01	0.000	0.001	0.001	0.006	0.004	0.003	0.001	0.003	-	-	-
Standard Error			0.006	0.032	0.003	0.00	0.000	0.000	0.000	0.003	0.002	0.001	0.000	0.001	-	-	-
Uncertainty			0.017	0.097	0.010	0.01	0.001	0.001	0.001	0.010	0.007	0.004	0.001	0.004	-	-	-
%Uncertainty			0.2%	2.4%	1.8%	0.3%	not calculated for pressure										

Table G-25. Uncertainty Analysis for Interceptor B (14.50 ft/s)

ID	Run Name	F_∇	R_t	Trim	Heave	S	Total Pressure (psi)										
			lbf	deg	in	ft^2	P1	P2	P3	P4	P5	P6	P7	P8	P9	P10	P11
60	IB_14.50	2.679	9.709	4.057	0.689	4.17	0.102	0.100	0.105	0.114	0.143	0.181	0.221	0.284	-	-	-
67	IB_14.50B	2.679	9.686	4.088	0.687	4.16	0.102	0.099	0.104	0.113	0.138	0.175	0.217	0.274	-	-	-
75	IB_14.50C	2.679	9.677	4.099	0.685	4.16	0.103	0.099	0.103	0.112	0.134	0.177	0.219	0.274	-	-	-
Average			9.691	4.081	0.687	4.16	0.102	0.100	0.104	0.113	0.138	0.178	0.219	0.277	-	-	-
Std Dev			0.016	0.022	0.002	0.01	0.000	0.001	0.001	0.001	0.004	0.003	0.002	0.006	-	-	-
Standard Error			0.009	0.013	0.001	0.00	0.000	0.000	0.001	0.001	0.003	0.002	0.001	0.003	-	-	-
Uncertainty			0.028	0.038	0.003	0.01	0.001	0.001	0.002	0.002	0.008	0.005	0.004	0.010	-	-	-
%Uncertainty			0.3%	0.9%	0.5%	0.3%	not calculated for pressure										

Table G-26. Uncertainty Analysis for Interceptor B (14.50 ft/s)

ID	Run Name	F_∇	R_t	Corrected Trim	Corrected Heave	S	Total Pressure (psi)										
			lbf	deg	in	ft^2	P1	P2	P3	P4	P5	P6	P7	P8	P9	P10	P11
217	IB_17.00_DL	3.142	10.831	4.730	0.956	3.96	0.100	0.102	0.118	0.156	0.214	0.285	0.371	0.456	-	-	-
219	IB_17.00B_DL	3.142	10.832	4.730	0.941	3.96	0.100	0.103	0.118	0.155	0.213	0.284	0.369	0.453	-	-	-
221	IB_17.00_DL	3.142	10.810	4.728	0.912	3.96	0.100	0.102	0.117	0.155	0.213	0.284	0.370	0.455	-	-	-
Average			10.824	4.729	0.936	3.96	0.100	0.102	0.118	0.155	0.214	0.285	0.370	0.455	-	-	-
Std Dev			0.013	0.001	0.023	0.00	0.000	0.000	0.000	0.001	0.001	0.001	0.001	0.001	-	-	-
Standard Error			0.007	0.001	0.013	0.00	0.000	0.000	0.000	0.000	0.000	0.000	0.000	0.001	-	-	-
Uncertainty			0.022	0.002	0.039	0.01	0.000	0.000	0.001	0.001	0.001	0.001	0.001	0.002	-	-	-
%Uncertainty			0.2%	0.0%	4.2%	0.2%	not calculated for pressure										

Table G-27. Uncertainty Analysis for Interceptor C (10.50 ft/s)

ID	Run Name	F_∇	R_t	Trim	Heave	S	Total Pressure (psi)										
			lbf	deg	in	ft^2	P1	P2	P3	P4	P5	P6	P7	P8	P9	P10	P11
83	IC_10.50	1.940	6.732	2.894	0.258	4.40	0.089	0.083	0.083	0.085	0.105	0.128	0.158	0.189	-	-	-
92	IC_10.50B	1.940	6.685	2.910	0.259	4.40	0.089	0.083	0.083	0.085	0.106	0.128	0.158	0.193	-	-	-
104	IC_10.50C	1.940	6.534	2.888	0.247	4.40	0.089	0.083	0.084	0.088	0.103	0.126	0.157	0.189	-	-	-
Average			6.650	2.897	0.255	4.40	0.089	0.083	0.083	0.086	0.105	0.127	0.158	0.190	-	-	-
Std Dev			0.103	0.011	0.007	0.00	0.000	0.000	0.001	0.002	0.001	0.001	0.001	0.002	-	-	-
Standard Error			0.060	0.007	0.004	0.00	0.000	0.000	0.000	0.001	0.001	0.001	0.000	0.001	-	-	-
Uncertainty			0.179	0.020	0.012	0.01	0.001	0.000	0.001	0.003	0.002	0.002	0.001	0.004	-	-	-
%Uncertainty			2.7%	0.7%	4.5%	0.1%	not calculated for pressure										

Table G-28. Uncertainty Analysis for Interceptor C (13.00 ft/s)

ID	Run Name	F_∇	R_t	Trim	Heave	S	Total Pressure (psi)										
			lbf	deg	in	ft^2	P1	P2	P3	P4	P5	P6	P7	P8	P9	P10	P11
87	IC_13.00	2.402	8.614	3.186	0.482	4.31	0.098	0.093	0.100	0.116	0.151	0.194	0.245	0.298	-	-	-
96	IC_13.00B	2.402	8.533	3.196	0.476	4.31	0.096	0.092	0.100	0.118	0.151	0.194	0.241	0.296	-	-	-
102	IC_13.00C	2.402	8.498	3.209	0.472	4.31	0.096	0.093	0.101	0.120	0.152	0.194	0.244	0.293	-	-	-
Average			8.548	3.197	0.477	4.31	0.097	0.093	0.100	0.118	0.151	0.194	0.243	0.296	-	-	-
Std Dev			0.059	0.012	0.005	0.00	0.001	0.001	0.001	0.002	0.000	0.000	0.002	0.002	-	-	-
Standard Error			0.034	0.007	0.003	0.00	0.001	0.000	0.000	0.001	0.000	0.000	0.001	0.001	-	-	-
Uncertainty			0.103	0.020	0.009	0.00	0.002	0.001	0.001	0.003	0.000	0.000	0.004	0.004	-	-	-
%Uncertainty			1.2%	0.6%	1.8%	0.0%	not calculated for pressure										

Table G-29. Uncertainty Analysis for Interceptor C (15.00 ft/s)

ID	Run Name	F_∇	R_t	Trim	Heave	S	Total Pressure (psi)										
			lbf	deg	in	ft^2	P1	P2	P3	P4	P5	P6	P7	P8	P9	P10	P11
86	IC_15.00	2.772	9.950	3.612	0.684	4.20	0.099	0.100	0.114	0.146	0.198	0.258	0.328	0.397	-	-	-
94	IC_15.00B	2.772	9.898	3.624	0.688	4.20	0.099	0.101	0.116	0.146	0.196	0.257	0.325	0.396	-	-	-
99	IC_15.00C	2.772	9.696	3.608	0.685	4.20	0.099	0.100	0.116	0.147	0.200	0.260	0.329	0.402	-	-	-
Average			9.848	3.614	0.686	4.20	0.099	0.100	0.115	0.146	0.198	0.258	0.327	0.398	-	-	-
Std Dev			0.134	0.008	0.002	0.00	0.000	0.001	0.001	0.001	0.002	0.002	0.002	0.003	-	-	-
Standard Error			0.078	0.005	0.001	0.00	0.000	0.000	0.001	0.000	0.001	0.001	0.001	0.002	-	-	-
Uncertainty			0.233	0.014	0.004	0.00	0.000	0.001	0.002	0.001	0.003	0.003	0.003	0.005	-	-	-
%Uncertainty			2.4%	0.4%	0.5%	0.1%	not calculated for pressure										

Table G-30. Uncertainty Analysis for Interceptor C (16.00 ft/s)

ID	Run Name	F_∇	R_t	Trim	Heave	S	Total Pressure (psi)										
			lbf	deg	in	ft^2	P1	P2	P3	P4	P5	P6	P7	P8	P9	P10	P11
225	IC_16.00_DL	2.957	10.803	3.856	0.683	4.14	0.100	0.103	0.120	0.157	0.215	0.284	0.366	0.443	-	-	-
227	IC_16.00B_DL	2.957	10.758	3.847	0.658	4.14	0.100	0.103	0.120	0.157	0.215	0.284	0.367	0.444	-	-	-
230	IC_16.00C_DL	2.957	10.761	3.858	0.673	4.14	0.102	0.104	0.121	0.158	0.214	0.285	0.367	0.442	-	-	-
Average			10.774	3.854	0.671	4.14	0.101	0.103	0.120	0.157	0.214	0.284	0.366	0.443	-	-	-
Std Dev			0.025	0.006	0.012	0.00	0.001	0.001	0.001	0.001	0.000	0.000	0.000	0.001	-	-	-
Standard Error			0.015	0.003	0.007	0.00	0.001	0.000	0.000	0.000	0.000	0.000	0.000	0.000	-	-	-
Uncertainty			0.044	0.010	0.022	0.00	0.002	0.001	0.001	0.001	0.000	0.001	0.000	0.001	-	-	-
%Uncertainty			0.4%	0.3%	3.2%	0.1%	not calculated for pressure										

APPENDIX H. PREDICTION CALCULATIONS

The appendix contains a summary of the performance prediction calculations for the bare hull and each of the trim tab configurations. For bare hull, Savitsky's method (1964) was used with a correction factor on resistance suggested by Blount and Fox (1976). For trim tabs, the same was done, but the predicted force of the trim tabs was incorporated into Savitsky's method according to Brown's method (1971).

BARE HULL - CALCULATIONS SUMMARY

Model Properties and Physical Constants					
Δ	47	lbf	**Water Temp.**	20	°C
V	0.755	ft^3	**ρ, FW**	1.934	$slugs/ft^3$
B_p	12.00	in	**ν,FW**	1.28E-05	ft^2/s
LCG	25.50	in	**VCG**	5.28	in
f	0.00	in	**Shaft Angle**	20	deg
g	32.20	ft/s^2	**Lp/BPA**	5	
Deadrise	20	deg	**CA**	0	
			Static Trim	-2.3	deg

Blount-Fox '76 Correction Factor Parameters	
LCG/BPX	2.125
LCG/LP	0.425

	Savitsky Method Calculated Values							Wetted Surface					Resistance Coefficients			
#	**F_∇**	**Model Speed**	**Resistance**	**Blount -Fox '76 Correction Factor**	**Corrected Resistance**	**Effective τ**	**Running τ**	**Lc**	**Lk**	**Lm**	**λ**	**S**	**Rn**	**CF**	**CF*S/S0**	**CR**
		ft/s	*lbf*		*lbf*	*deg*	*deg*	*ft*	*ft*	*ft*		ft^2				
1	1.11	6.003	3.297	1.603	5.284	3.00	5.30	4.84	7.05	5.94	5.94	6.32	2.79E+06	3.65E-03	4.34E-03	2.42E-02
2	1.48	8.004	4.085	1.710	6.985	3.36	5.66	4.59	6.56	5.58	5.58	5.94	3.49E+06	3.51E-03	3.91E-03	1.73E-02
3	1.85	10.005	4.975	1.471	7.320	3.83	6.13	4.26	5.99	5.12	5.12	5.45	4.01E+06	3.42E-03	3.51E-03	1.07E-02
4	1.94	10.506	5.203	1.412	7.347	3.95	6.25	4.16	5.84	5.00	5.00	5.32	4.11E+06	3.41E-03	3.41E-03	9.54E-03
5	2.03	11.006	5.431	1.357	7.369	4.08	6.38	4.07	5.69	4.88	4.88	5.19	4.20E+06	3.39E-03	3.32E-03	8.52E-03
6	2.13	11.506	5.655	1.307	7.389	4.20	6.50	3.97	5.54	4.76	4.76	5.06	4.28E+06	3.38E-03	3.22E-03	7.64E-03
7	2.22	12.007	5.873	1.262	7.411	4.32	6.62	3.87	5.40	4.63	4.63	4.93	4.35E+06	3.37E-03	3.13E-03	6.87E-03
8	2.31	12.507	6.070	1.222	7.418	4.43	6.73	3.77	5.26	4.52	4.52	4.81	4.42E+06	3.36E-03	3.04E-03	6.18E-03
9	2.40	13.007	6.271	1.187	7.443	4.53	6.83	3.67	5.13	4.40	4.40	4.69	4.48E+06	3.36E-03	2.96E-03	5.60E-03
10	2.49	13.507	6.460	1.157	7.471	4.62	6.92	3.58	5.01	4.30	4.30	4.57	4.54E+06	3.35E-03	2.88E-03	5.09E-03
11	2.59	14.008	6.655	1.130	7.521	4.68	6.98	3.49	4.90	4.20	4.20	4.47	4.60E+06	3.34E-03	2.81E-03	4.65E-03
12	2.68	14.508	6.823	1.107	7.555	4.74	7.04	3.40	4.80	4.10	4.10	4.37	4.65E+06	3.33E-03	2.74E-03	4.24E-03
13	2.77	15.008	6.981	1.088	7.593	4.77	7.07	3.32	4.71	4.02	4.02	4.27	4.71E+06	3.33E-03	2.68E-03	3.88E-03
14	2.86	15.509	7.129	1.071	7.635	4.79	7.09	3.25	4.63	3.94	3.94	4.19	4.77E+06	3.32E-03	2.62E-03	3.56E-03
15	2.96	16.009	7.268	1.057	7.681	4.79	7.09	3.17	4.56	3.86	3.86	4.11	4.84E+06	3.31E-03	2.56E-03	3.27E-03
16	3.05	16.509	7.402	1.045	7.733	4.77	7.07	3.11	4.49	3.80	3.80	4.04	4.90E+06	3.30E-03	2.51E-03	3.01E-03
17	3.14	17.010	7.504	1.034	7.762	4.75	7.05	3.04	4.44	3.74	3.74	3.98	4.97E+06	3.30E-03	2.47E-03	2.75E-03

TRIM TAB A - CALCULATION SUMMARY

Model Properties and Physical Constants					
Δ	47	lbf	**Water Temp.**	20	°C
V	0.755	ft^3	**ρ, FW**	1.934	$slugs/ft^3$
B_p	12.00	in	**ν,FW**	1.28E-05	ft^2/s
LCG	25.50	in	**VCG**	5.28	in
f	0.00	in	**Shaft Angle**	20	deg
g	32.20	ft/s^2	**Lp/BPA**	5	
Deadrise	20	deg	**CA**	0	
			Static Trim	-2.3	deg

Blount-Fox '76 Correction Factor Parameters	
LCG/BPX	2.125
LCG/LP	0.425

Trim Tab Parameters			
Number of Tabs	n	2	
Tab Deflection	αf	1	deg
Tab Chord	Lf	0.167	ft
Span-beam ratio	σ	0.783	

	Savitsky Method Calculated Values							Wetted Surface					Resistance Coefficients			
#	**F_∇**	**Model Speed**	**Resistance**	**Blount -Fox '76 Correction Factor**	**Corrected Resistance**	**Effective τ**	**Running τ**	**Lc**	**Lk**	**Lm**	**λ**	**S**	**Rn**	**CF**	**CF*S/S0**	**CR**
		ft/s	*lbf*		*lbf*	*deg*	*deg*	*ft*	*ft*	*ft*		ft^2				
1	1.11	6.003	3.265	1.603	5.233	2.97	5.27	4.85	7.08	5.96	5.96	6.35	2.80E+06	3.69E-03	4.41E-03	2.38E-02
2	1.48	8.004	4.023	1.710	6.879	3.29	5.59	4.61	6.63	5.62	5.62	5.98	3.52E+06	3.40E-03	3.83E-03	1.71E-02
3	1.85	10.005	4.869	1.471	7.164	3.69	5.99	4.29	6.09	5.19	5.19	5.53	4.06E+06	3.07E-03	3.19E-03	1.07E-02
4	1.94	10.506	5.084	1.412	7.179	3.80	6.10	4.21	5.95	5.08	5.08	5.40	4.17E+06	3.00E-03	3.05E-03	9.61E-03
5	2.03	11.006	5.296	1.357	7.186	3.91	6.21	4.11	5.81	4.96	4.96	5.28	4.27E+06	2.93E-03	2.91E-03	8.63E-03
6	2.13	11.506	5.506	1.307	7.195	4.01	6.31	4.02	5.67	4.85	4.85	5.16	4.36E+06	2.87E-03	2.78E-03	7.79E-03
7	2.22	12.007	5.714	1.262	7.210	4.11	6.41	3.93	5.54	4.73	4.73	5.04	4.44E+06	2.81E-03	2.67E-03	7.06E-03
8	2.31	12.507	5.898	1.222	7.207	4.20	6.50	3.83	5.41	4.62	4.62	4.92	4.52E+06	2.76E-03	2.55E-03	6.41E-03
9	2.40	13.007	6.086	1.187	7.225	4.28	6.58	3.74	5.29	4.52	4.52	4.81	4.59E+06	2.71E-03	2.45E-03	5.85E-03
10	2.49	13.507	6.256	1.157	7.235	4.34	6.64	3.65	5.18	4.42	4.42	4.70	4.66E+06	2.67E-03	2.36E-03	5.36E-03
11	2.59	14.008	6.438	1.130	7.276	4.39	6.69	3.57	5.08	4.32	4.32	4.60	4.73E+06	2.63E-03	2.27E-03	4.94E-03
12	2.68	14.508	6.596	1.107	7.304	4.43	6.73	3.49	4.98	4.23	4.23	4.51	4.80E+06	2.59E-03	2.19E-03	4.56E-03
13	2.77	15.008	6.748	1.088	7.340	4.45	6.75	3.41	4.90	4.15	4.15	4.42	4.87E+06	2.55E-03	2.12E-03	4.22E-03
14	2.86	15.509	6.892	1.071	7.382	4.45	6.75	3.34	4.82	4.08	4.08	4.34	4.95E+06	2.52E-03	2.06E-03	3.91E-03
15	2.96	16.009	7.046	1.057	7.446	4.44	6.74	3.27	4.76	4.01	4.01	4.27	5.02E+06	2.49E-03	2.00E-03	3.65E-03
16	3.05	16.509	7.192	1.045	7.513	4.41	6.71	3.20	4.70	3.95	3.95	4.21	5.10E+06	2.46E-03	1.95E-03	3.42E-03
17	3.14	17.010	7.326	1.034	7.578	4.38	6.68	3.14	4.65	3.90	3.90	4.15	5.18E+06	2.43E-03	1.90E-03	3.20E-03

TRIM TAB B- CALCULATION SUMMARY

Model Properties and Physical Constants					
Δ	47	lbf	**Water Temp.**	20	°C
V	0.755	ft^3	**ρ, FW**	1.934	$slugs/ft^3$
B_p	12.00	in	**ν,FW**	1.28E-05	ft^2/s
LCG	25.50	in	**VCG**	5.28	in
f	0.00	in	**Shaft Angle**	20	deg
g	32.20	ft/s^2	**Lp/BPA**	5	
Deadrise	20	deg	**CA**	0	
			Static Trim	-2.3	deg

Blount-Fox '76 Correction Factor Parameters	
LCG/BPX	2.125
LCG/LP	0.425

Trim Tab Parameters			
Number of Tabs	n	2	
Tab Deflection	αf	3	deg
Tab Chord	Lf	0.167	ft
Span-beam ratio	σ	0.783	

	Savitsky Method Calculated Values							Wetted Surface					Resistance Coefficients			
#	**F_∇**	**Model Speed**	**Resistance**	**Blount -Fox '76 Correction Factor**	**Corrected Resistance**	**Effective τ**	**Running τ**	**Lc**	**Lk**	**Lm**	**λ**	**S**	**Rn**	**CF**	**CF*S/S0**	**CR**
		ft/s	*lbf*		*lbf*	*deg*	*deg*	*ft*	*ft*	*ft*		ft^2				
1	1.11	6.003	3.209	1.603	5.143	2.90	5.20	4.86	7.15	6.01	6.01	6.39	2.82E+06	3.68E-03	4.42E-03	2.33E-02
2	1.48	8.004	3.915	1.710	6.695	3.15	5.45	4.65	6.76	5.70	5.70	6.07	3.57E+06	3.38E-03	3.86E-03	1.65E-02
3	1.85	10.005	4.689	1.471	6.900	3.43	5.73	4.37	6.30	5.33	5.33	5.68	4.17E+06	3.04E-03	3.24E-03	1.02E-02
4	1.94	10.506	4.885	1.412	6.897	3.51	5.81	4.29	6.18	5.24	5.24	5.57	4.30E+06	2.97E-03	3.11E-03	9.05E-03
5	2.03	11.006	5.078	1.357	6.890	3.57	5.87	4.21	6.06	5.14	5.14	5.47	4.42E+06	2.90E-03	2.98E-03	8.08E-03
6	2.13	11.506	5.269	1.307	6.885	3.64	5.94	4.13	5.95	5.04	5.04	5.36	4.53E+06	2.84E-03	2.86E-03	7.25E-03
7	2.22	12.007	5.449	1.262	6.876	3.69	5.99	4.05	5.84	4.94	4.94	5.26	4.64E+06	2.78E-03	2.75E-03	6.53E-03
8	2.31	12.507	5.612	1.222	6.858	3.74	6.04	3.97	5.74	4.85	4.85	5.16	4.74E+06	2.73E-03	2.65E-03	5.88E-03
9	2.40	13.007	5.785	1.187	6.867	3.78	6.08	3.89	5.64	4.76	4.76	5.07	4.84E+06	2.68E-03	2.56E-03	5.34E-03
10	2.49	13.507	5.953	1.157	6.885	3.81	6.11	3.81	5.55	4.68	4.68	4.98	4.94E+06	2.64E-03	2.47E-03	4.87E-03
11	2.59	14.008	6.127	1.130	6.924	3.82	6.12	3.73	5.47	4.60	4.60	4.90	5.04E+06	2.60E-03	2.39E-03	4.47E-03
12	2.68	14.508	6.272	1.107	6.946	3.83	6.13	3.66	5.40	4.53	4.53	4.82	5.14E+06	2.56E-03	2.32E-03	4.10E-03
13	2.77	15.008	6.421	1.088	6.985	3.82	6.12	3.60	5.33	4.46	4.46	4.75	5.24E+06	2.52E-03	2.26E-03	3.78E-03
14	2.86	15.509	6.567	1.071	7.033	3.79	6.09	3.53	5.28	4.41	4.41	4.69	5.34E+06	2.49E-03	2.20E-03	3.49E-03
15	2.96	16.009	6.716	1.057	7.098	3.76	6.06	3.47	5.24	4.35	4.35	4.63	5.45E+06	2.46E-03	2.15E-03	3.24E-03
16	3.05	16.509	6.867	1.045	7.174	3.71	6.01	3.42	5.20	4.31	4.31	4.58	5.56E+06	2.43E-03	2.10E-03	3.02E-03
17	3.14	17.010	7.020	1.034	7.262	3.66	5.96	3.36	5.17	4.27	4.27	4.54	5.68E+06	2.41E-03	2.06E-03	2.82E-03

TRIM TAB C- CALCULATION SUMMARY

Model Properties and Physical Constants					
Δ	47	lbf	**Water Temp.**	20	°C
V	0.755	ft^3	**ρ, FW**	1.934	$slugs/ft^3$
B_P	12.00	in	**ν,FW**	1.28E-05	ft^2/s
LCG	25.50	in	**VCG**	5.28	in
f	0.00	in	**Shaft Angle**	20	deg
g	32.20	ft/s^2	**Lp/BPA**	5	
Deadrise	20	deg	**CA**	0	
			Static Trim	-2.3	deg

Blount-Fox '76 Correction Factor Parameters	
LCG/BPX	2.125
LCG/LP	0.425

Trim Tab Parameters			
Number of Tabs	n	2	
Tab Deflection	αf	5	deg
Tab Chord	Lf	0.167	ft
Span-beam ratio	σ	0.783	

	Savitsky Method Calculated Values							Wetted Surface					Resistance Coefficients			
#	F_∇	Model Speed	Resistance	Blount -Fox '76 Correction Factor	Corrected Resistance	Effective τ	Running τ	Lc	Lk	Lm	λ	S	Rn	CF	CF*S/S0	CR
		ft/s	*lbf*		*lbf*	*deg*	*deg*	*ft*	*ft*	*ft*		ft^2				
1	1.11	6.003	3.163	1.603	5.069	2.83	5.13	4.88	7.23	6.05	6.05	6.44	2.84E+06	3.66E-03	4.44E-03	2.29E-02
2	1.48	8.004	3.829	1.710	6.548	3.01	5.31	4.69	6.89	5.79	5.79	6.16	3.62E+06	3.36E-03	3.89E-03	1.60E-02
3	1.85	10.005	4.553	1.471	6.699	3.19	5.49	4.44	6.52	5.48	5.48	5.83	4.29E+06	3.02E-03	3.31E-03	9.71E-03
4	1.94	10.506	4.736	1.412	6.687	3.22	5.52	4.37	6.43	5.40	5.40	5.75	4.44E+06	2.94E-03	3.19E-03	8.60E-03
5	2.03	11.006	4.918	1.357	6.673	3.26	5.56	4.31	6.34	5.32	5.32	5.67	4.58E+06	2.88E-03	3.07E-03	7.65E-03
6	2.13	11.506	5.098	1.307	6.662	3.28	5.58	4.24	6.26	5.25	5.25	5.58	4.72E+06	2.82E-03	2.96E-03	6.83E-03
7	2.22	12.007	5.277	1.262	6.658	3.30	5.60	4.17	6.18	5.17	5.17	5.51	4.86E+06	2.76E-03	2.86E-03	6.12E-03
8	2.31	12.507	5.440	1.222	6.648	3.31	5.61	4.10	6.10	5.10	5.10	5.43	4.99E+06	2.71E-03	2.77E-03	5.50E-03
9	2.40	13.007	5.613	1.187	6.663	3.31	5.61	4.04	6.04	5.04	5.04	5.36	5.12E+06	2.66E-03	2.68E-03	4.98E-03
10	2.49	13.507	5.785	1.157	6.691	3.31	5.61	3.97	5.98	4.98	4.98	5.30	5.25E+06	2.62E-03	2.61E-03	4.52E-03
11	2.59	14.008	5.974	1.130	6.752	3.28	5.58	3.91	5.93	4.92	4.92	5.24	5.39E+06	2.58E-03	2.54E-03	4.15E-03
12	2.68	14.508	6.149	1.107	6.809	3.25	5.55	3.86	5.89	4.87	4.87	5.19	5.53E+06	2.55E-03	2.49E-03	3.81E-03
13	2.77	15.008	6.327	1.088	6.882	3.21	5.51	3.80	5.86	4.83	4.83	5.14	5.67E+06	2.52E-03	2.43E-03	3.51E-03
14	2.86	15.509	6.510	1.071	6.972	3.16	5.46	3.75	5.85	4.80	4.80	5.11	5.82E+06	2.49E-03	2.39E-03	3.25E-03
15	2.96	16.009	6.700	1.057	7.080	3.10	5.40	3.70	5.84	4.77	4.77	5.08	5.97E+06	2.46E-03	2.35E-03	3.02E-03
16	3.05	16.509	6.900	1.045	7.208	3.04	5.34	3.66	5.85	4.75	4.75	5.06	6.14E+06	2.44E-03	2.32E-03	2.83E-03
17	3.14	17.010	7.113	1.034	7.358	2.96	5.26	3.62	5.86	4.74	4.74	5.05	6.31E+06	2.42E-03	2.29E-03	2.65E-03

APPENDIX I. EQUIVALENCE MATCHING CALCULATIONS

This appendix contains the calculations for the predicted equivalent interceptor deployments for each of the three trim tabs selected.

Equivalence Model Comparison

General Tab Dimensions		
Chord	2.000	in
Span	5.000	in

Equivalence Model Equations	
1. Dawson and Blount (2002)	$\alpha_i = 0.175\alpha_t + 0.0154{\alpha_t}^2$
2. Villa and Brizzolara (2009)	$\alpha_i = 0.102\alpha_t + 0.0134{\alpha_t}^2$

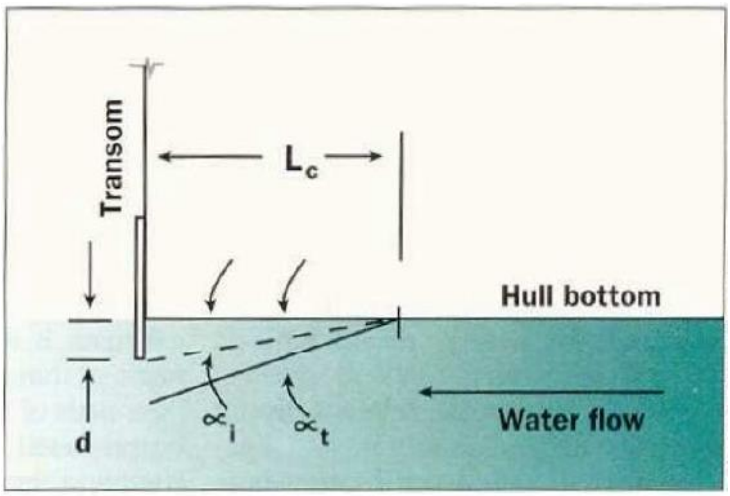

Figure I-1. Angel Definition
Source: (Dawson & Blount, 2002)

Trim Tab	α_t	α_i (deg)		Equivalent Interceptor Deployment (in)		
	deg	Eq 1	Eq 2	Experimental	Eq 1	Eq 2
A	1.00	0.19	0.12	0.0230 ± 0.0050	0.0066	0.0040
B	3.00	0.66	0.43	N/A	0.0230	0.0149
C	5.00	1.25	0.85	0.0450 ± 0.0040	0.0436	0.0295